THE ROLE OF TISSUE TRANSGLUTAMINASE ACTIVE SITE MUTANTS IN THE CELL CYCLE AND DRUG RESPONSE

by

Özge Deniz Yeşil

Submitted to Graduate School of Natural and Applied Sciences

in Partial Fulfillment of the Requirements

for the Degree of Master of Science in

Biotechnology

Yeditepe University

2021

THE ROLE OF TISSUE TRANSGLUTAMINASE ACTIVE SITE MUTANTS IN THE CELL CYCLE AND DRUG RESPONSE

APPROVED BY:

Prof. Dr. Dilek TELCİ TEMELTAŞ ……
(Thesis Supervisor)
(Yeditepe University)

Assist.Prof. Dr.Hüseyin ÇİMEN ……
(Yeditepe University)

Assist.Prof.Dr. Zeynep Büşra BOLAT
(Istanbul Sabahattin Zaim University) ……

DATE OF APPROVAL: …. /…. /2021

I hereby declare that this thesis is my own work and that all information in this thesis has been obtained and presented in accordance with academic rules and ethical conduct. I have fully cited and referenced all material and results as required by these rules and conduct, and this thesis study does not contain any plagiarism. If any material used in the thesis requires copyright, the necessary permissions have been obtained. No material from this thesis has been used for the award of another degree.

I accept all kinds of legal liability that may arise in case contrary to these situations.

Name, Last name ……

Signature …...…….……...

ACKNOWLEDGEMENTS

First and foremost, I would like to thank sincerely my thesis advisor, Prof. Dr. Dilek TELCİ TEMELTAŞ for her support and supervision through my thesis studies. Indeed, I believe that without being a member of Telci Lab, I could not be the person that I am today in all-field of life both from personal and academic perspectives. Besides, I would like to thank all DT Lab members especially Fatma SERTGÖZ and Halime İLHAN SIĞINÇ for their kind support and helps during my thesis.

In addition, I would like to convey my warmest gratitude to my dearest friends Naz ÜNSAL, Selin MUMCU, Hazal YILMAZ, İpek BEDİR and Ayça Ece NEZİR due to their kind supports during my thesis projects especially while having hard times in M.Sc. period and when even I lost my belief in myself, they believed and motivated me to remember who I am.

More importantly, I would like to share my gratitude at the highest level for my father and the role model in my life, Cafer YEŞİL, my beloved mother Fahriye Yeşil, my sisters İlkay YEŞİL ROY and Doğa YEŞİL and my life partner Mehmet Alper BAYSAL. If I did not have the support, courage, and love from my partner in life whilst having my mental breakdowns, I would not be able to finish this thesis. Finally, I would like to express my everlasting love to both my dear cat-daughter Kleopatra and to my grandmother Gülcan HÜNER. They are the brightest and guiding stars in my universe. I feel their spiritual connections and blessings in my life, and I always will.

ABSTRACT

THE ROLE OF TISSUE TRANSGLUTAMINASE ACTIVE SITE MUTANTS IN THE CELL CYCLE AND DRUG RESPONSE

Renal cell carcinoma (RCC) accounting for 85 percent of all kidney cancer cases constitutes 2 percent of all cancer-related death worldwide. The rapid development of the disease and poor survival rate entitles RCC as one of the most prevalent and carcinogenic neoplasms in urologic diseases. Despite recent advances in cancer treatment, recurrence of tumor, chemoresistance, and metastasis remain to be significant consequences of aggressive RCC. As a result, new treatment alternatives that necessitate the discovery of novel therapeutic targets are still needed. From this point of view, tissue transglutaminase TG2 draws attention due to its role in the progression, development, survival of various neoplasms including RCC. TG2 can gain these roles owing to its enzymatic activities which are GTPase and transamidase activities. Accumulating evidence showed that the GTPase activity of TG2 mostly participates in anti-apoptotic functions in cells while transamidase activity of TG2 is generally required for its interaction with the cell adhesion receptors. Therefore, in this study, TG2-variants which are transamidase active type TG2-R580A, transamidase-deficient, and low GTP-binding active form TG2-C277S and GTP-binding-active TG2-W241A were expressed in the RCC cell line to elucidate the role of transamidase and GTP-binding function of TG2 in the regulation of cell cycle and drug resistance of RCC. Based on our data, catalytically inactive transamidase domain-containing but GTPase active form TG2-W241A expressing RenCa showed the highest cell proliferation rate and increased cell cycle profile. In addition, although being subjected to a well-known mTOR inhibitor, everolimus, TG2-W241A RenCa cells were the only group that was not cytotoxically affected by this drug treatment. The fact that TG2-W241A expressing cells continued to proliferate whilst being exposed to everolimus suggested that the GTP-binding activity of TG2 may be important in circumventing cell death. Overall, these findings showed for the first time the indispensable role of the GTP binding function of TG2 on cell proliferation and everolimus resistance in RCC. This project was funded by FP-7 TRANSPATH 289964 grants.

ÖZET

DOKU TRANSGLUTAMİNAZI AKTİVE BÖLGE MUTANTLARININ İLAÇ DİRENCİ VE HÜCRE BÜYÜMESİNDEKİ ROLÜ

Tüm böbrek kanseri hücrelerinin yüzde 85'ini oluşturan böbrek hücreli karsinoma (BHK) tüm dünya çapında kansere bağlı ölümlerin yüzde 2'sini oluşturmaktadır. Hastalığın hızlı nüksü ve kansere bağlı sağkalım oranın düşük oluşu BHK'yı ürolojik hastalıklarda en yaygın ve karsinojenez neoplazmlardan biri olarak nitelendirmiştir. Kanser tedavisindeki son gelişmelere rağmen, tümörün nüksü, ilaç direnci ve metastaz agresif BHK'nın önemli sonuçlarındandır. Sonuç olarak, yeni terapötik hedeflerin keşfedilmesini gerektiren yeni tedavi alternatiflerine hala ihtiyaç duyulmaktadır. Bu açıdan, doku transglutaminaz TG2, BKH de dahil olmak üzere çeşitli neoplazmların ilerlemesi, gelişimi ve hayatta kalmasındaki rolü nedeniyle dikkat çekmektedir. TG2, GTPase ve transamidase enzimatik aktiviteleri kanser gelişiminde önemli rol oynamaktadır. Şimdiye kadar TG2'nin enzimatik aktiviteleri hakkında yayınlanan veriler, TG2'nin GTPase aktivitesinin çoğunlukla hücrelerde antiapoptotik fonksiyonlara katıldığı bildirirken, TG2'nin transamidaz aktivitesinin hücre adezyon reseptörleri ile etkileşiminde önemli olduğunu göstermektedir. Bu nedenle, bu çalışmada, transamidaz aktif tip TG2-R580A, transamidaz eksikliği ve düşük GTP bağlayıcı aktif form TG2-C277S ve GTP bağlayıcı aktif TG2-W241A olan TG2 varyantlarının RenCa BHK hücre hattında ifade edilmeleri ile TG2'nin transamidaz ve GTP bağlayıcı fonksiyonunlarının hücre siklüsü ve ilaç direncindeki öneminin aydınlatılması hedeflenmiştir. Verilerimize dayanarak, TG2-W241A ifade eden RenCa hücreleri en yüksek hücre proliferasyon oranını ve artan hücre döngüsü profilini gösterdiği tespit edilmiştir. Ek olarak, iyi bilinen bir mTOR inhibitörü olan everolimus'a maruz kalmasına rağmen, TG2-W241A RenCa hücreleri, bu ilaç tedavisinden sitotoksik olarak etkilenmeyen tek grup olmuştur. Everolimus'a maruz kalan TG2-W241A RenCa hücrelerinin büyümeye devam etmesi, TG2'deki GTP bağlanma aktivitesinin, Everolimus indüklü hücre ölümüne direnç gösterdiğini öne sürmüştür. Özetle bulgularımız ilk kez TG2'nin GTP bağlanma fonksiyonunun BHK'da hücre çoğalması ve everolimus direnci üzerindeki vazgeçilmez rolünü göstermiştir. Bu proje FP-7 TRANSPATH 289964 projesince finanse edilmiştir.

TABLE OF CONTENTS

LIST OF FIGURES

LIST OF TABLES

LIST OF ABBREVIATIONS

AKT	Protein kinase B
APS	Ammonium persulfate
ATTC	American type culture collection
ATP	Adenosine triphosphate
BSA	Bovine serum albumin
CCRCC	Clear cell renal cell carcinoma
cDNA	Complementary deoxyribonucleic acid
CDC	Collecting duct carcinoma
CDK1	Cyclin-dependent kinase inhibitor
chRCC	Chromophobe renal cell carcinoma
CHIP	Carboxyl-terminus of hsp70-interacting protein
DMEM	Dulbecco’s modified eagle’s medium
DMSO	Dimethyl sulfoxide
DR-4/5	Death receptor 4/5
ECM	Extracellular matrix
EDTA	Ethylenediaminetetraacetic acid
EGFR	Epidermal growth factor receptor
EMT	Epithelial-to-mesenchymal transition
ERK1/2	Extracellular signal-regulated protein kinases 1 and 2
FBS	Fetal bovine serum
FAK	Focal adhesion kinase
FN	Fibronectin
GLOBOCAN	Global cancer incidence, mortality, and prevalence

GTP	Guanosine triphosphate
HDAC	Histone deacetylase
HIF-1α	Hypoxia-Inducible Factor α
HPRCC	Inherited papillary renal cell carcinoma
HRE	Hypoxia response element
hTG2	Human tissue transglutaminase 2
ID1	DNA binding 1
IL-6	Interleukin-6
IL-1β	Interleukin 1-β
ISUP	International society of urologic pathologist
ITGβ1	Integrin β 1
JNK	c-JUN N-terminal kinase
MiT	Microphthalmia transcription factor
MMP-9	Matrix metalloproteinase-9
mTOR	Mechanistic target of rapamycin
mTORC1	Mechanistic target of rapamycin complex 1
mRCC	Metastatic renal cell carcinoma
PARP	Poly-ADP-ribose polymerase
PDGF	Platelet-derived growth factor
PDGFR	Platelet-derived growth factor receptor
PRCC	Papillary renal cell carcinoma
PVDF	Polyvinylidene difluoride
RCC	Renal cell carcinoma
RRE1&2	Retionic acid responsible elements 1 and 2
RT	Reverse transcriptase

SDS-PAGE	Sodium dodecyl sulfate-polyacrylamide gel electrophoresis gel electrophoresis
SDC-4	Syndecan-4
TBS	Tris-buffered saline
TBS-T	Tris-buffered saline with tween-20
TEMED	N, N, N', N'-Tetramethylethylenediamine
TG	Transglutaminase
TG2	Tissue transglutaminase 2
TNF-α	Tumor necrosis factor α
TRAIL	Tumor necrosis factor-related apoptosis-inducing ligand
TG2	Tissue transglutaminase 2
VHL	Von-Hippel Lindau
VEGF	Vascular endothelial growth factor
WHO	World health organization
WST	Water soluble tetrazolium salt

1. INTRODUCTION

1.1. GROSS ANATOMY AND FUNCTIONS OF KIDNEY

The urinary system of humans is composed of kidneys, ureters, bladder, and urethra. Among the members of the urinary system, bilateral kidney pairs have various roles in physiological processes occurring in the body [1,2]. Kidneys are bean-shaped organs that reside along the posterior abdominal wall and on both sides of the retroperitoneal space in vertebrates. More precisely, kidneys are located between the level of the 12^{th} thoracic vertebrae and the 3^{rd} lumbar rib (Figure 1.1.). Body homeostasis is sustained by these profoundly vascularized and complex organs. For instance, metabolic wastes such as ammonia and urea are filtered and removed from the blood through renal filtration and subsequently excreted as urine. Yet, concomitantly to provide homeostasis to the body, kidneys regulate the pH and electrolyte balance, and water levels in tissue fluids. Moreover, the kidney participates in the activation of vitamin D to provide a balance in calcium and phosphate ions in the body. Therefore, calcitriol which is the active form of vitamin D is produced in kidneys. Besides calcitriol, hormones such as erythropoietin, angiotensin, renin, and aldosterone, are secreted from kidneys, as well. In this way, the production of erythrocytes, and the adjustment of blood volume and pressure are regulated through kidneys. The last but not least, the metabolism of toxins is also part of the kidney's functions [2,3].

The functional and basic units of the kidneys are called nephrons. Owing to those basic subunits, the urination and filtration functions of the kidney take place in the mammalian urinary system. Although the number of nephrons is diverse in humans due to several genetic and environmental effects, approximately, two million nephrons are found in each kidney pair of humans. Critical reduction of nephrons in number may result in several diseases such as chronic kidney disease and hypertension [4]. The renal corpuscle which is also known as the glomerulus is located at the cortex of the nephron. The filtration of blood is initially started in the glomerulus whose selective permeability is provided by the filtration barrier to filtrate blood and to obtain an ultrafiltrate. The specialized visceral epithelium found in Bowman's capsule, the glomerular basement membrane, and endothelial cells composing

the glomerular capillaries are the units of the filtration barrier. Concomitantly, the ultrafiltrate is circulated from the nephron to the collecting duct and subsequently to ureters to be excreted as urine [2].

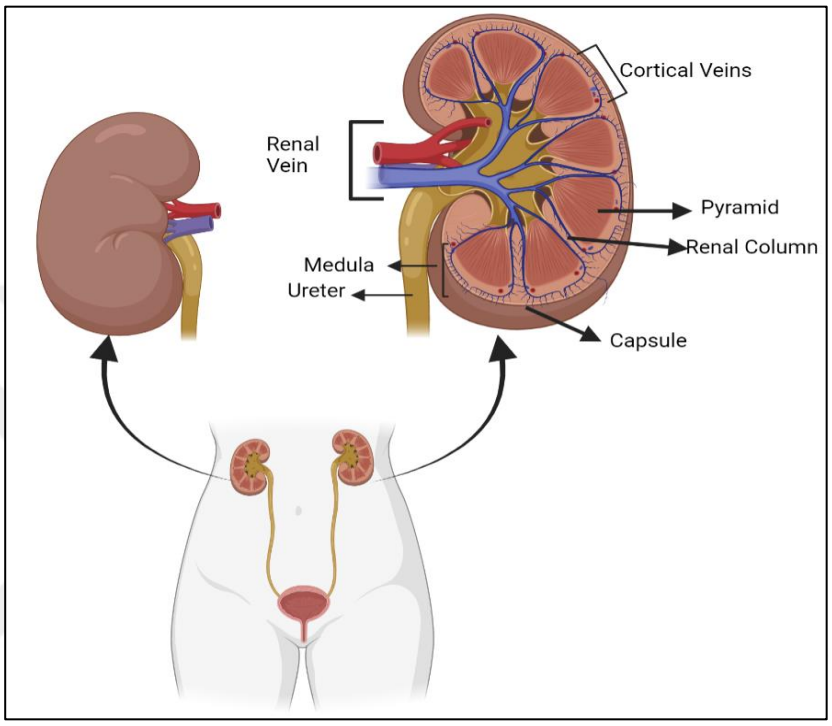

Figure 1.1. Gross anatomy of the kidney. Kidneys are found bilaterally in the retroperitoneal space at the 12th thoracic vertebrate and 13th lumbar rib. Due to the location of the liver, the right pair of the kidney is placed slightly lower level than the left pair.

1.2. KIDNEY CANCER

Kidney cancer is a prevailing genitourinary malignancy by placing 12th rank worldwide and ninth in European cancer statistics [5]. The incidence rate of kidney cancer varies in different factors such as genetic background, environmental effects, and lifestyles of a person. Moreover, in the geographical point of view, it has the highest occurrence rate in first world countries such as Europe and America, whereas, lowest in Africa and Asia (Figure 1.2.). Kidney cancer is also called renal carcinoma (RCC) and it is not a homogenous but heterogenous renal neoplasm derived from the renal tubular epithelium. 90-95 percent of kidney tumors and 2-3 percent of cancer cases occur due to renal cell carcinoma [6].

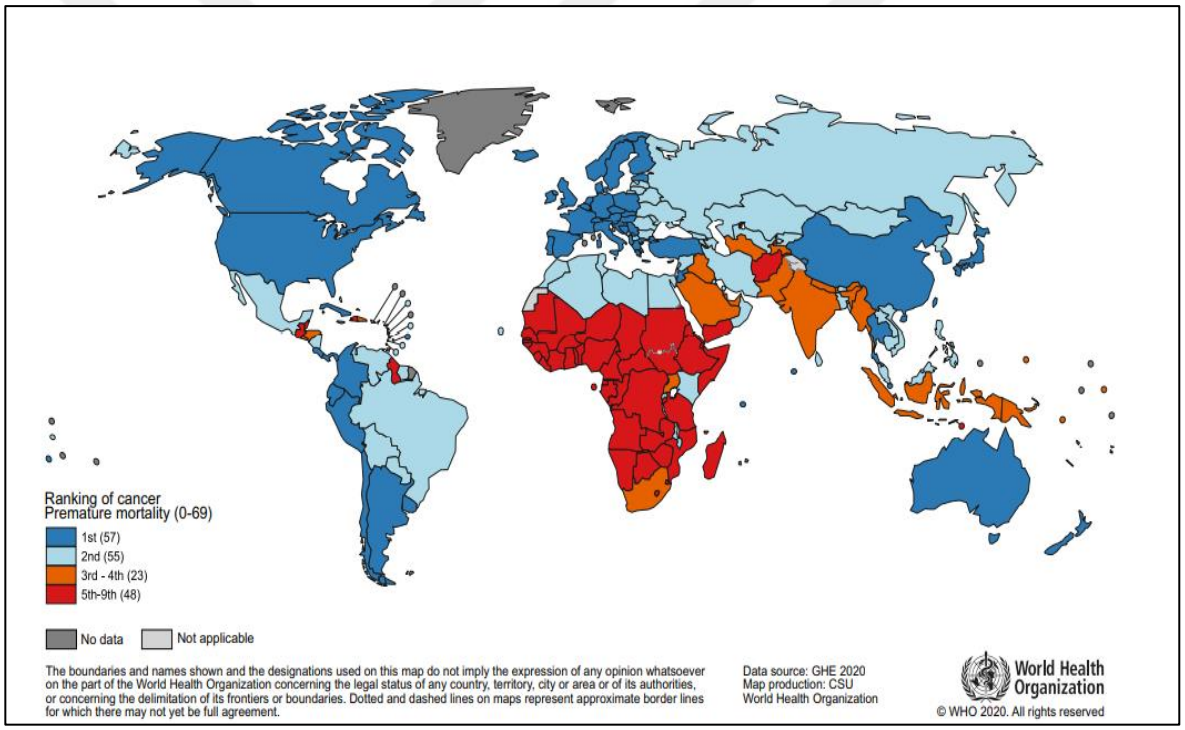

Figure 1.2. Mortality rate of renal cell carcinoma in the patients with <70- years old [7].

A recent study published by GLOBOCAN claims that except basal cell carcinoma, 28.4 million new tumor cases are estimated to show up from 2020 to 2040 and increase the incidence rate to 47 percent. Moreover, this study issued that 431.288 new cases accounted for approximately 2 percent of all adult malignancies, occurred due to renal cell carcinoma in 2020. In 2020, 179.368 new mortality cases were observed because of kidney tumors [7].

1.3. CLASSIFICATION AND SUBTYPES OF RENAL CELL CARCINOMAS

In 1968, the classification of renal tumors is asserted according to a system published by Thoenes *et al.* relying on cytological and histopathological characteristics of the renal neoplasms [7,8]. Renal tumors' classifications are revised in 2016 by the World Health Organization (WHO) regarding recent advances, pathologies, and molecular biology of RCC [9].

Renal cell cancers are categorized into different subtypes based on their morphological features. The most common subtypes of RCC are clear cell RCC, chromophobe RCC and papillary RCC which are accounting for 65-70 percent, 5-7 percent, and 15-20 percent of all renal tumors in respective order [9, 10]. Besides these major subtypes of RCC, a vast range of novel subtypes of RCC are present (Figure 1.4.). These new subtypes of RCC are classified according to cellular morphology and prevailing cytoplasmic stainings such as clear cell RCC and renal oncocytoma. Moreover, a combination of both cytoplasmic staining and cellular features also create another subtype, for instance, clear cell papillary RCC [11]. There are more categories for the designation of rare and novel subtypes of RCC. Renal medullary and collecting duct carcinomas are named based on the anatomical site of the tumor, succinate dehydrogenase deficient and microphthalmia transcription factor (MiT) family translocation RCC are designated regarding depicter molecular mutations. Furthermore, family predisposition is also utilized to classify RCC subtypes such as hereditary leiomyomatosis RCC syndrome-associated RCC [11,12].

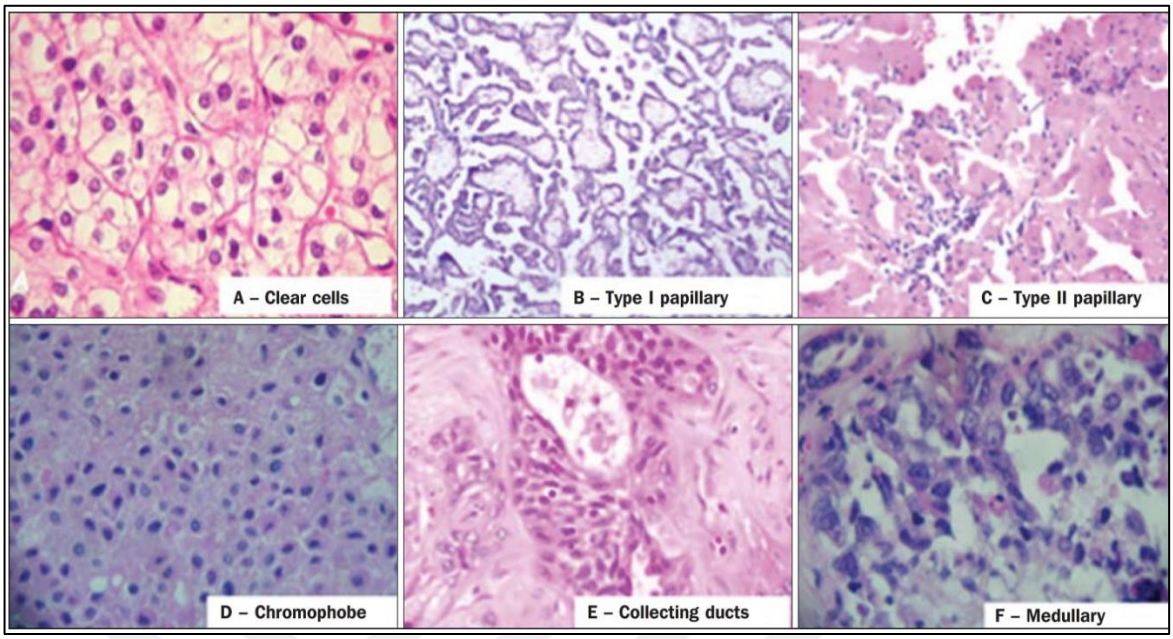

Figure 1.3. Histological representative images for renal cell carcinoma's subtypes. A-F) Clear cell, type 1 papillary, type 2 papillary, chromophobe, collecting ducts, and medullary renal cell carcinomas were demonstrated respectively [13].

1.3.1. Clear Cell RCC

One of the major subtypes of renal cell carcinoma is clear cell RCC (CCRCC) which occurs in epithelial cells by coating the proximal tubule. CCRCC is termed as clear due to its optically clear cytoplasm and cell membrane since the cancer cells lose glycogen and cytoplasmic lipids during tissue processing. In some high-grade CCRCC neoplasm cases or near areas of necrosis or internal bleeding, CCRCCs are observed to have granular eosinophilic cytoplasm. There is not a strict predominant patient group in CCRCC. Yet, the occurrence rate of the RCC is higher in the male group who is older than 40 years of age comparing the female group in the same age category by having a 1:5 male to female ratio. CCRCC possesses both hereditary and sporadic forms [3]. CCRCC is generally affiliated with cytogenetic malignancies comprising a mutation in a tumor suppressor gene called Von Hippel-Lindau (VHL) located at 3p25-26 and deprivation of genetic material due to deletion in chromosome 3 (3p). The VHL is also an E3 ubiquitin ligase which involves the ubiquitylation of the transcription factors named hypoxia-inducible factor (HIF1α) and

HIF2α to trigger their proteolytic degradation when the cells are exposed to normoxic conditions. As being a transcription factor, both HIF1α and HIF2α participate in the regulation of a vast range of genes responsible for chromatin remodeling, angiogenesis, and metabolism. In 90 percent of the sporadic form of CCRCC, biallelic loss of VHL occurs and due to that HIFs improperly stabilized, therefore, proangiogenic gene expression is a marker of CCRCC's carcinogenesis occurs. On the hereditary side of the VHL mutation, VHL disease passes onto the offspring in an autosomal dominant manner. Patients with VHL disease deal with bilateral and multifocal CCRCC [14–17].

Besides the functional link between VHL and HIF1α, VHL also participates in the downregulation of AKT protein which is a substantial player of the Phosphoinositide 3-kinase (PI3K) pathway. This protein is an important marker in CCRCC-like aggressive-termed tumor cells. In the upregulation of AKT gene expression, most of the hallmarks of cancer such as resistance to growth suppressors and cell death can arise since cell division and growth are induced and cell survival is enhanced while cell-death processes such as autophagy are diminished. Thus, elevated activation of AKT is related to aggressiveness of tumor cells, inactivation of cell cycle checkpoint protein p27, and cytoplasmic translocation [6].

Aside from VHL, the elevation of vascular endothelial growth factor (VEGF) and platelet-derived growth factor (PDGF)'s levels are also associated with the arising of angiogenic potential and aggressiveness of CCRCC [18].

1.3.2. Papillary RCC

The term papillary implicates the tumor cells constituted from tubulo-papillary or papillary constructs which are less than 0.5cm in diameter. Papillary renal cell carcinoma (PRCC) is the second most prevalent subtype of RCC with differing unique histologic and cytogenetic characteristics. PRCC accounts for approximately 10-15 percent of total RCC cases [19,20]. This renal neoplasm mostly occurs in the sporadic form however in some cases PRCC is also inherited to patients whose families have a familial history of PRCC. Inherited PRCC (HPRCC) generally arises due to mutations in *MET* oncogene located at chromosome 7q31. Without any familial record of RCC, only 13 percent of PRCC cases occur due to *MET*

mutations. Moreover, HPRCC increases the predisposition to form bilateral and multifocal papillary renal carcinomas rather than a sporadic form of PRCC. Apart from the genetic mutations, karyotypic anomalies such as trisomy of chromosomes 7 and 17 result in PRCC [21]. Albeit renal neoplasms do not possess papillary structure, these cytogenetic aberrations are utilized to diagnose PRCC. Well-circumscribed PRCC is observed to be soft and to have a red-brown cut surface with fibrous capsules. In addition, around PRCC, necrosis, and hemorrhage are monitored. Among other aggressive variants of RCC, PRCC has a better prognosis. Following 5 years of surgery, the tumor-specific mortality rate of PRCC is 91 percent although other RCC subtypes such as CCRCC and chromophobe RCC have 72 and 88 percent survival rates, respectively [3].

1.3.3. Chromophobe RCC

The chromophobe renal cell carcinoma (chRCC) which was first identified in 1985, accounts for around 5 percent of all RCC cases [9,22,23]. This type of RCC has particular biologic, ultrastructural, and morphological characteristics which differentiate chRCC from other subtypes of RCC. chRCC has two morphological variants classified as eosinophilic and classical variants according to physical features of the tumor cell cytoplasm [9]. While classic variants have clear cytoplasm, eosinophilic variants have eosinophilic cytoplasm as their name suggests. chRCC generally occurs in sporadic form, however, also familial predisposition leads to the occurrence of chRCC if the patients have the hereditary Brit-Hogg-Dubé or Cowden (a mutation of PTEN) syndrome in the family record [11,24,25].

1.3.3. Renal Medullary Carcinoma

Renal medullary carcinoma (RMC) is originated from the renal medulla and an idiocratic type of RCC due to its association with sickle cell hemoglobinopathies. This highly aggressive and slightly rare neoplasm is enunciated in 1995 for the first time [26]. Unfortunately, RMC is mostly reported in young adult groups along with a slight long-term disease-free survival and an average of 19-week survival period. Although applied neoadjuvant therapies extend the survival period and attenuate the effects of the disease, the reoccurrence of the tumor occurs rapidly and leads to a high mortality rate. In addition, the

occurrence of RMC is considered to ensue after the loss of expression of SMARCB1 gene. Hence, the nuclear transcription regulator gene SMARCB1 (INI1) expressed on chromosome 22 is supported to inevitably be involved in the diagnosis of RMC [26–28].

1.3.4. Collecting Duct RCC

Collecting duct renal carcinoma develops in the medullary zone of the kidney. Morphologically distinct characteristics of these tumors are dysplasia in the surrounding collecting duct, desmoplastic response in the stroma, and a tubule papillary configuration of cells. In addition to these three unique features of collecting duct RCC, augmented solid regions, glands, and tubules are generally exhibited as well. Although collecting duct renal carcinoma is a rare subtype of RCC by accounting for 1 percent of all RCC cases, it demonstrates an aggressive behavior by posing high mortality and yet a short survival rate [29–31].

1.3.5. Xp11 Translocation Carcinoma

Starting from the early 1990s, Xp11 translocation carcinoma was identified Starting thoroughly and characteristics of the disease were described. Preliminary, both papillary and Xp11 translocation RCC were thought to be the same type of malignancy yet just differ in having particular translocations. However, today the difference of these malignancies was discovered, and they are classified in different subclasses of RCC. Xp11 translocation carcinoma is prevalently and predominantly determined in females, young adults, and even children account for nearly one-third of all renal cell carcinomas [32]. Although the pediatric age group is the most affected group of the Xp11 carcinoma, a raft of adult group cases is also reported to suffer from this neoplasm. The translocation in the name of the carcinoma define the translocation of TFE3 gene found in Xp11.2 region of chromosome with adjacent genes; PSF t(X;1) (p11.2; p34), ASLP t(x;1) (p11.2;p34) and PRCC genes t(x;1)(p11.2;q21). The histological characteristics of this malignancy are defined as vesicular structures together with either layer of tumor cells or conducted nests [9].

1.4. GRADING OF RCC

The Fuhrman nuclear grading system divides RCC into four different categories based on nucleolar size, nuclear size, and nuclear anaplasia (seen in Table 1). According to the highest grade throughout the whole tumor, a nuclear grade is determined, and it is independent of the prevalent nuclear grade. Using a light microscope, the nuclear grade of a tumor is examined at 100x and 400x magnifications. Nevertheless, Fuhrman nuclear grading system has only been validated in CCRCC and has yet to be confirmed in other RCC subtypes. Therefore, in 2012 International Society of Urologic Pathologists (ISUP) build a consensus to develop a less complex alternative to Fuhrman grading in order to obtain results that correlates ideally with prognosis. The ISUP's proposal of a novel strategy for grading RCC is nucleolar grading. Both the ISUP and Fuhrman grading systems are relevant in being used in CCRCC and PRCC gradings while not appropriate for chromophobe renal cell carcinoma [3,6].

Table 1.1. RCC grading according to Fuhrman nuclear grading system (Adapted from Primo N. Lara *et al*., 2015) [9].

Grade	Nucleus	Nucleolus
1	Small (10-µm diameter), round uniform resembling nucleus of a mature lymphocyte	Inconspicuous or absent nucleoli (viewed at 4oX magnification)
2	Larger nuclei (15-µm diameter) with slight nuclear irregularity	Small nucleoli (only visible at 400X magnification)
3	Large nuclei (20-µm diameter), with obvious nuclear integrity	Large, prominent nucleoli (visible at 100x magnification)
4	Same as grade 3 but more bizarre with multilobation and large clumps of chromatin	Large, prominent nucleoli (visible at 100x magnification)

1.5. MOLECULAR TARGETED THERAPIES FOR RENAL CELL CARCINOMA

Although even being undergone nephrectomy, 20 to 40 percent of patients encounter recurrence of the disease and developed metastasis. The 5-year survival rate for patients with metastatic RCC is lower than 10 percent because of poor prognosis. Thus, understanding the molecular mechanism behind the recurrence of metastatic RCC is required to improve prognosis [33].

Indeed, most RCC cases are defined to occur spontaneously, the significance of chromosome 3 in RCC was discovered for the hereditary type of CCRCCs linked with von Hippel-Lindau disease by a study. Chromosome 3 was defined to involve numerous tumor suppressor genes and mutation in these genes are associated with RCC such as SETD2, VHL, BAP1, and PBRM1 [34]. VHL is an E3 ubiquitin ligase and known as a tumor suppressor. VHL regulates several proteins involving HIF1-α which is a transcription factor modulating numerous pro-angiogenic factors such as vascular endothelial growth factor (VEGF) for degradation [35]. On the other hand, activation of HIF-1α occurs due to mutations which lead to loss or silencing of VHL. Therefore, the identification of these molecular interactions presents a compelling case for targeting and developing VEGFR in metastatic RCC.

Since RCC is one the most angiogenesis-promoting solid neoplasm, angiogenesis is the primary goal of targeted therapies for mRCC patients. In fact, to detect and diagnose RCC, renal angiography was a formerly prominent method in this disease [36]. As a result of increased angiogenesis in mRCC, hypervascularity is monitored. This hypervascularity conveys the presence of overexpressed HIF-dependent angiogenic factors such as VEGF. Depending on the loss of pVHL, notable overexpression of VEGF is observed which results in increased formation of new blood vessels. Furthermore, either together or separately other several angiogenic factors contribute to a process of formation of new blood vessels called neoangiogenesis in solid tumors. Therefore, new strategies have been developed against ligands of VEGF or VEGFR to hinder VEGF in mRCC [37]. In agreement with this notion, the FDA has authorized the number of drugs that hinder VEGF, or its receptor called kinase insert domain receptors (KDR) such as sunitinib, lenvatinib, pazopanib, axitinib, and sorafenib in mRCC (Figure 1.4.).

A first-generation tyrosine kinase inhibitor (TKI), sunitinib, was approved by FDA in 2006 as regular therapy for mCCRCC patients. Sunitinib is a multi-targeted therapy as it effectively inhibits PDGFR(α and β), KIT, VEGFR (1,2 and 3), RET, Fms-like tyrosine kinase 3 (FLT3), and CSF-1R [38–41]. In a group of RCC patients who have not received any previous treatment, progression-free survival (PFS) was determined as 11 months after sunitinib treatment, while overall survival (OS) was determined as 26.4 months [38,42]. Adverse effects (AEs) of sunitinib were recorded as oral changes, hypertension, diarrhea, skin toxicity, and anorexia. Furthermore, the incidence rate of common toxicity criteria (CTC) grade 3 or 4 toxicities is low and sunitinib treatment is tolerated well in patients [43].

Pazopanib is also a TKI inhibitor targeting FGFR, cKIT**,** PDGFR (α and β), and VEGFR (1,2 and 3). In 2009, both FDA and European Medicines Agency (EMA) approve the use of pazopanib in mRCC patients treated with prior chemotherapy [41]. Comparing to a placebo group, PFS and OS were found as 9.2 and 22.9 months for the pazopanib-treated group respectively while 4.2 and 20.5 months were detected in placebo-treated group. Hepatotoxicity and gastrointestinal side effects were reported in pazopanib treatment [44,45].

Sorafenib is another multikinase inhibitor that inhibits PDGFβ, cKIT, VEGFR (1,2 and 3), RET, and Fms-like tyrosine kinase 3 (FLT3) [46,47]. Sorafenib was primarily discovered as a Raf kinase inhibitor showing an antiapoptotic effect in carcinomas [47]. Antitumor activity of sorafenib was identified in animal models such as murine renal adenocarcinoma, RenCa. In the VHL-knockout xenograft model, sorafenib treatment prevented angiogenesis and tumor growth [48]. In sorafenib-treated patients, some AEs such as nausea, rash, diarrhea, and fatigue can be observed. PFS of sorafenib-treated patient and placebo group was assessed as 5.5 and 2.8 months respectively [49].

Lenvatinib is a potent tyrosine kinase inhibitor for VEGFR (1–3), FGFR (1–4), PDGFR, c-KIT, and RET. FDA and EMA approved it for the treatment of patients who have locally recurrent, metastatic, or progressive mRCC in combination with an anti-angiogenic therapy such as everolimus [50,51]. The median PFS was reported as 7.4 months for lenvatinib however PFS is increased when lenvatinib is used together with everolimus [52]. Moreover, OS for lenvatinib alone is 19.1 months. Hypertension, nausea, diarrhea, vomiting, and fatigue are the AEs of lenvatinib treatment [52]. Another specific tyrosine kinase inhibitor

of VEGFR (1-3) is axitinib. Axitinib is authorized by EMA and FDA for the treatment of advanced RCC in 2012 [41,53]. In comparison to other TKIs, axitinib is observed to demonstrate an increased risk of hypertension as an AE as well as gastrointestinal symptoms. PFS was evaluated as 6.7 months for patients treated with axitinib [54,55].

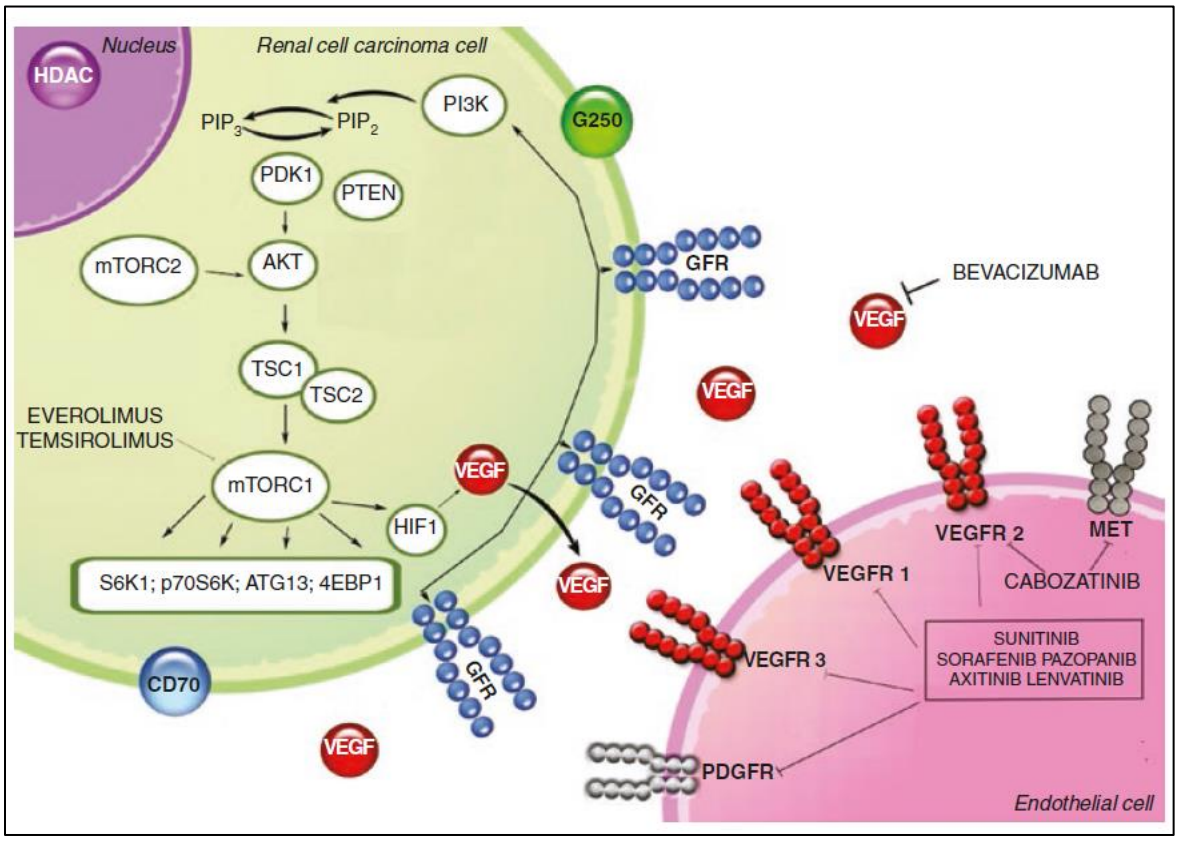

Figure 1.4. mTOR and tyrosine kinase inhibitors approved in metastatic renal cell carcinoma and their targets [6].

The molecular mechanism associated with the development of RCC is the mTOR pathway which is an important element in the regulation of PI3K-AKT signaling. Abnormal activation of the mTOR pathway has been projected as being involved in cell growth, invasion, and metastasis of tumor cells. Besides, overexpression of mTOR leads to the induction of angiogenesis through enhanced expression of VEGF signaling. Given the connection of the mTOR pathway with several tumorigenesis processes, mTOR is considered as one of the key targets in the treatment of RCC [56]. As a matter of fact, mTOR is a notable participant in tumor development. Therefore, in the clinical treatment of tumors,

rapamycin analogs (rapalogs) have been licensed. mTOR inhibitors with distinct functional molecular mechanisms have a promising role in the targeted therapy in solid tumors. Rapamycin was originally discovered to be an antiproliferative, antifungal, and immunosuppressive element. Later studies have been shown that rapamycin binds 12 kDa FK506-binding protein (FKBP12) and consequently blocks mTORC1. Nevertheless, due to the low solubility and pharmacokinetics of rapamycin, it is not suitable to target carcinomas. Thus, water-soluble rapalogs having similar pharmacological properties to rapamycin have been produced. Everolimus and temsirolimus are water-soluble rapalogs proved to possess tumor-suppressive characteristics in vivo. Furthermore, both rapalogs have been used in the clinical treatment of mRCC. Besides advanced RCC, non-small cell lung cancer, hepatocellular carcinoma, advanced gastric cancer, mantle cell lymphoma, and endometrial cancers can be targeted via these rapalogs. In 2009, oral administered rapalog and mTOR inhibitor, everolimus (RAD001), was authorized by the FDA to use in advanced RCC patients taking medications for VEGFR inhibition as antiangiogenic. According to phase I clinical trials of everolimus, daily oral administration dose of everolimus was chosen as 10 mg for patients with metastatic mainly CCRCC. The phase 3 trial on everolimus published by Motzer *et al*. in 2008, proved the efficacy of sequential treatment for patients with mCCRCC for the first time [57]. In this trial, everolimus treatment was applied to 416 patients with mRCC after the failures of given first or several prior treatments such as VEGFR-TKI therapy. After the applied double-blind treatment, the median PFS of everolimus was reported as 49 months while it was 1.9 months for the placebo group according to blind independent central review. AEs were also recorded as fatigue and dyspnea. As a result of RECORD-3 (Renal Cell cancer treatment with Oral RAD001 given daily) phase III, evaluation of everolimus on mRCC patients showed a reduction in the tumor progression by 67 percent compared to the placebo group.

1.6. TRANSGLUTAMINASES

A large protein family known as transglutaminase (TGs) possesses functionally and structurally related family members which are especially well-known for their ability to catalyze proteins by Ca^{+2} dependent manner and modulate posttranslational modifications. Modifications of proteins by transglutaminase occur by appending covalent bonds between

γ-carboxamide groups and free-amine groups of peptide-bound glutamine, site-specific deamination, and crosslinking between proteins (Figure 1.5.) [58]. The designation, transglutaminase, was first defined in a study reported by Waelsch *et al* in the 1960s. In this study, from a guinea pig liver extract, Heinrich Waelsch identified a soluble liver protein that catalyzes the integration of low-molecular primary amines into proteins [2-4]. The term, transglutaminase, was later revised by the Enzyme Commission based on the R-glutamyl-peptide and amine- γ-glutamyltransferase structure in tTG [60].

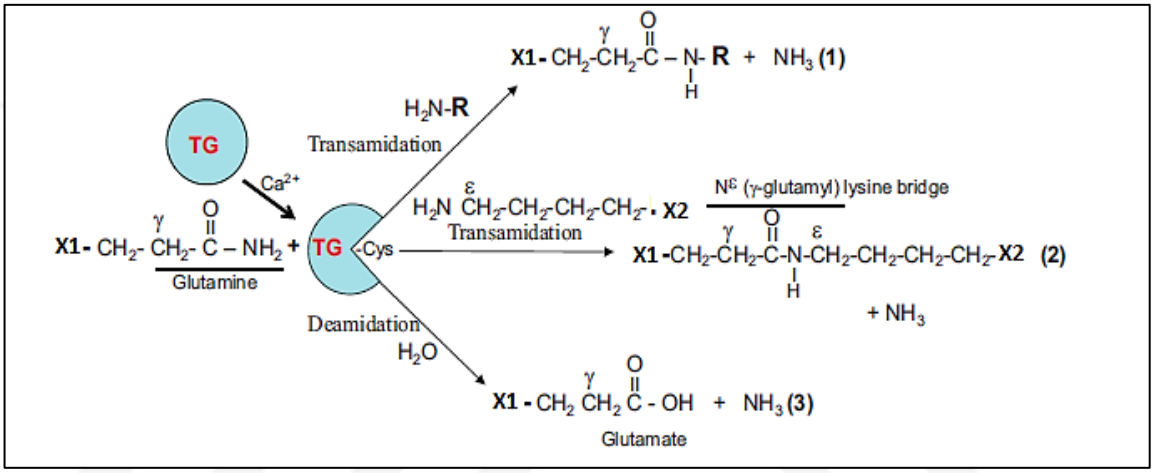

Figure 1.5. Transglutaminase catalyzes transamidation and deamidation reactions. Constructing a covalent bond between primary amines and a glutamine residue of the X1 protein (an acceptor protein) by crosslinking reaction due to transamidation activity of TGs requires the availability of calcium ions. The transamidation reactions mentioned above results in ε-(γ-glutamyl) lysine isopeptide bond **(2)** due to the crosslinking reaction occurring either between monoamines/polyamines and proteins **(1)** or protein-protein residues. As it can be seen in **(3)**, X1 protein may undergo a deamination reaction in an acidic environment and in the presence of water molecules used by TGs to catalyze deamination reactions. Adapted from Eckert *et.al.*,2014 [58].

Nine different transglutaminase members have been discovered until now. Eight of the members have a catalytically active site and one known as Erythrocyte membrane protein band 4.2 (band 4.2) is a catalytically inactive member. Furthermore, except for band 4.2, all TGs proteins have a catalytical site in which they share an equivalent amino acid sequence [58]. A substitution between a cysteine group to alanine within the active site of band 4.2

protein results in the inactivated catalytic domain. Yet, erythrocyte membrane band 4.2 has been observed to share over 30 percent similarity with other TG family members [60]. The family member proteins participate in a wide range of cellular functions to sustain membrane integrity, modulate signal transductions, attend as scaffolds, and regulate cell adhesion [58,61]. Besides, TGs participate in cancer development, cell survival, and differentiation. In addition to these functions of TGs, the integration of amines into proteins by TG-catalyzed manner, may alter immunogenicity, function, and stability of substrate proteins and lead to autoimmune diseases such as celiac disease [62]. Although transglutaminases attain many cellular functions, the unique structure and multifunctionality, and ubiquitous expression of transglutaminase 2 (TG2) draw attention among the other family members and make TG2 the most-studied member of the family [63].

1.7. TRANSGLUTAMINASE 2 (TG2)

The multifunctional protein TG2 is a 76 kDa protein located on chromosome 20q11-12 in the human genome [58]. TG2 can be translocated to different locations in the cell via chemical stimuli coming from cellular stressors (e.g. depletion of Ca^{+2} ions reservoir of intracellular stock or triggering extracellular Ca^{+2} ions influx, reactive oxygen species, nucleotides, membrane protein-protein, and membrane lipids interactions) [9]. Although TG2 is most commonly thought of as a cytosolic protein, it may be found in nearly every cellular compartment, including the nucleus, plasma membrane, recycling endosomes, and mitochondria [10].

Modulating TG2 expression is predominantly accomplished at the transcriptional level [66]. The promoter of human TG2 (hTG2) possesses four Sp1 binding sites which are generally found in human promoters and involved in responses to a wide range of activators (Figure 1.6.) [66–69]. Retinoids are the most well-known activators of TG2 [70]. Moreover, other response elements for stress-induced transcription factors are transforming growth factor β1 (TGF-β1), nuclear factor kappa B (NF-κB), and hypoxia-inducible factor (HIF) are found on the TG2 promoter [68,71,72] (Figure 1.6.). In addition to these stressors, there are also other well-known response elements for inflammatory stress-induced transcriptional factors placed on the TG2 promoter named as tumor necrosis factor α (TNF-α) and inflammatory

cytokines, for instance, interleukin 6 (IL-6), interleukin 1 β (IL-1β) [73–76]. Apart from the induction of TG2 expression level, the TG2 promoter also regulates the silencing of the TG2 expression. Several studies have been shown that in less aggressive cancer cell types such as breast cancer, non-small lung cancer, and glioma, the TG2 promoter is hypermethylated due to epigenetic modifications. Histone deacetylase (HDACs) is another epigenetic modification that causes to down-regulate TG2 promoter activity. However, overall, TG2 may be categorized as a stress response protein induced correlatedly to the received stimuli from the cellular protective feedback loop [67,77–79]. TG2 is abundantly expressed in fibroblasts, endothelial cells, vascular cells, macrophages/monocytes, and leukocytes [58,65,80,81]. Although the expression level of TG2 depends on external stimuli, and maturation or differentiation in some types of cells whereas in cell lines such as endothelium and smooth muscle cells, TG2 activation is kept constitutive at a high level [82].

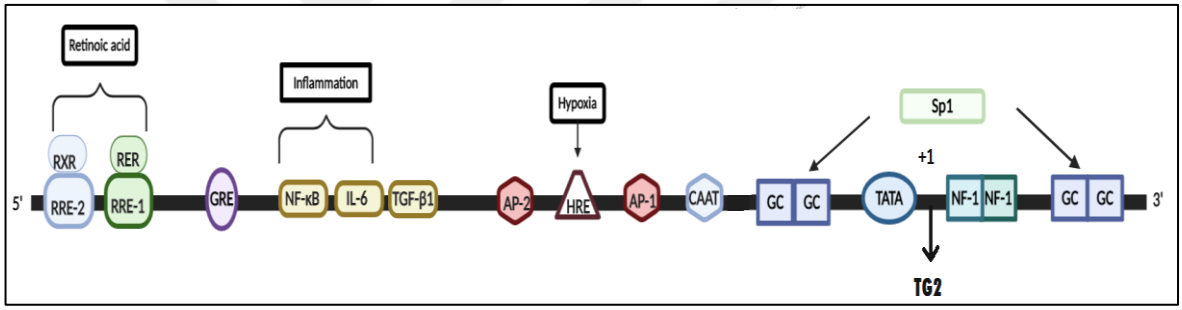

Figure 1.6. Representation of human TG2 (hTG2) response elements participating in the TG2 expression. The figure shows response elements on the hTG2 promoter. In the 5'flanking region of hTG2 Retinoic acid response elements (RRE-1 and 2) are located at -1731 and -1720 bp respectively. Glucocorticoid response element is at -1399 bp and after that inflammation and hypoxia response elements called nuclear factor-κB (NF-κB), interleukin-6 (IL-6), hypoxia response element (HRE) is presented. Besides, transforming growth factor-β1 (TGF-β1) is placed at -868bp. Finally, the GC-rich region responsible for the encoding of two Sp 1 transcriptional factors is located between CAAT and TATA box at the 3' flanking region. Adapted from Gundemir *et.al*., 2012 [67].

TG2 protein structure is comprised of four domains which are the N-terminal β-sandwich domain, catalytic domain, and two C-terminal β-barrel 1 and β-barrel 2 domains respectively (Figure1.7).

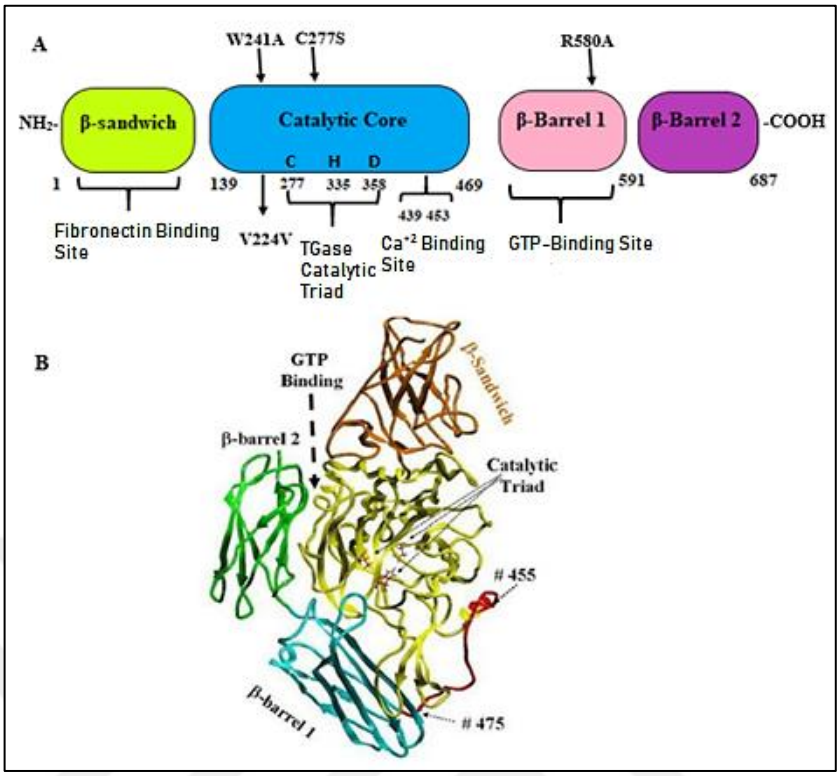

Figure 1.7. Schematic representation of TG2 protein's functional and structural domains. A) TG2 is composed of four different functional domains which are β-sandwich (green), catalytic core (blue), first and second β-barrels (pink and purple). B) 3D crystal structure of TG2 in which GTP-binding (left) and catalytic triad domain related to transamidation activity are shown. Adapted from Lai *et al*. [83].

The intracellular Ca^{+2} concentration is an important element that results in the change of TG2 conformation and consequently its cellular function. When the intracellular Ca^{+2} concentration decreases to 10-20nM, intracellular TG2 acts as Ca^{+2}-independent GTPase by transforming its structure to the closed conformation. As a constituent of α_1-adrenergic receptor complexes, the GTP-binding form of TG2 contributes to the transmembrane signaling of phospholipase Cδ [84,85]. On the other hand, when the intracellular Ca^{+2} rises over 700-800nM and a particular stimulus is received by cells, transamidase activity of TG2 is activated upon the alteration in TG2 structure. This structural change converts TG2 to the open conformation by which it gains crosslinking activity [84,86]. TG2-regulated crosslinking of ECM proteins occurs in specific circumstances, for example, tissue remodeling and regeneration. In some cases, increase in the extracellular Ca^{+2} concentration,

instead of transamidation activity, TG2 may regulate outside-in signaling by transmembrane receptors and cell-ECM interactions [87].

The catalytic trio of cysteine proteases is found in the catalytic domain of TG2. The catalytic triad responsible for TG2's transamidation activity is made up of cysteine 277 (C277), histidine 335 (H335), and aspartate 358 (D358) residues [67,88]. In addition to the catalytic triad, at the opposite side of the catalytic domain, two conserved tryptophan residues W332 and 241 are found. Switching W241 to an alanine W241A via a mutation causes to knocking out of transamidation activity of the TG2 protein without affecting its GTP/GDP binding activity [67,89–91]. The binding of Ca^{+2} or GTP/GDP affects the activation of TG2 and, also transamidation activity of TG2 inversely depends on GDP/GTP dissociation and Ca^{+2} ions binding. TG2 is only catalytically active when found in the ‘’open’’ form and bound to Ca^{+2}, whereas it switches into inactive ‘’closed’’ conformation when bound to GTP/GDP [67,86,92]. GTP works as an allosteric inhibitor for TG2 and leads to shifting of the domains through the binding on the surface of both domain 1 and 2 placed on the amino-terminal side and on the β-Barrel 1 domain where it interacts with R580A to hold TG2 protein in the closed structure [1,18,21–26]. The signal transduction ability of TG2 gains functions when the protein halts into this closed conformation and as a consequence that TG2 works as a member of the G-protein family [95].

More particularly, it is important to elucidate how transamidase active, GTP-bound, and/or both forms of TG2 may induce tumor progression and cancer survival in different tumor types (Figure 1.8). To determine roles of GTP-binding and transamidation of TG2 on cancer cell characteristics, cells of epidermal squamous, lung [96], colon [97], ovarian [98], and breast [99,100] cancers were transduced with TGase activity or GTP-binding deficient mutants of TG2. All these studies cumulatively showed GTP-bound conformation of TG2 promotes the downstream signaling pathways for survival to induce tumor cell development. On the other hand, other studies reported that transamidation TG2 leads to inactivation of main tumor suppressor proteins or alteration of ECM [101].

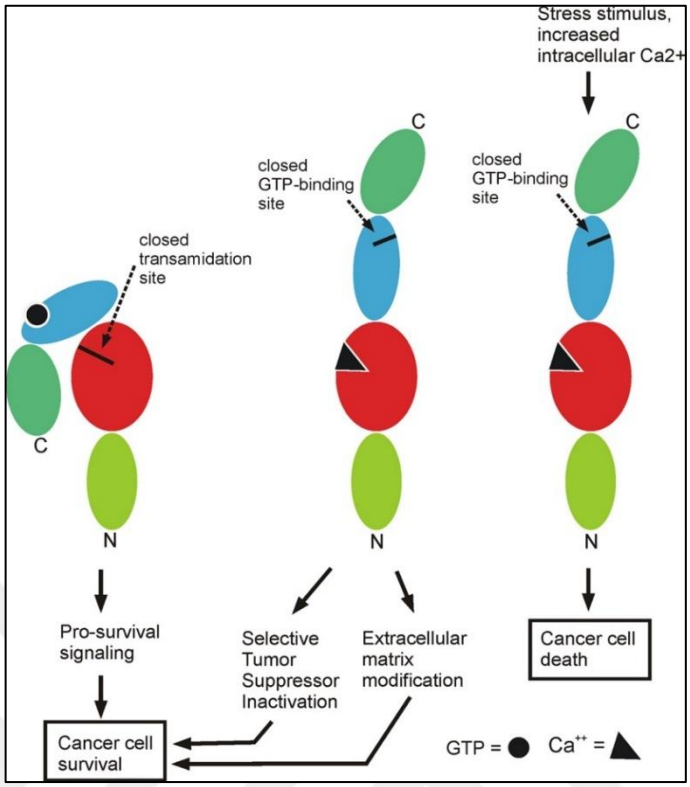

Figure 1.8. The effect of GTP-binding and transamidating active forms of TG2 on cancer cell death and survival. The transamidating active form of TG2 can lead to cell death under the influence of increased intracellular Ca^{+2} or stimulus received after stress conditions. The GTP-binding active type of TG2 promotes tumor cell survival by inactivation of tumor suppressors or alteration of ECM [101].

TG2 is an isoenzyme that attends both enzymatic and non-enzymatic cellular activities. Among the transglutaminase family members, ubiquitously expressed TG2, is the most studied member of the family because of its multifunctionality. Several studies have been shown that besides intracellular expression of TG2, it is also defined to be expressed on the cell surface and extracellular matrix (ECM) to modulate outside-in signaling cascades by transmembrane receptors such as platelet-derived growth factor receptors (PDGF-R) and vascular endothelial growth factor (VEGF). Moreover, TG2 provides cell-extracellular matrix (ECM) communication by acting as an adhesion molecule through its interactions with integrin beta 1 (ITGβ1), fibronectin (FN), and syndecan-4 (SDC-4) [102–105]. In addition to non-enzymatic functions, TG2 also participates in the regulation of transamidation reactions of proteins where either a cross-linkage via the formation of an

isopeptide bond between lysine and glutamine moieties or post-translational modifications of these proteins occur. TG2 activity is also implicated in several pathological conditions such as celiac disease, cancer, infectious diseases, and neurodegenerative diseases such as Huntington's disease and Alzheimer and all these conditions are gathered on the common ground based on their inflammatory characteristics.

1.7.1. The interplay between Cancer and TG2

Hanahan and Weinberg defined ten hallmarks of cancer in their review, ‘’*The Hallmarks of Cancer: The Next Generation*’’ in 2011. According to the review published by Hanahan *et.al*., cancer is described as a disease that can evade growth suppressors, resisting cell death, activate invasion and metastasis, increase tumor-promoting inflammation, and sustain proliferative signaling [106]. In addition to the aforementioned capabilities of cancer, elevated expression TG2 has been consistently demonstrated as being a hallmark of many cancer cell types such as breast carcinoma [107], malignant melanomas [108], ovarian carcinoma [109,110], pancreatic carcinoma [111], glioblastoma [112], and lung carcinoma [78] by many studies [60]. Since increased chronic inflammation is one of the factors playing important role in tumor initiation and progression, the interplay between increased TGs activation, especially TG2 expression, in response to secreted inflammatory cytokines can clarify the vital role of TG2 in many cancer cells. The evidential studies have been shown that TG2 expression is not just being induced by inflammatory cytokines such as IL-6, IL-1, TGF-β, and TNF-α, but also inflammatory signaling circuit may be reprogrammed in epithelial tumor cells due to increased TG2 activation. Furthermore, the reprogrammed inflammatory signaling cascade may result in gaining the ability to develop drug resistance and to metastasize in epithelial cancer cells. However, the molecular mechanism that identifies TGs’ role in cancer progression remains controversial. For instance, while TG2 expression levels are inclined in metastatic and drug-resistant tumor cells, the expression level is declined in primary tumors [78,110,111,113,114].

Several studies also show that increased cancer cell survival, invasion, and tumor progression are predominantly associated with the extracellular TG2 [58,115]. Upon the release of inflammatory cytokines, TG2 expression is increased. Ultimately, synthesis and

deposition of collagen and fibronectin are accelerated whereas extracellular TG2 contributes stabilization of ECM by crosslinking both fibronectin and collagen. That TG2-modulated ECM crosslinking may result in a desmoplastic reaction similar to desmoplastic response and fibrosis of tumors which consists of an interaction between altered ECM and the invading tumors [116]. Therefore, TG2-regulated crosslinking is attributed to have an impact on the behavior of tumor cells as this process results in alterations of stiffness of the ECM and consequently induces a malignant tumor characteristic. For instance, ECM stiffening enhanced focal adhesion genesis, and collagen crosslinking are required by breast cancer cells [117].

1.7.2. The Interplay of TG2 in Metastasis, Drug Resistance, and Epithelial to Mesenchymal Transition (EMT)

Advanced cancers are considered to be compelling because of their ability to develop resistance against the applied therapy and to metastasize which are also hallmarks of advanced cancer. These hallmarks of advanced cancer also serve as biomarkers in order to define new therapeutic approaches to cancer therapy. For instance, one of the paramount pathways in close relation with advanced cancers is an epithelial-to-mesenchymal transition (EMT). EMT is a pathway that starts in embryogenesis and can be reactivated upon epigenetic alteration signals in adult tissues [58,118]. Moreover, processes such as wound healing, regeneration of the damaged tissue, and fibrosis in organs occur due to EMT. Tumor cells benefit from this dynamic switch to gain stem-cell characteristics [58,119–121]. During this transition, epithelial carcinomas acquire mesenchymal markers' expressions such as vimentin, desmin, and fibronectin while losing epithelial genes expressions e.g., E-cadherin which is an epithelial tight junction protein. The tumor cells have undergone EMT lead to the constitution of micrometastases, intravasation, and extravasation. Inducing of EMT in tumor cells can occur due to several molecular signaling pathways such as NF_KB, FAK, and AKT (Figure 1.10.). Indeed, TG2 is known to be responsible for the activation of these signaling pathways which elicit EMT. Furthermore, normal epithelial and fibroblast cells demonstrate EMT characteristics, for instance, increased survival rate and anchorage-independent cell growth due to microvesicles released by TG2-overexpressing cells. Moreover, a vast range of studies demonstrates that when TG2-expression is inhibited,

resistance to tumor treatments and the drug, and invasiveness of cancer are suppressed or vice versa [58,78,109,112,122,123].

1.7.3. The Role of TG2 in the Regulation of Cell Growth Pathways

Evading the cell suppressors and sustaining proliferative signaling which are the major hallmarks of cancer provide tumor cells gain limitless proliferation and switched from a quiescent state to dynamic proliferation in the existence of mitogenic growth signals [124]. The extracellular matrix (ECM) molecules, growth factors, and cell-to-cell interactions are regulators of mitogenic signaling [125].

Several studies demonstrate that cell proliferation and cell survival can be induced due to functional interaction of TG2 with transforming growth factor-beta (TGF-β) which is a multifunctional cytokine that participated in a variety of activities subsuming immune function, proliferation, and differentiation. It has been shown that TGF-β modulates TG2 expression through tumor suppressor gene, SMADs, and TGF-β-activated kinase 1 resulting in the activation of NF-$_{K}$B, increased cell proliferation which leads to metastasis and spheroid formation [126]. Besides the TGF-β pathway, there are other signaling pathways interacting with TG2 to enhance tumor proliferation. For instance, the study published by Fu *et al*. implicated that knock-down of TG2 diminish the growth of glioma stem cells by reducing a protein expression called DNA binding 1 (ID1) [127]. In contrast, overexpression of ID1 results in the rebuilding of proliferation by pointing ID1 as a downstream mediator of TG2 through PI3K/AKT pathway's activation. Furthermore, aggregation of β-catenin which is normally promoted by activation of the Wnt pathway has also been correlated with TG2. The activation of the Wnt pathway resulting in the accumulation of β-catenin leads to translocation of β-catenin to nucleus and stimulation of c-Myc and cyclinD-1 expressions by which proliferation of ovarian tumor cells are retained [125]. In addition, through the extracellular signal-regulated protein kinases 1 and 2 (ERK1/2) pathway, TG2 has been defined to induce gastric cancer cell growth [128].

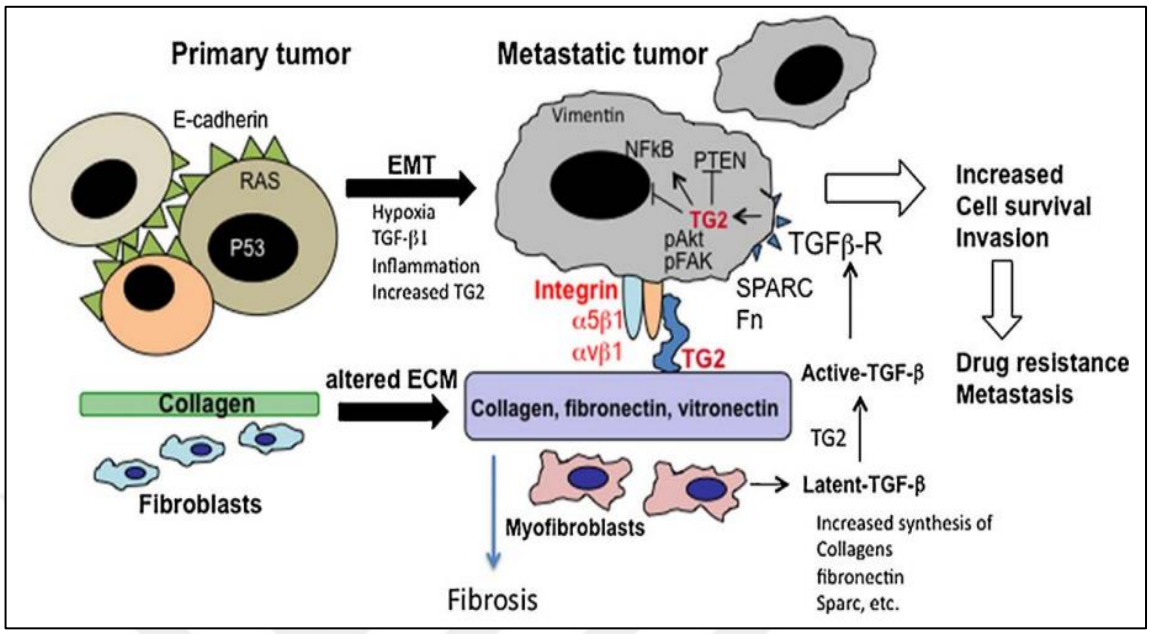

Figure 1.9. The transition of primary tumors to invasive carcinoma occurs in the TG2-overexpressed tumor microenvironment. Expression of TG2 activates oncogenic signaling such as NF-$_K$B, FAK, Akt, and PTEN and promotes the Epithelial-to-Mesenchymal Transition (EMT). Extracellular TG2-induced crosslinking and synthesis of ECM proteins lead to stiffness of ECM which results in enhanced PI3K activation, invasion of epithelial cells, and focal adhesion [129].

1.7.4. The Role of TG2 in Resisting to Cell Death

Resisting from cell death is one of the abilities that tumor cells gain to evade any cell death mechanism forced to go through due to applied chemotherapies [130,131]. A caspase-dependent and programmed cell death mechanism, apoptosis, occur in tumor cells in order to get rid of mutated and damaged cells [131]. However, cancer cells can evade this fate, and neoplasia of cancer cells arises. From this point of view, these characteristics of cancer cells lead to challenging treatments, recurrence of the disease, and resistance to therapies [131]. To overcome therapeutic challenges for cancer treatment, several studies have shown that TG2 has a role in the apoptotic process and determines the fate of cancer cells based on the structural conformation and cellular context. Based on these studies, overexpression of TG2 has a connection with apoptotic processes and can involve in the process as pro- or anti-

apoptotic protein. For instance, utilizing A23187 which is a calcium ionophore as a TG2-inducer leads to a dramatic increase in apoptosis of cancer cells [132,133]. Crosslinking of transcription factor Sp1 by TG2 triggers apoptosis in cancer cells [134]. In contrast to the pro-apoptotic function of TG2, several studies have highlighted that TG2 can involve in the inhibition of apoptosis as being an anti-apoptotic protein through modifications of Bax and caspase-3 expressions [72,135–137]. The function of TG2 in the removal of apoptotic cells via phagocytosis and in cross-linking while necrosis implies that TG2 limits possible damaging inflammation and tissue injury occurred in response to cell death [138–140].

The extrinsic pathway of apoptosis is triggered when tumor necrosis factor-related apoptosis-inducing ligand (TRAIL) binds to death receptors such as death receptor 4 (DR4)/TRAIL-R1 and DR5/TRAIL-R2 which results in the eradication of cancer cells [141]. Furthermore, Li *et al.* demonstrated that TG2 is one of the most significantly elevated genes after the generation of procured TRAIL resistance in lung carcinoma. However, sensitization and induction of apoptosis reoccur when TRAIL resistance is inhibited [141]**.** Epidermal growth factor receptor (EGFR) which participates in the induction of c-JUN N-terminal kinase (JNK) and extracellular signal-regulated (ERK) results in elevated levels of TG2 expression, TRAIL resistance, and diminishing of matrix metalloproteinase 9 (MMP-9) associated with migration and invasion of cancer cells. Thus, in TRAIL-resistant cancer cells, EGF is represented as a critical upstream signaling route of TG2 [142].

1.7.5. The Role of TG2 in Chemoresistance

The most challenging part of cancer therapies is the drug resistance that tumor cells develop. Therefore, understanding the underlying causes of drug resistance is an indispensable action to take during anti-cancer treatments [142]. Indeed, through several mechanisms, aberrant expression of TG2 has been indicated to be related to induced chemoresistance. A vast range of neoplasms has been notified to acquire TG2-regulated chemoresistance by many studies, for instance, Mehta *et al.* demonstrated that doxorubicin-resistant breast cancer cells overexpress TG2 [143]. Moreover, sustained TG2 expression conduces the activation of numerous signaling pathways which lead cancer cells to gain drug resistance ability. Drug resistance in cancer cells can occur by either blocking extrinsic or intrinsic pathways of

apoptosis. While TRAIL resistance provides extrinsic resistance to apoptosis, cisplatin, and doxorubicin-resistant cancers have been reported to result in the activation of signaling pathways leading to intrinsic resistance to apoptosis [144]. Recently, the latest studies implicate that TG2-mediated chemoresistance is also defined in newer treatment methods such as mTORC1 [145,146] and histone deacetylase [147] targeted inhibitors indicating that TG2 participates in a wide range of drug-resistance mechanisms [142].

1.8. TG2 IN RENAL CELL CARCINOMA

Increased activation of TG2 is observed in many tumor cells as well as RCC [148,149]. Decreased cancer-free survival rate and increased metastasis rate are attributed to RCC tumors upon TG2 overexpression. According to data published by Hidaka *et al.*, miR-1285 controls TG2 in RCC, and the expression of miR-1285 is inversely proportional to that of TG2. In addition, the same study also showed that miR-1285 expression diminishes TG2 expression and resulting in decreased cell proliferation [148]. In RCC types such as Caki-1, A-498, ACHN, and 768-O , knockdown of TG2 causes enhanced p53 expression levels and induced apoptosis [149,150]. The process that leads to p53 degradation and enhanced cell survival depends on the TG2 crosslinking of p53. This implies that through decreasing p53 levels, TG2 aids RCC development. Furthermore, in xenograft models, TG2 inhibitor GK921 inhibits the development of ACHN and CAKI-1 RCC tumors [149–151].

In RCC cells, glycolysis is increased and high TG2 levels boost glucose intake and lactate generation while lowering mitochondrial aconitase levels[101,149]. TG2 knockdown reverses these effects [152]. The ubiquitination pathway also affects TG2 function, as CHIP (carboxyl-terminus of hsp70-interacting protein) an E3 ubiquitin ligase reduces TG2 levels, and CHIP knockdown is linked to increased TG2 levels and aggressive neoplasms of RCC [153]. Eckert *et al.* implied that this might be a sole response in RCC cells [101].

TG2 is also involved in cell adherence and stemness in RCC cells. Actin stress fiber production and adherence to fibronectin, collagen type I, and laminin are decreased in RCC cells when TG2 is silenced, resulting in not only decreased migration and invasion but also reduced cancer stem cell marker expression [154]. According to these findings, TG2 might be a potential cancer treatment target in RCC [155].

1.9. AIM

Tissue transglutaminase 2 (TG2) is a member of the transglutaminase enzyme family that is widely expressed. TG2's importance stems from its multifunctionality, which allows it to participate in a variety of biological processes including crosslinking, cell adhesion, differentiation, cell proliferation, scaffolding, and apoptosis. Furthermore, abnormal TG2 expression has been linked to poor cancer-specific survival, increased metastatic capacity and progression, cancer stemness, EMT, poor prognosis, and increased treatment resistance in RCC, which is the most common kind of kidney cancer. Our previous findings published by Ulukan *et al.* showed that GTP-binding active but transamidase inactive mutant TG2-W241A acts as a proto-oncogene in RCC by promoting NF-$_{K}$B mediated EMT activation. While GTP-binding deficient and transamidase active TG2-R580A and low-GTP-binding affinity mutants TG2-C277S did not participate in EMT promotion. As NF-$_{K}$B signaling might be important in cell proliferation and regulation of the cell cycle, this thesis firstly aims to further elucidate the role of TG2-variants in these processes. TG2-variants which are transamidase active type TG2-R580A, transamidase-deficient, and low GTP-binding active form TG2-C277S and GTP-binding-active TG2-W241A were expressed in RenCa cells for this purpose. As initial evidence by Ulukan *et al.* also suggested that TG2-W241A could be important for the response of RenCa cells to 1, 5 and 10 μM of Everolimus treatment, the second aim of this thesis was to investigate the importance of TG2 variants on the viability of RenCa cells in the presence of 0.25, 0.5, 0.75 and 1 μM of everolimus, lower doses that cause everolimus resistance in long term [155]. Annexin V cell death assay was employed to analyze cell death response to 1 μM of Everolimus treatment in RenCa cells transduced with the TG2 variants.

2. MATERIALS

2.1. INSTRUMENTS

Centrifuge (Sigma, 3-18K, UK), -80°C freezer (Thermo Forma - 86 C ULT Freezer, USA), pH meter (Hanna instruments PH211, Germany), SprectraMax Paradigm Spectrometry Multi-Mode Plate Reader, CO_2 incubator (In-Vitro Cell ES NU-5800, NuAire, USA), Laminar flow cabinet (ESCO Labculture Class II Biohazard Safety Cabinet 2A, Singapore), Centrifuge (Sigma, 3-18K, UK), ThermoShaker (Inovia Tech, Turkey), Gyrorocker (Stuart,SSL3, UK), Vortex (Velp Scientfica, Italy), Waterbath (Stuart, SBS40, UK), Ultra low temperature Freezer (Witeg, Germany), pH meter (Milwaukee, Mi151, Germany), Guava easyCyte Flow Cytometer, Carl Zeiss PrimoVert Microscopy Axiocam 105 color (GmbH37081, Germany), Centrifuge (Hettich Micro 22R, UK), Centrifuge (Sigme 3-16K, England), Centrifuge (Gyrozen 416, Korea), Hot plate with magnetic Strirrer (Heidolp MR 3003 control, Germany), Weighing Scale (Shimaozu, Tw423L,Japan), Min, Trans-blot cell blotting system (Bio-rad 170-3935, USA), Mini-Protean tetra cell electrophoresis system (Bio-Rad 165-8001, USA), StepOnePlus Real-Time PCR System (Applied Biosystems, 4376600, the USA), Mp Minipure DestUp Distilled Water (SentezLab, Turkey), 96-well Thermal Cycler (ThermoFischer, the USA), Microcentrifuge (Beckman Coulter, A46473,Germany), Rotator (BioSan, RS-24, Latvia)

2.2. EQUIPMENT

Easypet Electronic pipette (Eppendorf, Germany), Conical centrifuge tubes (15 ml and 50 ml, Thermo Fischer, the USA), Safe-lock Eppendorf tubes (2ml and 1.5 ml, Germany), Micropipettes (10µL, 20µL, 100µL, 200µL, 1000µL, Thermo Scientific, USA), Serological pipettes (2 ml, 5 ml, 10ml and 25ml, SPL Life Sciences, USA), Cell culture flasks (T-25 and T-75) (TPP, Switzerland), 0.45 µm Minisart Syringe Filter, 0.22 µm Minisart Syringe Filter, TC-treated multiple-well plate for cell culture (6,12, 24 and 96-well plates) (Corning Costar, the USA), Cryovials (Isolab, Germany), Graduated cylinder (50, 250 and 100 ml, Isolab, Germany), Amersham Full-Range Rainbow Protein Marker (RPN800E, Merck,

Germany), PVDF and Nitrocellulose membrane 0.22 and 0.45µm (Thermo Fischer, the USA).

2.3. KITS

Ultrapure Midi Plasmid Isolation Kit (Invitrogen), ZymoPure Plasmid Mini-Prep (Zymo Research), WestenBright Sirius Detection Kit (Advansta, K-12043D10, the USA), Sensiscript RT Kit (Qiagen, 205213, the USA), PowerUp SYBR Green Master Mix (Thermo Fischer, the USA), RIPA Lysis Buffer (Santa Cruz, sc-24948, the USA)

2.4. CHEMICALS

RPMI-1640 Medium (Gibco, BE12-702F, UK), Dulbecco's Modified Eagle's Medium (DMEM) high glucose (Gibco 41966, UK), Heat-inactivated Fetal Bovine Serum (FBS) tested (Gibco, A3840401, UK), Antibiotic-Antimycotic (Gibco, the USA), Aphidicolin (Merck, 178273, Germany), 2-Propanol (AppliChem A3928, Germany), Absolute Ethanol (AppliChem A3928, Germany), Dulbecco's Phosphate Buffered Saline (DPBS) (LONZA, Z17-512F, USA), LB Agar, LB Broth (Sigma, USA), Polybrene (Merck, TR-1003G, Germany), 4-(2-hydroxyethyl)-1-piperazineethanesulfonic acid (HEPES) (Multicell 600-032-EG, Canada), Albumin Fraction V (Bioshop, ALB001, Canada).

2.5. PRIMER ASSAYS

Hs_TGM2_3_SG QuantiTect Primer Assay (202689401, the USA), Mm_Rn18s_3_SG QuantiTect Primer Assay (QT02448075, the USA)

2.6. CELL LINES

Human embryonic kidney cell line (HEK293FT, ThermoFisher R70007), Mouse renal adenocarcinoma cell line (RenCa, ATCC CRL-2947).

3. METHODS

3.1. METHODS IN CELL CULTURE

3.1.1. Cell Lines and Conditions for Culturing

Renal cell carcinoma cell line, RenCa, and human embryonic kidney cell line HEK-293 ft were obtained from American Type Cell Culture Collection (ATCC) and Thermo Fischer Scientific (Invitrogen) respectively. HEK-293 ft cell line and RenCa cell line were cultured in Dulbecco's modified medium (DMEM) and RPMI-1640 medium containing 10 percent (v/v) Fetal Bovine Serum (FBS) and one percent (v/v) Antibiotic-Antimycotic solution (PSA) composed of 10,000 units/ml of penicillin, 10,000 µg/ml of streptomycin and 25 µg/ml of Gibco Amphotericin B in respective order. The cell lines were incubated in the incubator with 37^{o}C temperature, 5 percent CO_2, and 80-95 percent humidified air conditions.

3.1.2. Cell Subculturing

Subculturing of the cells was applied when cells reached 70-80 percent confluency. For subculturing of the cells, the cell monolayer was washed using 1X Dulbecco's Phosphate-Buffered Saline (DPBS) with a pH of 7.4. After that, the cells were subjected to 0.05 percent (w/v) trypsin followed by incubation at 37^{o}C for 5 minutes. In order to eliminate trypsin activity, growth media containing 10 percent (v/v) FBS was added, and dislodged cells were collected. The cell suspension was centrifuged at 300x*g* for 5 minutes. The pellet was resuspended in growth media and placed into an appropriate cell culture flask.

3.1.3. Calculation of Cell Number

10 µl of the cell suspension remained after the subculturing process described above (Section 3.1.2.) was loaded into the middle square of the hemocytometer where a coverslip is placed. The number of cells was counted under the inverted light microscope at 10x objective. Cell

concentration (total cell number per milliliter) of the suspension was calculated based on the equation below.

Counted cell number x dilution factor x depth of hemocytometer = Cell number /ml

3.1.4. Cryopreservation of Cell Lines

Following the cell counting process described above (Section 3.1.3.), the excessive cell suspension was centrifuged once again, and the pellet was resuspended with a freezing mix containing 10 percent (v/v) of Dimethyl sulfoxide (DMSO) and 90 percent (v/v) FBS as to have cell suspension with a density of $1x10^6$ cells/ml per one cryovial. For long-term storage, cells were placed into cryovial and transferred to a -80°C refrigerator immediately. The cryovials can be transferred to a liquid nitrogen container in the following day to preserve cells for years.

3.1.5. Cell Thawing

From the liquid nitrogen container, formerly freezed stock cells were taken and rapidly heated to 37°C in the palm. The cell suspension was then gathered into a new sterile falcon tube and 5 ml of prewarmed culture media was added dropwise onto the cell with a steady mixing in order not to disrupt the cells due to an abrupt inclination in the osmatic pressure. Afterward, the cell suspension was centrifuged at 300*xg* for 5 minutes to discard DMSO that was present in the freezing mix solution. Pellet was resuspended in growth media and plated into a T-25 tissue culture flask. The very next day, the medium was changed to remove any residual of DMSO, which is known to be a toxic substance for the cells. Cells were passaged at least once before the experiment begins.

3.2. ISOLATION OF MUTANT TG2 CONSTRUCTS CONTAINING PLASMID DNA

Sub-cloning of the wt-TG2 gene was applied by using Plenti CMV BLAST DEST (706-1) vector and other TG2 variants which TG2-R580A, TG2-C277S, and TG2-W241A were produced after side directed mutagenesis as mentioned in Ulukan *et al.* 2020 [156].

3.2.1. Plasmid DNA Isolation

Previously sub-cloned TG-2 constructs, C-pLenti, wt-TG2 (V-pLenti), W-pLenti, and R-pLenti were inoculated in 100 ml of LB broth containing 0.1ug/ml ampicillin and left for overnight incubation in a 37^{o}C incubator which is continuously shaken at 180 rpm. 16-18 h later, OD values of the inoculated samples were measured. After OD values were measured within 2.0-4.0, the isolation of plasmids was performed as described previously in the study published by Ulukan *et al*.,2020 [156]. Inoculums were transferred to the 50 ml centrifuge tubes and centrifuged at 4000*xg* for 10 minutes to harvest the cells and the obtained bacterial pellet was used for plasmid isolation. 4 ml of resuspension buffer containing RNase A was added, and gently mixed with the obtained pellet until the solution became homogenous. 4 ml of lysis buffer was added onto the mixture and immediately inverted bottom to cap 5 times. After that 4 ml of precipitation buffer was mixed into the suspension and centrifuged at 12000*xg* for 15 minutes at room temperature. Meanwhile, equilibration columns were washed with 10 ml of equilibration buffer. After the centrifugation step, obtained supernatant was loaded into the equilibrated column, and drained by gravity flow. 10 ml of wash buffer was then added to the columns. A new collection tube was placed under the columns and 5 ml of elution buffer was added into columns. The obtained solution was suspended with 3.5 ml of isopropanol and followed by a centrifugation process at 12000*xg* for 30 minutes at 4°C. Afterward, the supernatant was discarded and 3ml of 70 percent ethanol was used to wash pellets. The previously mentioned centrifugation step was repeated for 5 minutes. Pellet was then left to dry and suspended in 50 µ of TE buffer. As a final step of the plasmid isolation, the concentration of the isolated plasmid DNA was quantified via nanodrop, and plasmid DNA was stored at -20°C for later use.

3.3. CONSTRUCTION OF TG2 MUTANTS EXPRESSING RENCA CELL LINE

3.3.1. Transfection of HEK293-FT Cells with Isolated DNA of Interest

In order to produce lentiviral particles carrying the genes of interest, HEK293FT cells were cultured into 100mm cell culture petri-dish at a density of $1x10^6$ cells/dish and left for overnight incubation. The following day, the media was renewed with the fresh preheated media replaced approximately two h before the transfection. 22.4 µg of the gene of interest, and 7.46 µg of both packaging plasmid (pPAX2) and enveloped plasmid (PMD2G) were mixed in a 50 ml falcon tube. After that, other reagents were included in the following order: 0.1X TE, 2.5 mM CaCl2 were gently mixed into the same 50 ml falcon tube, and then, 2X HBS solution with pH of 7.12 was placed into the solution drop by drop while air-agitating the mixture via 2 mL serological pipette. The mixture was then incubated for 12 minutes at room temperature and then placed dropwise on mixed by gently rotating the plate. 13 h later, previous media was removed, cells were washed with 1X PBS and 10 ml of fresh pre-heated media was placed. Following 24h later, media was collected into the falcon tube and kept at 4°C. Then, 10 ml of fresh pre-heated media was added to the petri dish. 48 h later, the media was recollected and mixed with the previously collected media. After 48 h later, collected supernatants were filtered and aliquoted, and stored at -80°C.

3.3.2. Transduction of RenCa Cells with Produced Lentiviral Particles

RenCa cells were cultured at a density of 20.000 cells/well of a 12-well plate. Following overnight incubation, the cells were incubated with 8 µg/ml polybrene in 2 percent (v/v) FBS containing complete RPMI medium for 12 h. Following polybrene incubation, the cells were gently washed with 1xDPBS twice and incubated with previously produced lentiviral particles. Following 24 h of transduction, a fresh culture medium including 10 percent (v/v) FBS, 100 units/ml penicillin, and 100 µg/ml streptomycin was provided to the transduced cells until they reached certain confluency. Afterward, 6 µg/ml blasticidin containing fresh medium was given to cells for the selection process.

3.4. IDENTIFICATION OF HUMAN TG2 GENE LEVEL IN TRANSDUCED RENCA CELL LINES

3.4.1. Total RNA Isolation

RenCa cell lines containing mutant TG2 constructs (TG2-R580A and TG2-C277S) were cultured as 300.000 cells are in each well of a 6-well plate and grown overnight in a humidified incubator at 37ºC with 5 percent (v/v) CO_2. The next day, cells were washed twice with 1xPBS. The cells were dislodged with 250 µl of Trizol Reagent and collected into 1.5 ml Eppendorf tubes. Samples were then left for incubation at room temperature for 5 minutes. 50 µl of chloroform was mixed with the suspension by pipetting vigorously several times until the mixture colour turns into soft pink color. The previous step was followed by 15 minutes of incubation at room temperature. After incubation, samples were centrifuged at 12.000*xg* for 15 minutes at 4ºC. The colorless upper phase was transformed into new sterile 1.5 ml Eppendorf tubes and supplied with an equal volume of isopropanol. Subsequently, the samples were incubated on ice for 10 minutes and centrifuged at 12.000*xg* at 4ºC for 10 minutes. After that 500 µl of 75 percent (v/v), ethanol was added into sample tubes and centrifuged at 7.500*xg* on ice for 10 minutes. Supernatants were then removed, and the pellet was air-dried. The remained pellet was resuspended in 20 µl RNase-free water. Finally, concentrations of total RNA in the previously mentioned cell lines were measured.

3.4.2. cDNA Synthesis

Master mix for cDNA synthesis was performed based on Table 3.2. and 1 µg of RNA template was prepared in 10 µl. That each 10 µl of RNA templates was mixed with 10 µl of 2X reverse transcription master mix in order to convert the reaction mix to 1X.

Table 3.1. Reagents and their volumes for 2X RT master mix preparation.

REAGENTS	**VOLUMES (µl)**
10X RT Buffer	2
25X dNTP Mix (100mM)	0.8
10X RT Random Primers	2
MultiScribe Reverse Transcriptase	1
Nuclease Free Water	4.2
RNA Template (1µg)	10
Total Reaction Volume	**20**

The obtained overall reaction mix of each sample was run in Thermal Cycler according to recommended thermal cycling conditions by manufacturers (Table 3.2.).

Table 3.2. The thermal cycling conditions for cDNA reverse transcription.

Settings	**Step 1**	**Step 2**	**Step 3**	**Step 4**
Temperature (^{o}C)	25	37	85	4
Time (min.)	10	120	5	Infinite

Finally, after the thermal cycling, the concentrations of synthesized cDNA were measured via Nanodrop.

3.4.3. Real Time-PCR (RT-PCR)

The level of expressions of hTGM2 and m18S RNA was quantified via RT-PCR by using Qiagen QuantiTect Primer Assay. The amount of cDNA that will be added into the reaction mix was chosen as 1000 ng. The RT-master mix was prepared by adding 5 µl of SYBR

Green, 1 µl of 10 µM primers, and 2 µl of nuclease-free water. The expression of the gene of interest which is hTG2 was normalized by using a housekeeping gene, mouse 18S rRNA. The results are expressed based on the relative expression level of the hTGM2 gene normalized by mouse 18S rRNA values (see Figure 4.2.). Real-time PCR stages and cycle conditions were performed as indicated in Table 3.3.

Table 3.3. Real-Time PCR cycling modes applied based on Applied Biosystem's Power-Up SyberGreen master mix.

Step	**Temperature**	**Duration**	**Cycles**
Uracil-DNA glycosylase (UDG) activation	50°C	2 minutes	Hold
Dual-Lock DNA Polymerase	95°C	2 minutes	Hold
Denature	95°C	15 seconds	40
Anneal	50-60°C	15 seconds	
Extend	72°C	1 minute	

3.5. DETECTION OF CELL GROWTH RATE AND DRUG RESISTANCE PROFILES OF TG2-MUTANTS EXPRESSING RENCA CELL LINES

3.5.1. Determination of Proliferation Rates of RenCa Cells

The cell viability assay was performed on non-transduced parental, wt-TG2, TG2-R580A, TG2-C277S, TG2-W241A expressing RenCa cell lines. Prior to experiments, cells were synchronized in serum-free medium at least for 4 h. To detect which enzyme activities of TG2 have a role in increased cell proliferation rates on TG2 active site mutants quantitatively, firstly standard curve plate was prepared by culturing 1, 2.5, 5, 10, 15, and $20x10^3$ cells per well. After overnight incubation of the standard curve plate, the plate was incubated with 1:10 WST-1 reagent diluted in culture medium for 1h. After the completion of the incubation, the absorbance values of the plate were measured at 450/630 nm. For the experiment, cells were seeded at a density of $5x10^3$ cells/well in a 96-well plate. Subsequently, cells were incubated overnight in a humidified atmosphere containing 5percent CO_2 at 37ºC. After the overnight incubation, the cells were incubated for 24, 48, and 72 h in the incubator. After the completion of each incubation time point, 5 µl of WST-1 reagent (Roche Diagnostic, Germany) was mixed with 45 µl of culture medium in order to dilute WST-1 reagent in 1:10 dilution and 50 µl of the prepared WST-1 reagent was placed into each well of the 96-well culture dish and incubated at 37°C for 1h. Following the incubation, the absorbance values were measured at 450/630 nm via SpectraMax Paradigm Multi-Mode Microplate Reader. The number of viable cells was then calculated according to the obtained absorbance values by using the standard curve plate.

3.5.2. Identification of the Effect of TG2 Variants on the Drug Resistance in RenCa Cells

In order to determine the chemoresistance that may be gained through TG2-mutants, wt-TG2, TG2-R580A, TG2-C277S, TG2-W241A expressing RenCa cells along within non-transduced parental were seeded at a density of $5x10^3$ cells/well in a 96-well plate. After that, the cells were incubated overnight in a humidified atmosphere containing 5percent CO_2 at 37ºC. Following overnight incubation, the cells were treated with 0.25, 0.5, 0.75, and 1µM

of mTOR inhibitor, everolimus, and incubated for 24, 48, and 72h in the incubator. After the completion of each incubation time point, cell viability was measured as indicated in Section 3.6.1.

3.5.3. Cell Death Assay

Parental non-transduced, wt-TG2 and mutant TG2 expressing RenCa cell lines were cultured into a 6-well plate at a density of $3x10^5$ cells per well and left for overnight incubation in a humidified incubator at 37ºC and 5 percent CO_2. After 16-18h of incubation, the cells were treated 1µM of everolimus for 48 and 72h. Subsequently, after completion of each drug incubation, first, the old medium of the cells which may contain the dead cells was collecting into 15 ml falcon tubes and centrifuged at 350*xg* for 5 min. Meanwhile, the cell monolayers were washed with 1x DPBS and detached from the plate surface by incubating them with 1X Trypsin for 5 min in the incubator. After the trypsinization, the cells were collected into new 15 ml falcon tubes, and then the surface of the 6-well plate was once again washed with 1xDPBS to gather remaining cells in the wells and transferred into the same falcon tubes. The tubes were centrifuged at 300*xg* for 5 min and the cells suspensions were collected in the same 15-falcon with the cell suspension containing the dead cells to count $10x10^4$ cells for further use in Annexin-V Fluos Staining assay. Counted $10x10^4$ cells were placed into new 1.5ml Eppendorf tubes. Regarding the manufacturer's protocol, the tubes were centrifuged at 200xg for 5 min and the pellets were resuspended in 100 µl of incubation buffer. The control group which was the non-treated parental RenCa cells were divided into four groups named control unstained, annexin only, PI only, and annexin& PI. The annexin-only group of the resuspended cells was incubated with 1 µl of Annexin-V labeling reagent for 15 min in a dark environment. After the annexin incubation, the resuspended cells were mixed with 100 µl of incubation buffer to complete the total volume to 200 µl. Finally, $10x10^4$ events were evaluated via flow cytometer by using unstained control parental cells for gating after being stained with PI.

3.5.4. Cell Cycle

In order to detect the effect of transamidase and GTP-binding activity of TG2 on RenCa cell proliferation rate, cell cycle profiles were analyzed via flow cytometry. Non-transduced parental, wt-TG2 expressing and mutant type of TG2 expressing (TG2-R580A, TG2-C277S, and TG2-W241A) RenCa cell lines were seed at 300.000 cells/well density on 6-well plate surface. Based on the doubling times of the cells, all cell lines were incubated with 10 percent and 2 percent FBS containing medium for either 12 or 24h. As a positive control of 5µM, aphidicolin treatment was applied to the cells for 12h. Following the incubation, the old medium of the cells was collected into new 15ml tubes then the cell monolayer was trypsinized by incubating the cells in the incubator at 37^{o}C for 5 min. After the trypsinization, detached cells containing medium were collected in the previous 15 ml tubes and centrifuged at 350 *xg* for 5 min in order to precipitate both viable and dead cells. Cells were fixated with 70 percent ethanol for 2h. Subsequently, 500 µl of 0.1 percent Triton-X was added into each cell suspension, and the cells were incubated at room temperature for 20 min. Later, tubes were centrifuged at 300*xg* for 5 min at 4^{o}C and 200 µl of 0.05mg/ml RNase A was added. The RNase added cell suspensions were incubated at 37^{o}C for 30 min. Afterward, the tubes were centrifuged once more at 300*xg* for 5 min at 4^{o}C. The cell pellets were dissolved and stained with 200 µl of 5µg/ml PI. Finally, cell cycle analysis was carried out via flow cytometry.

3.6. STATISTICAL ANALYSIS

All data mentioned in the Result Section of the study (in Section 4) were analyzed after obtained three independent experiments. According to the mean values of these data, figures are represented in Section 4, results part. Standard deviations were calculated by using the three independent replicates (means± SD). The required comparisons between groups were evaluated via parametric statistics using the Student's t-test, one-way or two-way ANOVA by using GraphPad Prism 9.0 (GraphPad Software, San Diego California, USA). p-values <0.05 and <0.0001 considered as statistically significant.

4. RESULTS

4.1. MONITORING OF TRANSFECTION EFFICIENCY IN HEK293-FT CELLS

Transfection of HEK293-FT cells with the gene of interest was carried out with the $CaCl_2$ method. To control the transfection efficiency in the HEK293-FT cell line, pUC19-eGFP transfected HEK293-FT cells were examined under fluorescence microscopy after 24 and 48h of incubations. At each incubation time point, successfully transfected GFP-positive HEK293-FT cells were captured, and green fluorescence emission was observed.

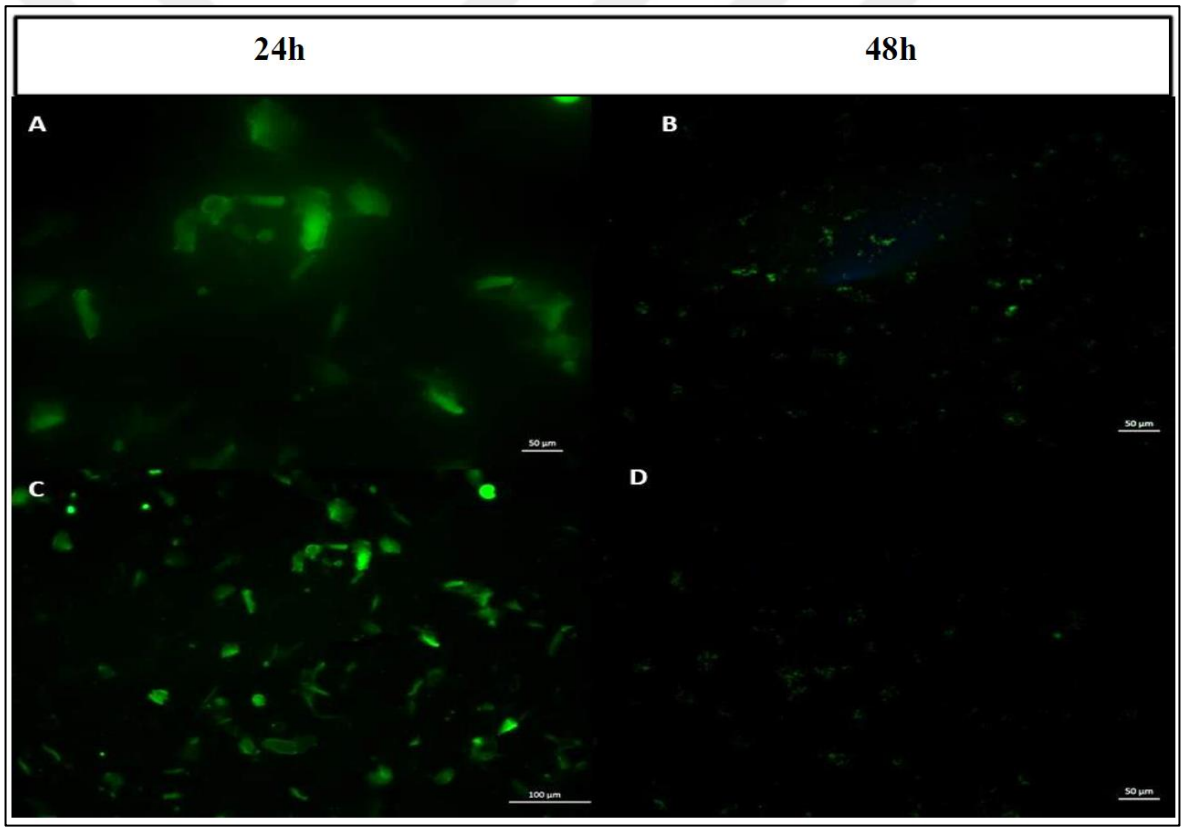

Figure 4.1. pUC19-eGFP transfected HEK293-FT cells. Transfected cells were captured via fluorescence microscopy taken at 20x and 40x objectives after A&C) 24 and B&D) 48h of incubations. The images above are the representative figures of three independent replicates of the calcium chloride transfection method. Scale bars 50 µm for Figure A, B, and D while 100 µm for Figure C.

4.2. DETECTION OF HUMAN TG2 EXPRESSION LEVEL IN TG2 VARIANTS EXPRESSING RENCA CELLS

The effect of GTP-binding or transamidase activity of TG2 variants in the cell proliferation and drug resistance which are related to both increased tumor aggression and aberrant growth in cancer cell lines were set to be identified in mouse kidney adenocarcinoma RCC cell line, RenCa. As is earlier mentioned in Section 3.3.2. RenCa cell lines were transduced with different TG2-variants separately. Consequently, to confirm transduction efficiency, mRNA level of hTGM2 was detected in parental RenCa and wild-type (wt-TG2), TG2-R580A, TG2-C277S, and TG2-W241A RenCa cells generated from parental RenCa cells by transduction with lentiviral vectors encoding the genes of interest. hTGM2 gene expression was determined via real-time PCR as described previously in Section 3.4.3. Before RT-PCR, RNA isolation and cDNA synthesis were done in respective order as mentioned in Section 3.4.1. and Section 3.4.2.

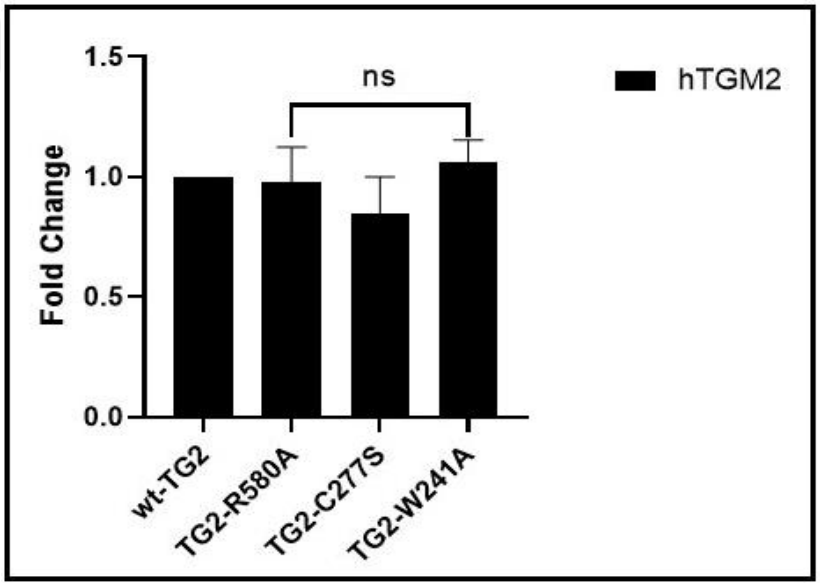

Figure 4.2. The relative hTGM2 gene expression at the mRNA level was analyzed via RT-PCR. Each hTGM2 expression obtained from wt-TG2 and TG2-mutants which are TG2-R580A, TG2-C277S, and TG2-W241A normalized to house-keeping gene 18S RNA. Error bars stand for standard deviation (means ±SD) obtained from three independent biological replicates. According to Wilcoxon non-parametric test, the deviations between the mutant cells are determined as nonsignificant (ns, $p>0.05$).

Fold change of hTGM2 gene expression in the mutant-TG2 expressing cells were analyzed after considering hTGM2 expression in wt-TG2 expressing cells as 1. According to a relative comparison of hTGM2 expression in wt-TG2 to other TG2 active site mutants, the fold change was 0.92, 0.85, and 1.1 for TG2-R580A, TG2-C277S, and TG2-W241A cells, respectively. Figure 4.2. clearly presents that the hTGM2 expression level in wt-TG2, TG2-R580A, and TG2-W241A expressing RenCa cell lines have gene expressions alike to each other. However, TG2-C277S expressing RenCa cells showed a relatively lower ($p>0.05$) hTGM2 expression pattern. Moreover, as a negative control hTGM2 expression in parental non-transduced RenCa cell line was analyzed and no hTGM2 expression was not detected.

4.3. IDENTIFICATION OF TG2 ACTIVE SITE MUTANTS' ROLE IN RENCA CELL PROLIFERATION

Although TG2 has opposing roles in different and even within the same cancer cell line based on the cellular stimuli, conformation, and subcellular location, this multifunctional protein has been demonstrated by several studies to participate in aberrant tumor growth [87]. Therefore, to answer the questions of which enzyme activity of TG2 has a role in cell proliferation, RenCa cell lines transduced with wt-TG2, TG2-R580A, TG2-C277S, and TG2-W241A along with non-transduced parental RenCa were subjected to WST-1 assay as described in Section 3.6. Cell proliferation percentages are evaluated according to parental RenCa cells' absorbance values which were considered as 100 percent at 24h.

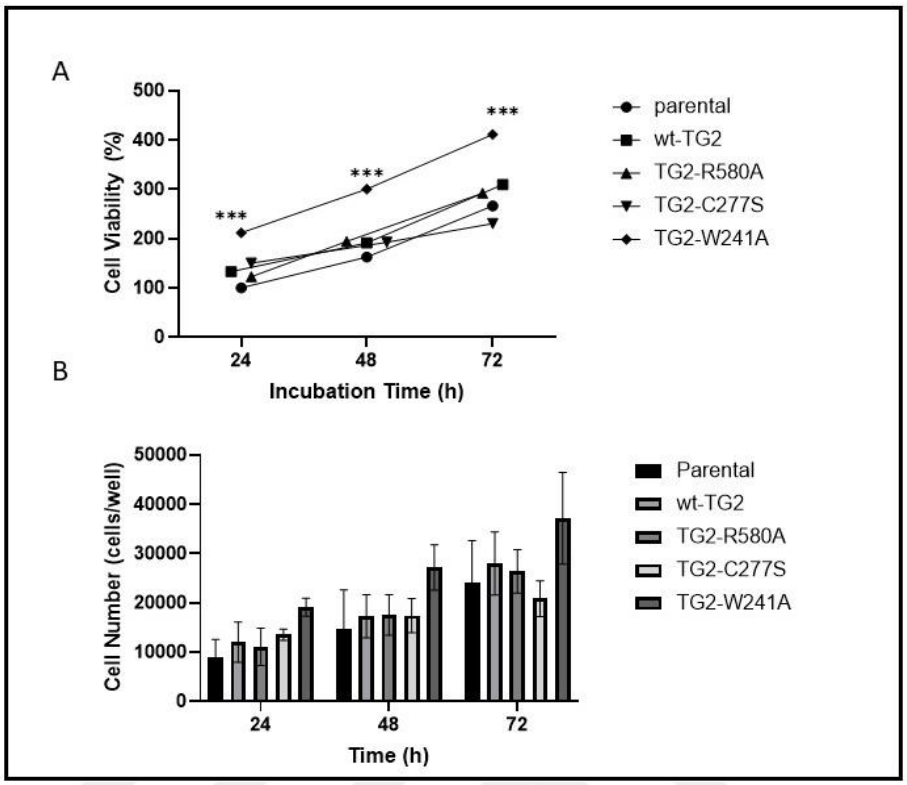

Figure 4.3. Identification of TG2 variants' role in the proliferation of RenCa. Cell proliferation rates were determined in non-transduced parental, wt-TG2, and TG2 active site mutant constructs containing RenCa cells after 24, 48, and 72h of incubations. A) The cell viabilities and B) the number of parental, wt-TG2, TG2-R580A, TG2-C277S, and TG2-W241A RenCa cell lines were evaluated based on the mean values obtained after three independent WST-1 assay repeats. Error bars stand for standard deviation (means ±SD). (Statistical significance was determined via two-way ANOVA, $p<0.0001$(***) were considered as significant).

As can be seen in Figure 4.3., cell viabilities of parental, wt-TG2, TG2-R580A, TG2-C277S, and TG2-W241A cells were evaluated as 100, 55, 63, 29 ve 83 percent for 24h of incubations in respective order. Furthermore, cell viabilities of the cells were increased to 183, 174, 160, 91, and 197 percent for 48h and 231, 209, 198, 135, and 248 percent for 72h of incubations again in the same respective order of the cells. Based on these data, an increase in cell proliferation was observed at the highest level in GTP-binding active TG2-W241A cells among the other cells. While parental, wt-TG2 and TG2-R580A expressing RenCa cells

were observed to have relatively similar proliferation percentages at the end of 48 and 72h of incubations, the proliferation rate of TG2-C277S was observed to be slowest. At the 24 h of incubation of the cells, there are 0.5, 0.6, 0.3 and 0.8-fold observed increase in wt-TG2, TG2-R580A, TG2-C277S, and TG2-W241A cell number in respective order, in comparison to the parental RenCa cell. Fold changes for cell proliferation were calculated as 1.7, 1.6, 0.9, and 2 for 48h and 2.1, 2, 1.4, and 2.5 for 72h of incubations respectively for wt-TG2, TG2-R580A, TG2-C277S, and TG2-W241A. Overall data supports that TG2-W241A possessed the highest proliferation rate compared to parental RenCa cells and the other TG2 mutant-expressing RenCa cells. The results showed that GTP-binding activity in RenCa cells results in enhanced cell proliferation which can be associated with induced tumor progression.

4.4. DETERMINATION OF TG2 ACTIVE SITE MUTANTS' ROLE IN RENCA CELL CYCLE

Several studies have shown that TG2 is a key player in various molecular and survival mechanisms of tumor cells which may affect tumor progression through cell proliferation and consequently cell cycle [157,158]. Therefore, to identify changes in the cell cycle profile of RenCa cell lines after transduced with TG2-variants, cell cycle analysis was carried out, for 12 and 24h of incubations.

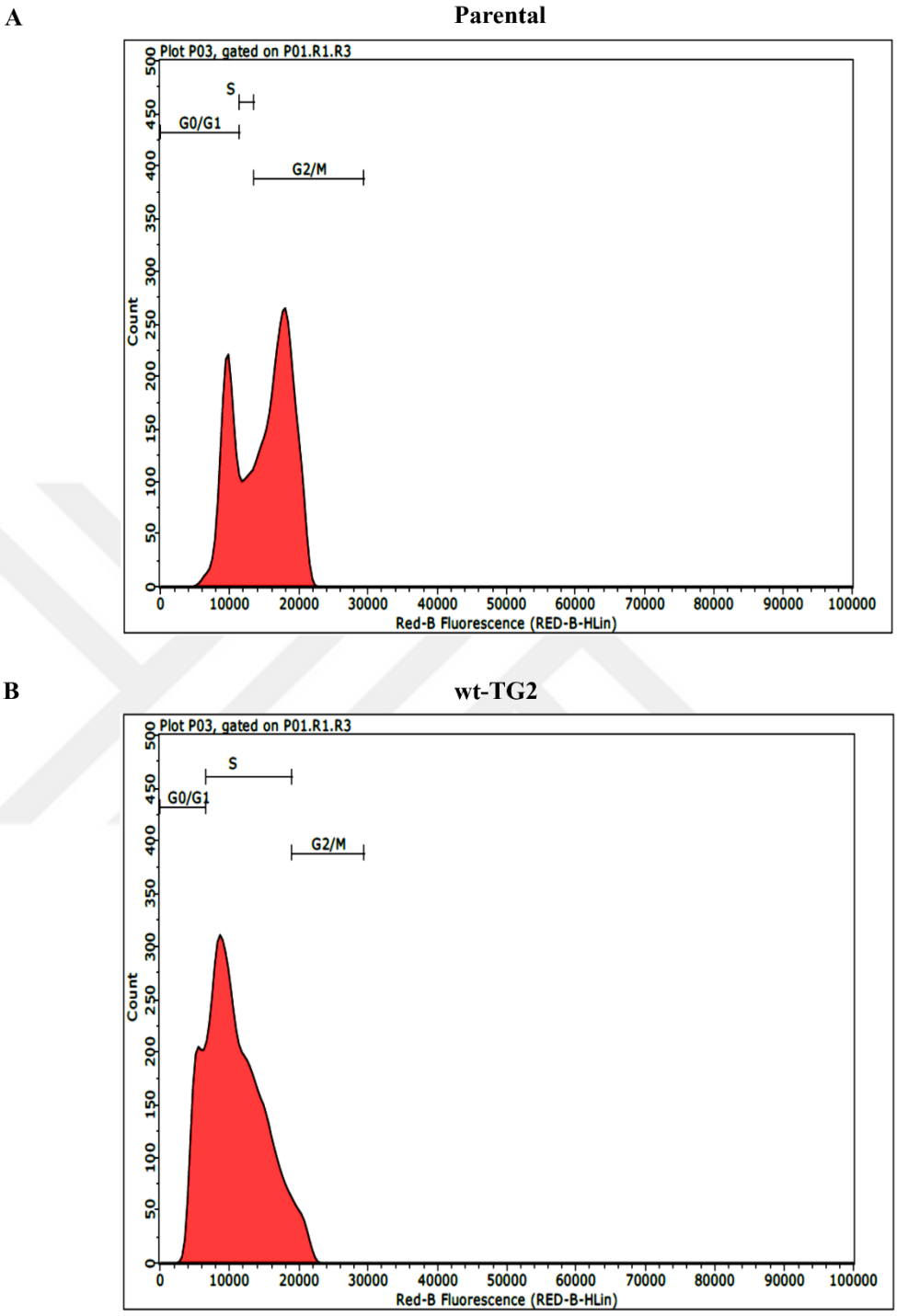

Figure 4.4. Cell cycle profiles of A-E) parental, wt-TG2 and mutant TG2 expressing (TG2-R580A, TG2-C277S and TG2-W241A) RenCa cell lines at the end of 12 h of incubations. Cell cycle analysis was done through PI-staining via flow-cytometry analysis and evaluated via Guave easyCyte Systems.

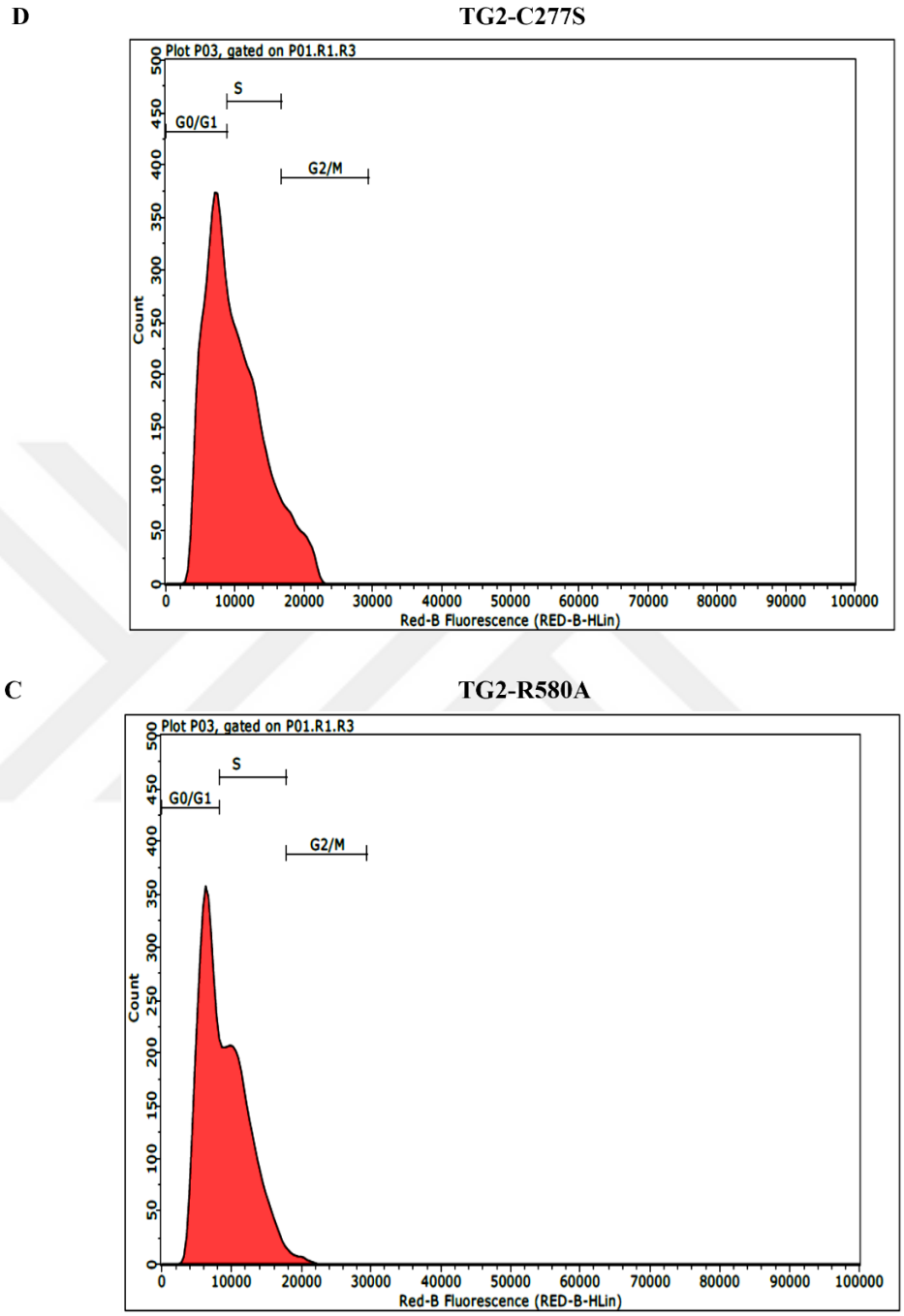

Figure 4.4. (Continue) Cell cycle profiles of A-E) parental, wt-TG2 and mutant TG2 expressing (TG2-R580A, TG2-C277S and TG2-W241A) RenCa cell lines at the end of 12 h of incubations. Cell cycle analysis was done through PI-staining via flow-cytometry analysis and evaluated via Guave easyCyte Systems.

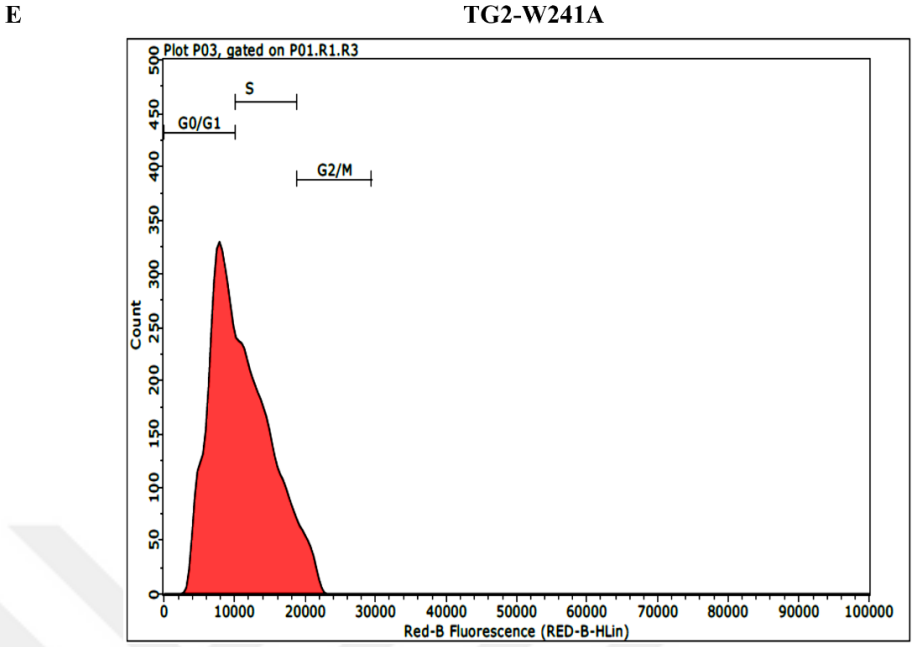

Figure 4.4. (Continue) Cell cycle profiles of A-E) parental, wt-TG2 and mutant TG2 expressing (TG2-R580A, TG2-C277S and TG2-W241A) RenCa cell lines at the end of 12 h of incubations. Cell cycle analysis was done through PI-staining via flow-cytometry analysis and evaluated via Guave easyCyte Systems.

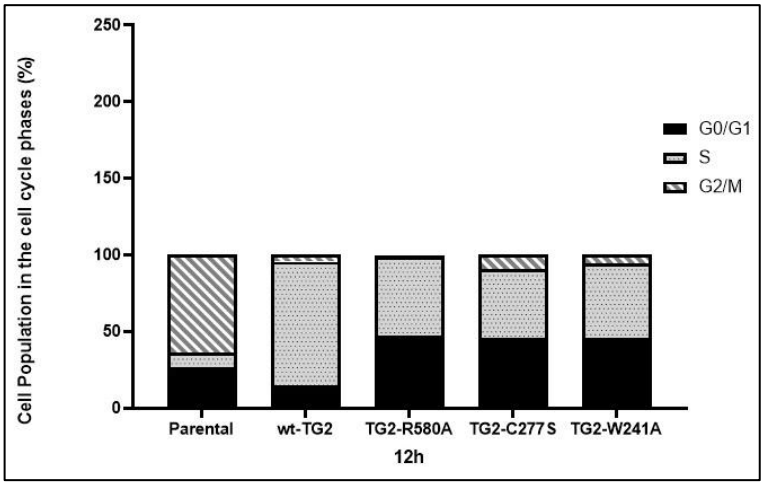

Figure 4.5. Non-transduced parental RenCa, wt-TG2, and mutant-TG2 expressing TG2-R580A, TG2-C277S, and TG2-W241A populations (percent) in each cell cycle phase (G0/G1, S, and G2/M) were evaluated after 12h of incubation via flow-cytometry analysis by using Guave easyCyte Systems.

Table 4.1. Cell cycle distribution of parental, wt-TG2, TG2-R580A, TG2-C277S, and TG2-W241A cell lines after 12 h of incubation.

	G0/G1	**S**	**G2/M**
Parental	38.2±10.3	17.0±7.0	45.2±16.1
wt-TG2	31.9±14.5	13.8±0.9	46.3±2.1
TG2-R580A	47.0±1.8	14.8±0.5	26.3±21.8
TG2-C277S	48.6±5.9	26.6±16.0	25.2±14.2
TG2-W241A	48.0±14.2	30.4±15.8	30.4±17.1

Upon the 12 of incubation of non-transduced parental RenCa, and wt-TG2 and TG2-active site mutants expressing RenCa cells, our results showed that except for parental RenCa cells, other cell lines were observed to be arrested in G1 and S phase by having a total 95.6, 98.7, 90.8 and 94.6 percent of cell population in these cell cycle phases respectively for wt-TG2, TG2-R580A, TG2-C277S and TG2-W241A expressing RenCa cells. The parental RenCa cell population in G1 and S phases was evaluated as 36.2 percent in total. The cell population in G2/M phases was 63.8, 4.4, 1.3, 9.2, and 5.5 percent for wt-TG2, TG2-R580A, TG2-C277S, and TG2-W241A expressing RenCa cells in respective order.

A **Parental**

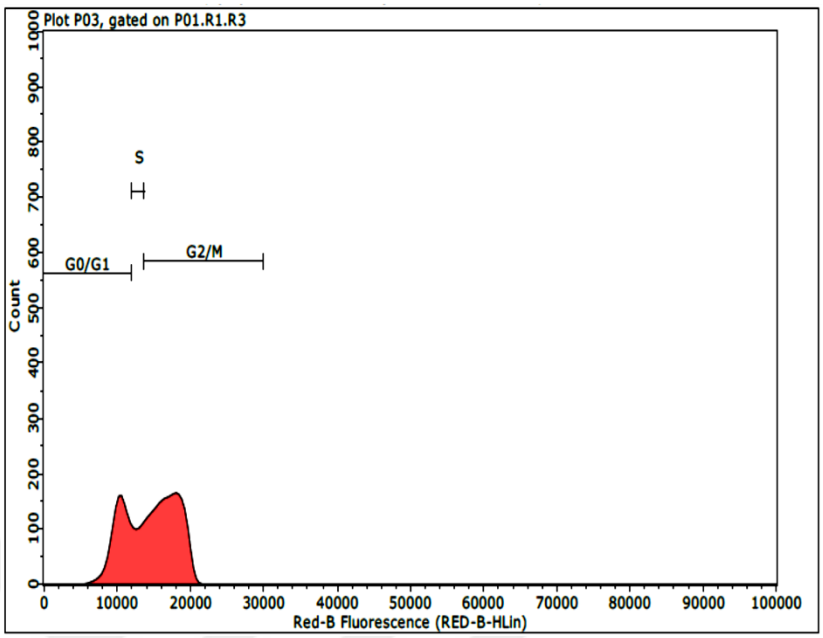

B **wt-TG2**

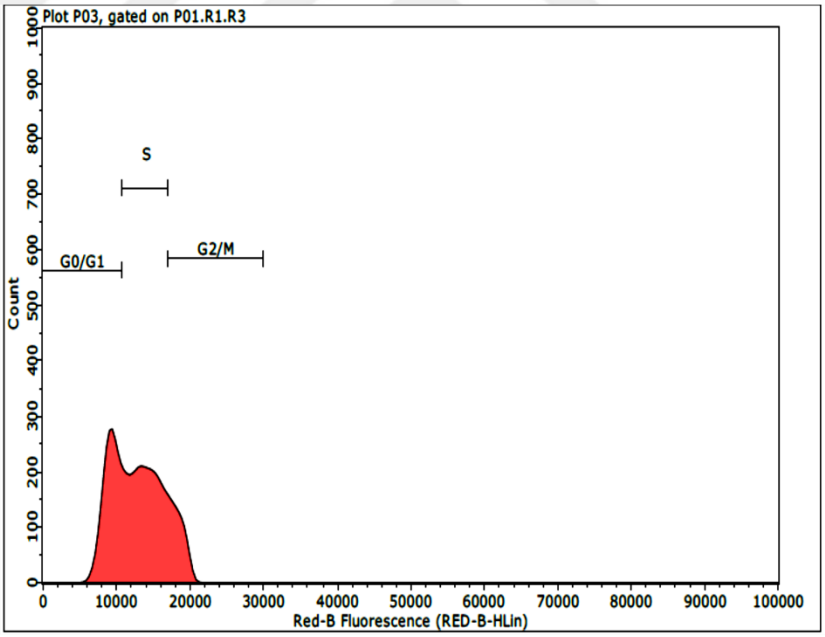

C **TG2-R580A**

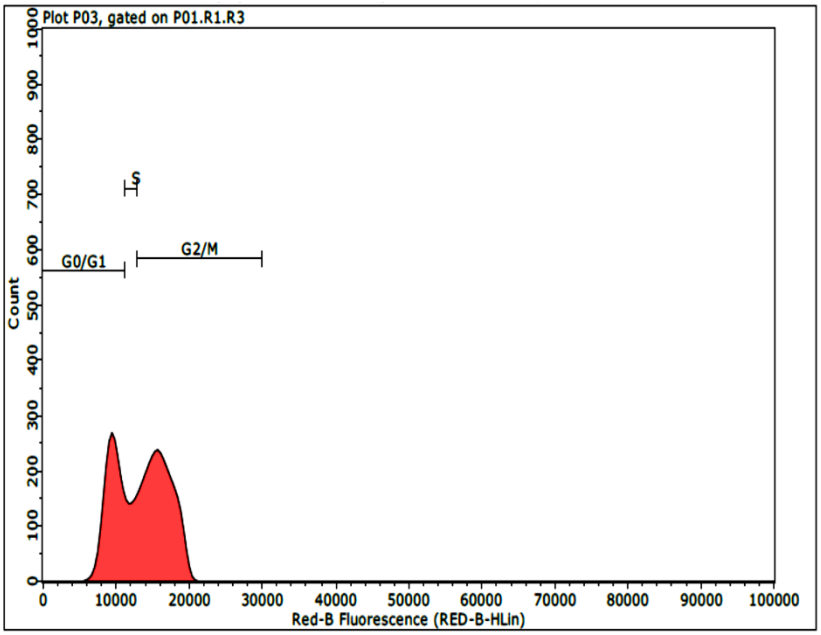

D **TG2-C277S**

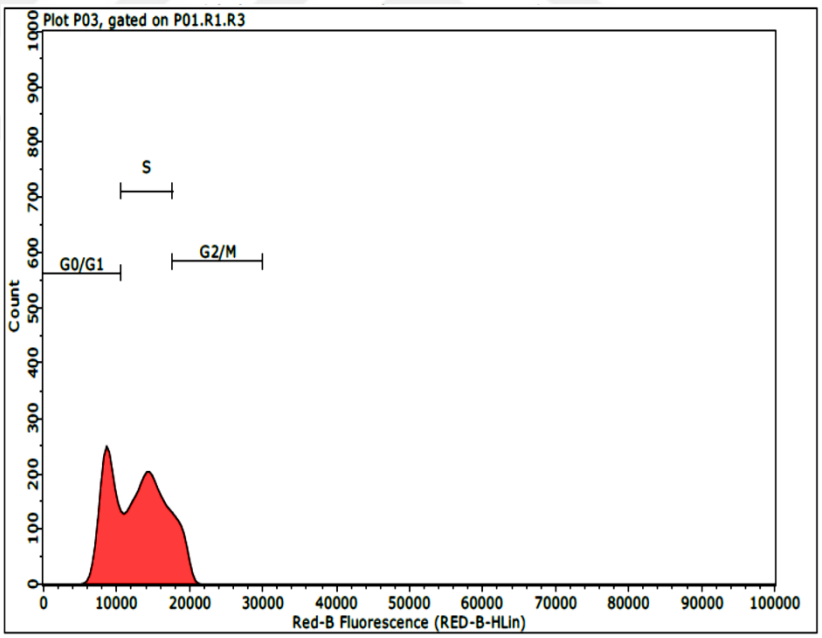

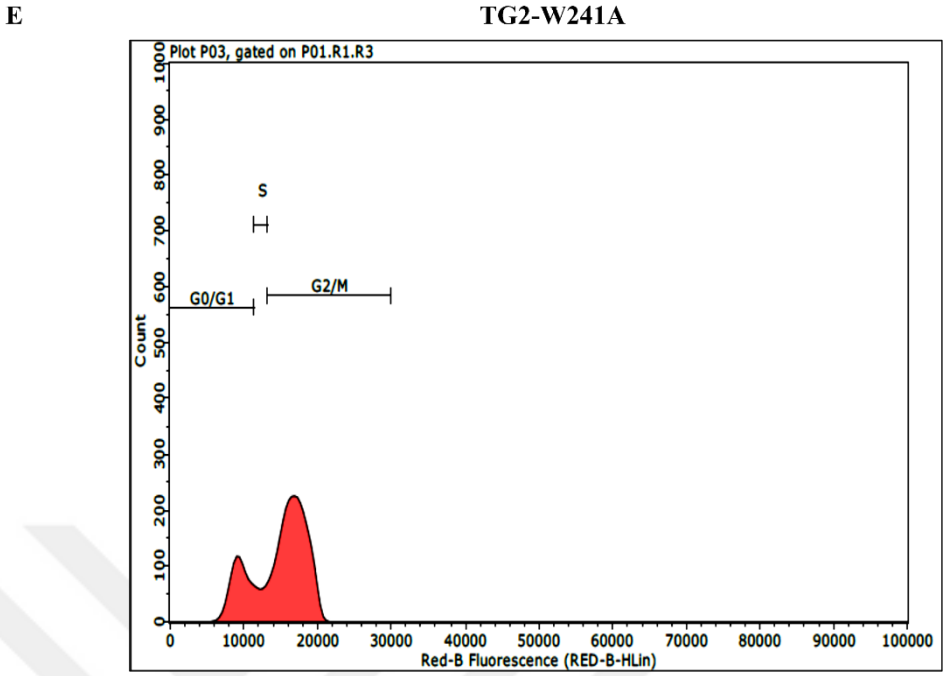

Figure 4.6. Non-transduced parental RenCa, wt-TG2, and mutant-TG2 expressing TG2-R580A, TG2-C277S, and TG2-W241A populations (percent) in each cell cycle phase (G0/G1, S, and G2/M) were evaluated after 24h of incubation via flow-cytometry analysis by using Guave easyCyte Systems.

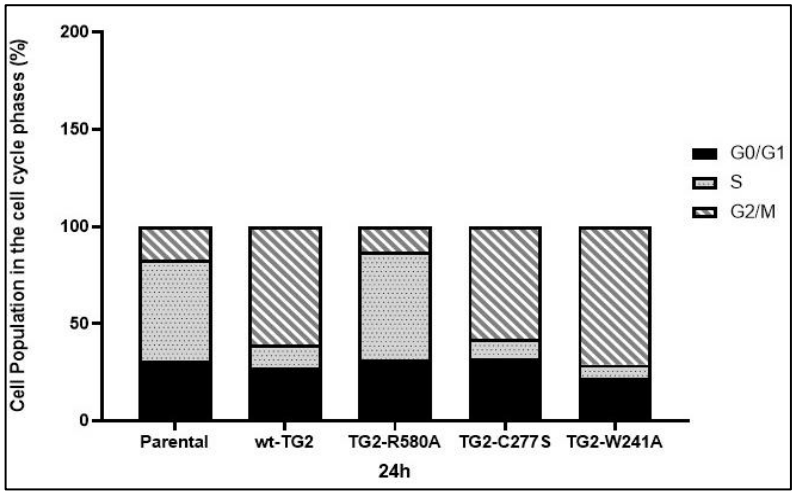

Figure 4.7. Non-transduced parental RenCa, wt-TG2, and mutant-TG2 expressing TG2-R580A, TG2-C277S, and TG2-W241A populations in each cell cycle phase (G0/G1, S, and G2/M) were evaluated after 24h of incubation via flow-cytometry analysis by using Guave easyCyte Systems.

Table 4.2. Cell cycle distribution of parental, wt-TG2, TG2-R580A, TG2-C277S, and TG2-W241A cell lines after 24 h of incubation.

	G0/G1	S	G2/M
Parental	44.8±12.1	34.3±15.8	21.2±4.0
wt-TG2	36.3±7.5	16.6±6.7	47.4±12.8
TG2-R580A	26.9±6.5	57.4±2.5	15.7±4.0
TG2-C277S	38.9±7.0	21.4±11.0	40.1±15.3
TG2-W241A	23.7±2.3	6.7±0.2	69.6±2.1

Figure 4.6.-4.7. and Table 4.2. demonstrated that after 24h of incubation, total cell population in both G1 and S phases were observed respectively as being 83.1, 39.3, 87.1, 42.3, and 28.9 percent for parental, wt-TG2, TG2-R580A, TG2-C277S, and TG2-W241A expressing RenCa cells. On the other hand, the cell population for each cell line arrested in the G2 phase of the cell cycle was evaluated as 16.9, 60.7, 12.9, 57.7, and 71.1. for parental, wt-TG2, TG2-R580A, TG2-C277S, and TG2-W241A expressing RenCa cells. Taken together with data obtained after 12h of incubation for cell cycle analysis, mutant TG2-construct expressing RenCa cells (TG2-R580A, TG2-C277S, and TG2-W241A) were observed to doubled DNA content at the end of 24h of incubation. Moreover, the TG2-W241A cells population was observed to be arrested in the G2/M phase more than other mutant types by having 71 percent of its population in the G2/M phase.

4.5. DETECTION OF EFFECTS OF TG2 ACTIVE SITE MUTANTS IN DRUG RESISTANCE AND CELL DEATH OF RENCA CELLS

A study published by Nayman *et al.* elucidated that RenCa cells are actually sensitive to everolimus treatment in a dose and treatment-duration-dependent manner[159]. In order to understand, whether TG2 variants possessing GTP-binding or transamidation active has an indispensable role in cell viability upon everolimus treatment, non-transduced parental, wt-TG2, TG2-R580A, TG2-C277S, and TG2-W241A were subjected to low doses of

everolimus (0.25, 0.5, 0.75, and 1 μM) which was previously shown to induce everolimus resistance in RenCa cells [160].

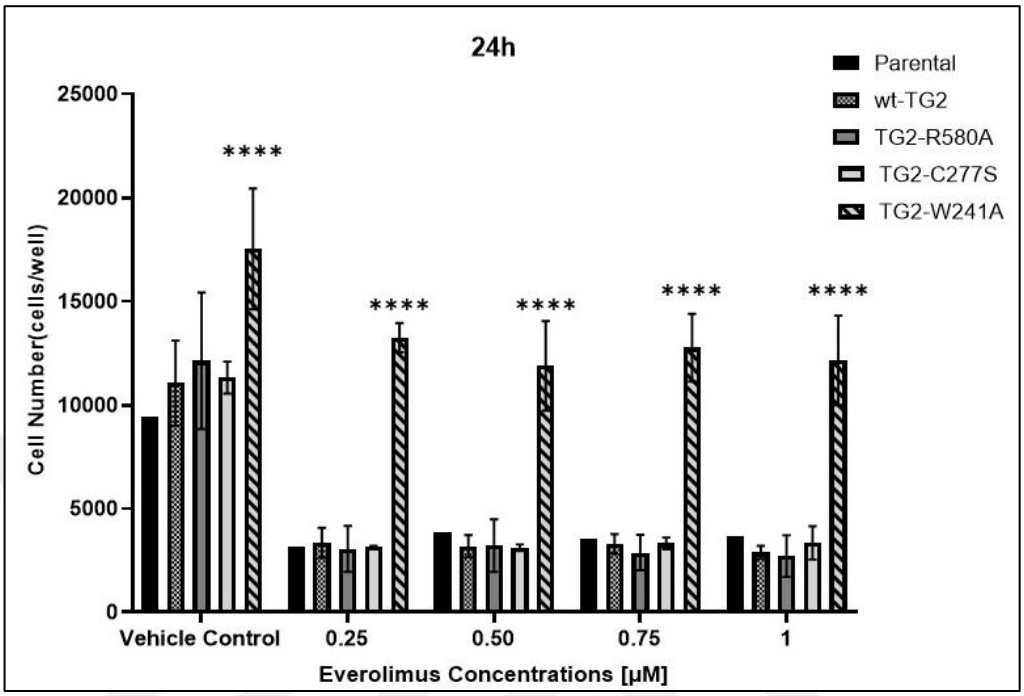

Figure 4.8. Everolimus response profile of non-transduced parental, wt-TG2, TG2-R580A, TG2-C277S, and TG2-W241A RenCa cell lines for 24h at 0.25, 0.5, 0.75, and 1 μM everolimus. The number of viable cells was determined using WST-1 assay. Error bars stand for the standard deviation of three independent biological replicates (mean± SD). Statistical significance was determined via two-way ANOVA, $p<0.0001$(****) were considered as significant.

Figure 4.8. represents that upon 0.25, 0.5, 0.75, and 1 μM of everolimus treatment on non-transduced parental, wt-TG2, TG2-R580A, TG2-C277S, and TG2-W241A RenCa cell lines for 24 h, the number of viable TG2-W241A cells were remarkably higher among the other RenCa cell lines ($p<0.0001$). The mean number of the viable cells was assessed as 3430, 3649, 3550, 3378, and 3192 for parental RenCa, 3349, 3191, 3291 and 2888 for wt-TG2, 3062, 3216, 2880, 2712 for TG2-R580A, 3173, 3113, 3327 and 3348 for TG2-C277S and finally 13.248, 11.887, 12.7611, and 12.148 for TG2-W241A cells respectively for 0.25, 0.5, 0.75, and 1 μM everolimus treatment. Each dose of everolimus showed the nearly same effect on the average cell viability within the same RenCa cell group.

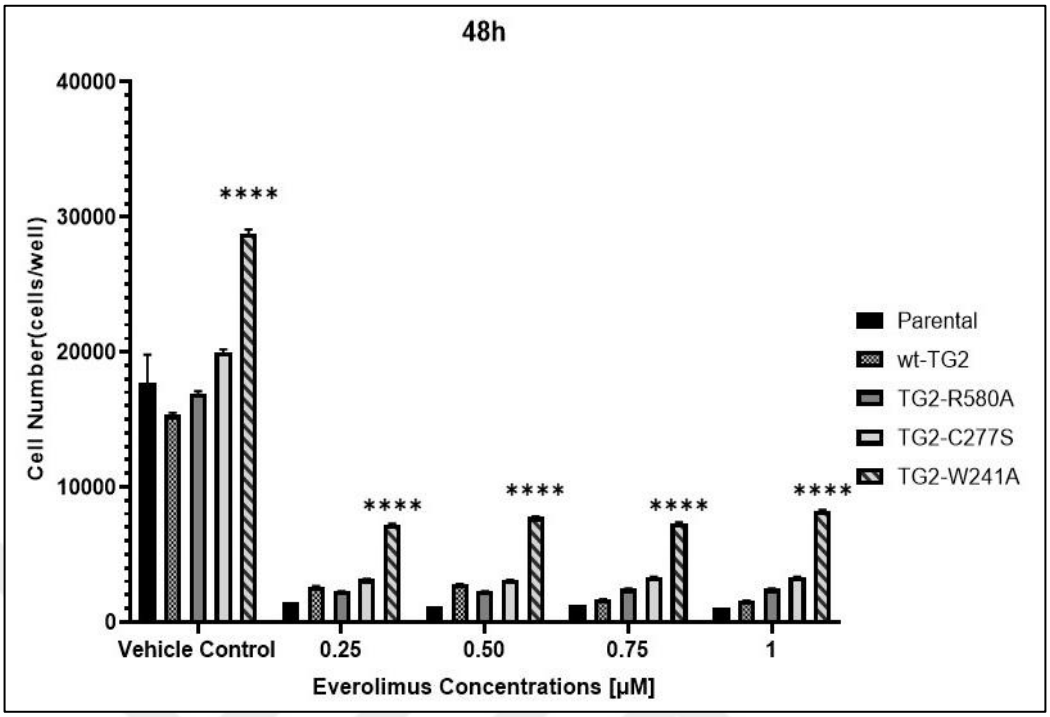

Figure 4.9. Everolimus response profile of non-transduced parental, wt-TG2, TG2-R580A, TG2-C277S, and TG2-W241A RenCa cell lines for 48h at 0.25, 0.5, 0.75, and 1 μM everolimus. The number of viable cells was determined using WST-1 assay. Error bars stand for the standard deviation of three independent biological replicates (mean± SD). Statistical significance was determined via two-way ANOVA, $p<0.0001$(****) were considered as significant.

As seen in Figure 4.9., upon the applied 0.25, 0.5, 0.75, and 1 μM everolimus treatment on non-transduced parental, wt-TG2, TG2-R580A, TG2-C277S, and TG2-W241A RenCa cell lines for 48 h, the number of viable TG2-W241A cells were again observed to have highest cell population among the other cell lines in all applied doses of everolimus. The number of viable cells were assessed as 1444, 1208, 1272, 1057, and 1187 for parental RenCa, 2631, 2796, 1669, 1574 for wt-TG2, 2270, 2268, 2455, 2457 for TG2-R580A, 2473, 2794, 2861, and 1158 for TG2-C277S and finally 7227, 7776, 7323, and 8257 for TG2-W241A cells respectively for 0.25, 0.5, 0.75, and 1 μM everolimus treatment. Each dose of everolimus again resulted in nearly the same average cell viability within the same RenCa cell group.

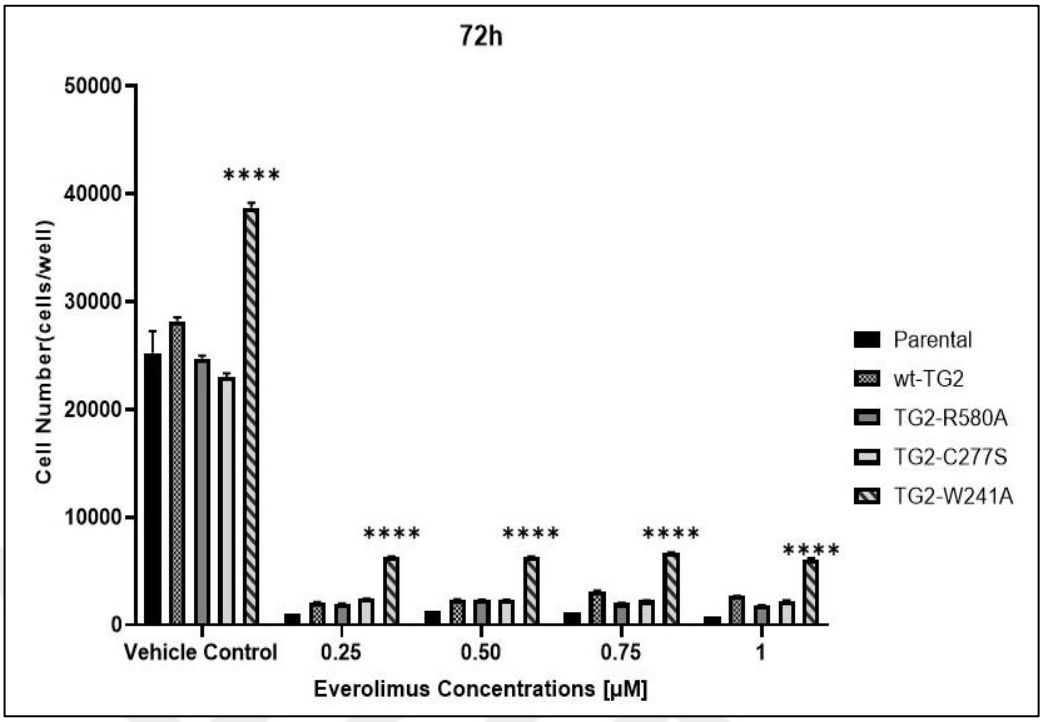

Figure 4.10. Everolimus response profile of non-transduced parental, wt-TG2, TG2-R580A, TG2-C277S, and TG2-W241A RenCa cell lines for 72h at 0.25, 0.5, 0.75, and 1 μM everolimus. The number of viable cells was determined using WST-1 assay. Error bars stand for the standard deviation of three independent biological replicates (mean± SD). Statistical significance was determined via two-way ANOVA, $p<0.0001$(****) were considered as significant.

Based on Figure 4.10. the cell viability in number was determined as 1082, 1296,1123, and 822 for parental RenCa, 2083,2340,3150, and 2677 for wt-TG2, 1982, 2318, 2017, and 1795 for TG2-R580A, 2408, 2317, 2260 and 2254 for TG2-C277S and finally 6269, 6287, 6650, and 6093 for TG2-W241A cells respectively for 0.25, 0.5, 0.75, and 1 μM everolimus treatment comparing to non-treated parental RenCa cell for 72h of everolimus treatment. Similar to 24 and 48h of treatment with everolimus, each dose of everolimus once again affected the cell viability in approximately the same profile within the same RenCa cell group. Together with obtained results represented above in Figure 4.8-4.10., wt-TG2, TG2-R580A, and TG2-C277S RenCa cells were observed to have approximately similar cell viability profiles in each treatment group and drug administration time compared to non-transduced parental RenCa cells. However, the cell viability was observed to be remarkably

higher in the GTP-binding active form of TG2 expressing RenCa cell line, TG2-W241A among all cell lines treated with 0.25-1 μM everolimus. Except for TG2-W241A cells, all cell lines were cytotoxically affected by everolimus treatment. However, as it was mentioned in Section 3.5., the initial cell number cultured for drug-resistance analysis via WST-1 assay was $5x10^3$ cells/well, and only transamidase inactive and GTP-binding active TG2-W241A cells surpassed the initial number of viable cells in spite of being subjected to one most potent remedy for RCC, everolimus. Overall, in the light of these results, it can be said that the GTP-binding activity of TG2 is inevitably important in gained drug resistance of advanced RCC type, RenCa.

4.6. EFFECT OF EVEROLIMUS ON APOPTOSIS OF TG2 ACTIVE SITE MUTANT RENCA CELLS

The role of TG2 in both pathological and physiological processes is multifaceted due to its conformational alterations, genetic variants, and multifunctionality [161]. Moreover, the understanding of TG2 via its differentially gained functions such as promoting cell death and induced cell survival owing to its GTP-binding and transamidating-active forms are worthwhile to avoid this obscureness. For this reason, the effect of GTP-binding and/or transamidating activity of TG2 on cell death was investigated by annexin-V Fluos PI double staining in parental, wt-TG2, TG2-R580A, TG2-C277S, and TG2-W241A undergone 1 μM everolimus treatment.

A **Parental**

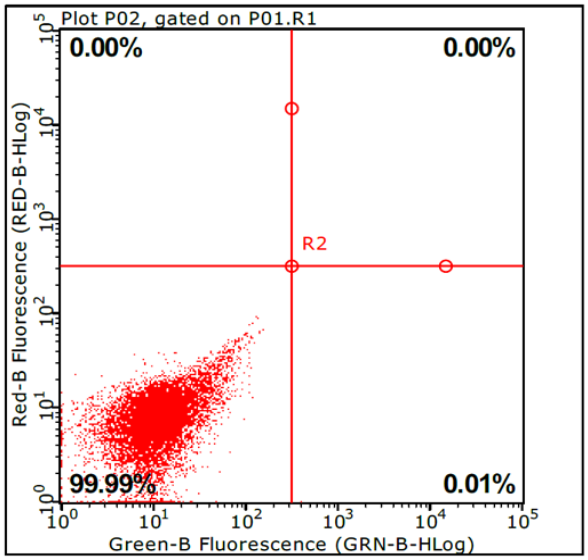

B **Parental-ev.**

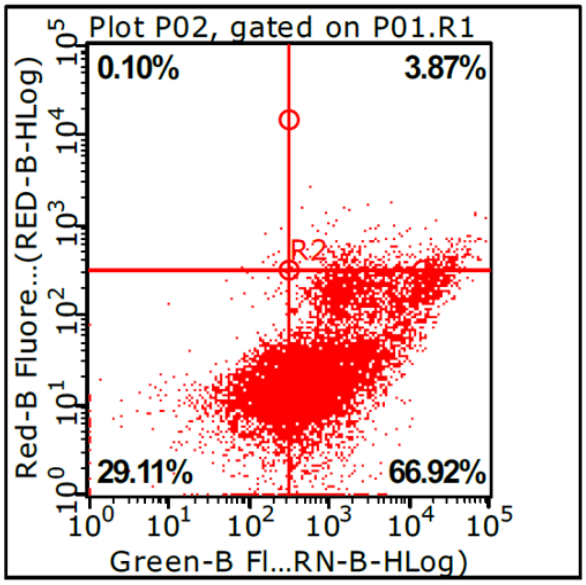

C wt-TG2-ev.

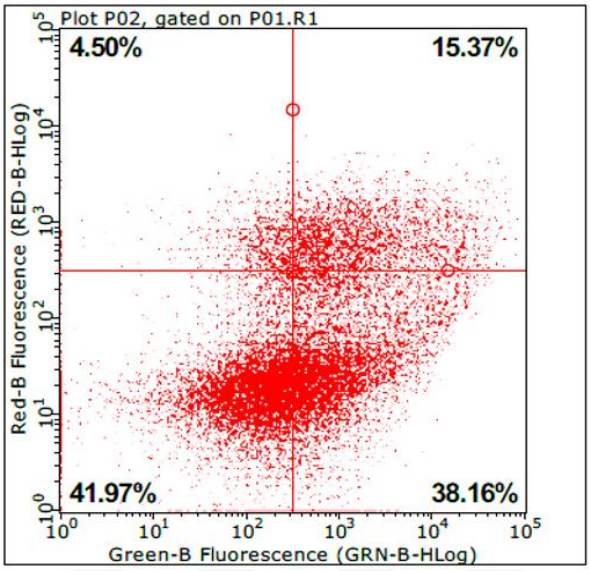

D TG2-R580A-ev.

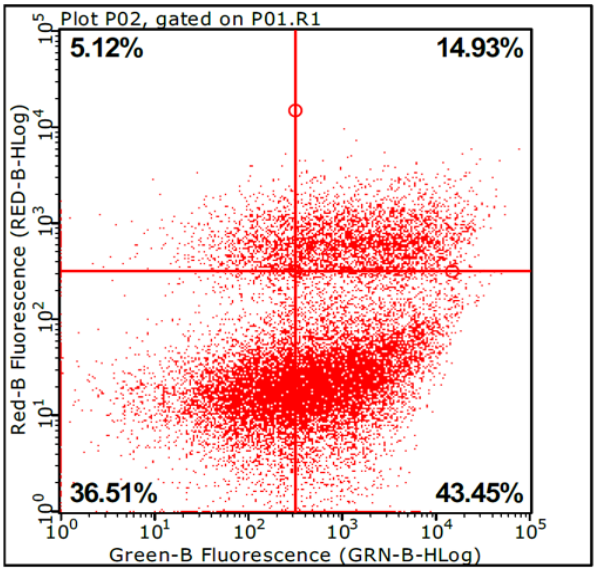

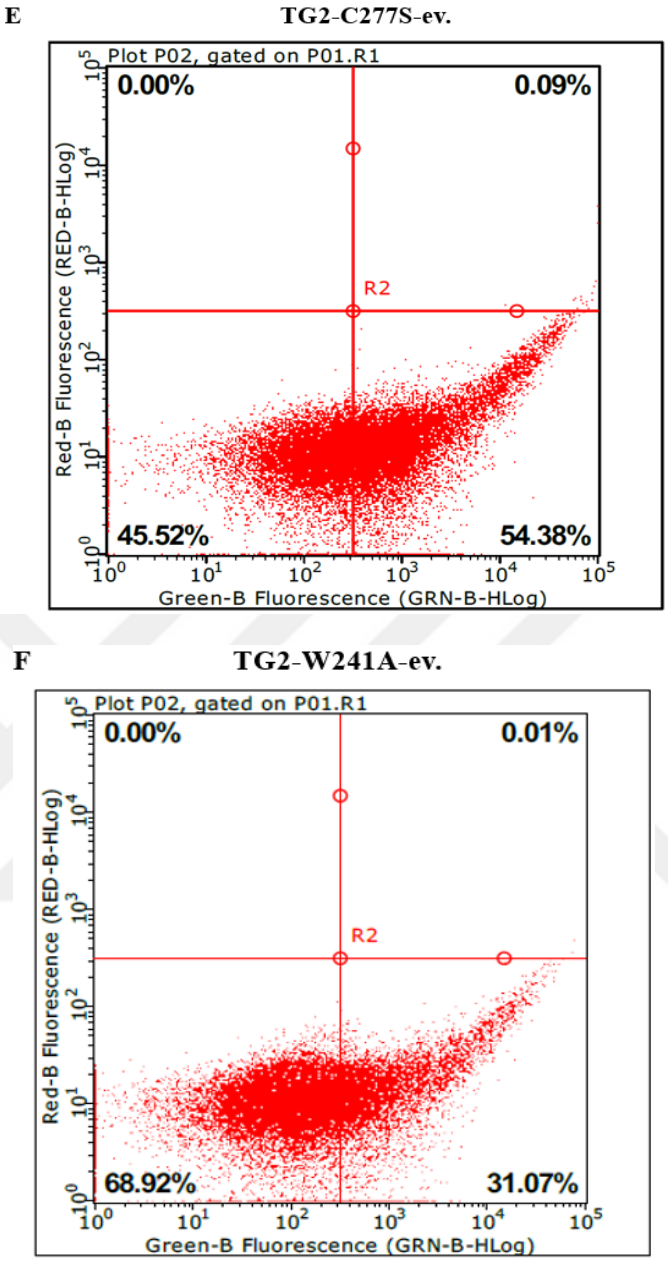

Figure 4.11. Apoptotic cell death of the parental non-transduced, wt-TG2 and mutant TG2 expressing RenCa cells were detected after 1 µM of everolimus treatment for 48h. A-F) The percentages of necrosis (upper left), late apoptosis (upper right), viable cells (lower left), and early apoptosis (lower right) in parental non-transduced, and everolimus treated parental, wt-TG2 and mutant TG2 expressing RenCa cells were represented in respective order. Representative images were selected from three independent Annexin-V experiments.

Table 4.3. Parental, parental-ev., TG2-R580A, TG2-C277S, and TG2-W241A RenCa cells' populations in necrosis, late and early apoptosis, and viable stages were evaluated after being treated with 1 μM of everolimus for 48h. Standard deviation was calculated according to three independent biological repeats (mean± SD). Statistical significance was determined by comparing each data to control parental cells via two-way ANOVA, $p<0.01$ (*) and $p<0.0001$(****) were considered significant.

	Viable	**Early Apoptosis**	**Late Apoptosis**	**Necrosis**	**p-value**
Parental	100 ± 1	0.01 ±0.0	-	-	-
Parental-ev.	36.2 ±10.2	49.9 ±14.7	6.0 ±3.0	0.2 ±0.1	**** P<0.0001
wt-TG2	44.9 ±5.3	42.7 ±11.6	14.1 ±1.8	3.2 ±1.8	**** P<0.0001
TG2-R580A	35.1 ±7.8	56.5 ±18.4	14.7 ±0.3	2.7 ±3.5	**** P<0.0001
TG2-C277S	42.9 ±4.4	56.1 ±2.5	2.1 ±2.9	1.5 ±2.5	**** P<0.0001
TG2-W241A	63.6 ±5.5	27.8 ±6.7	1.3 ±1.8	0.7 ±1.0	* P<0.01

According to Figure 4.11., after 48h treatment with everolimus, parental, wt-TG2, TG2-R580A, TG2-C277S, and TG2-W241A cells were observed to be undergone early apoptosis by 66.9, 38.16, 43.45, 54.38, and 31.1 percent. While parental, wt-TG2, and TG2-R580A cells were detected to undergo necrosis by 0.10, 4.5, 5.12 percent respectively, TG2-W241A and TG2-C277S cells did not show necrosis. Moreover, the cells were detected to undergo

late apoptosis stage by 3.87, 15.37, 14.93, 0.09, and 0.01 percent respectively, in the above order.

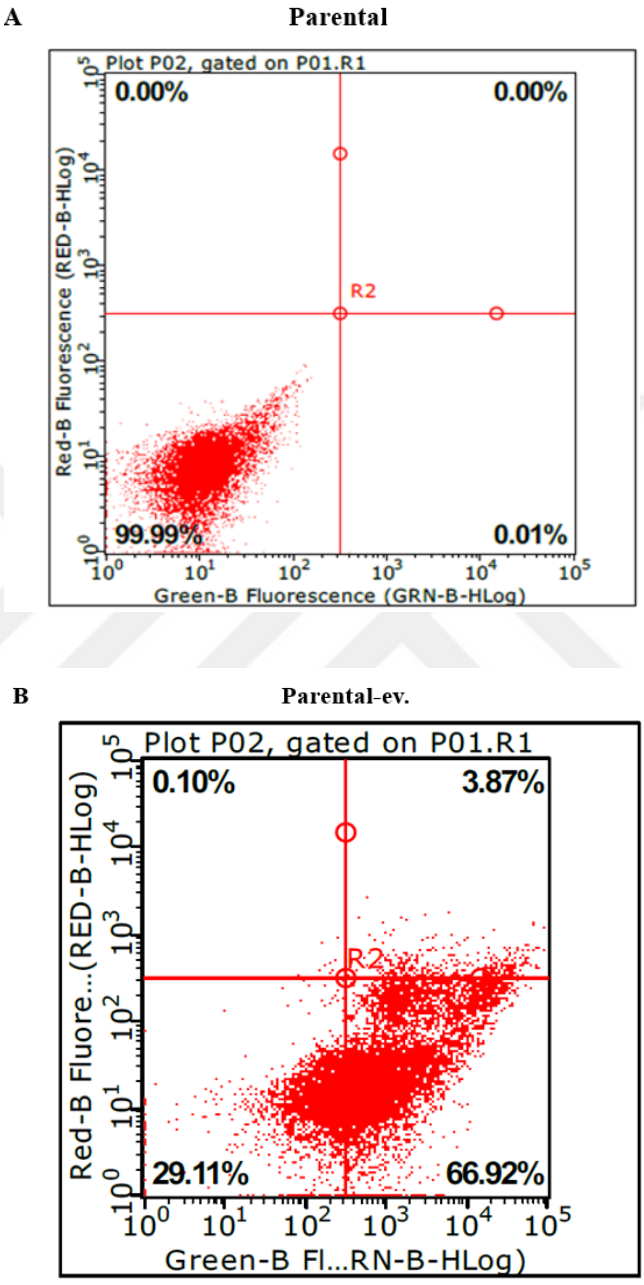

C wt-TG2-ev.

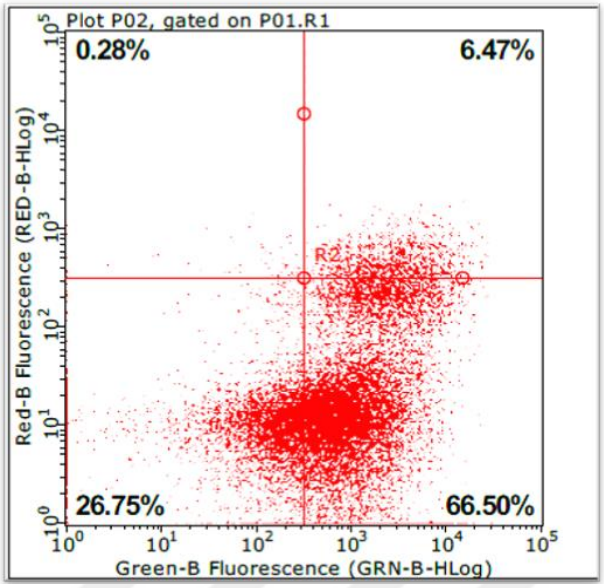

D TG2-R580A-ev.

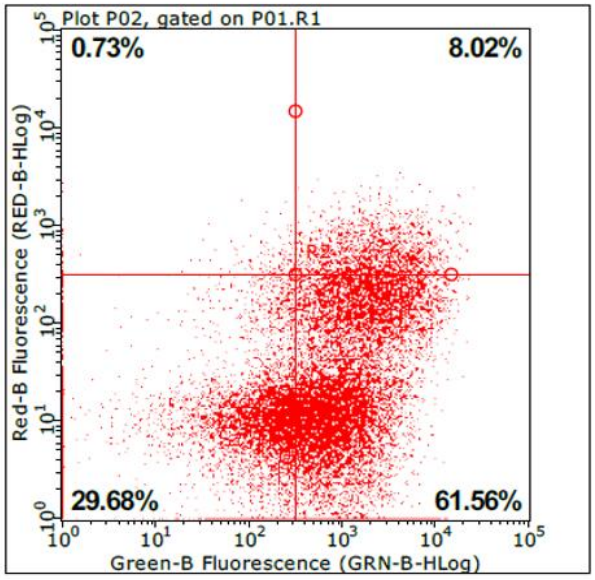

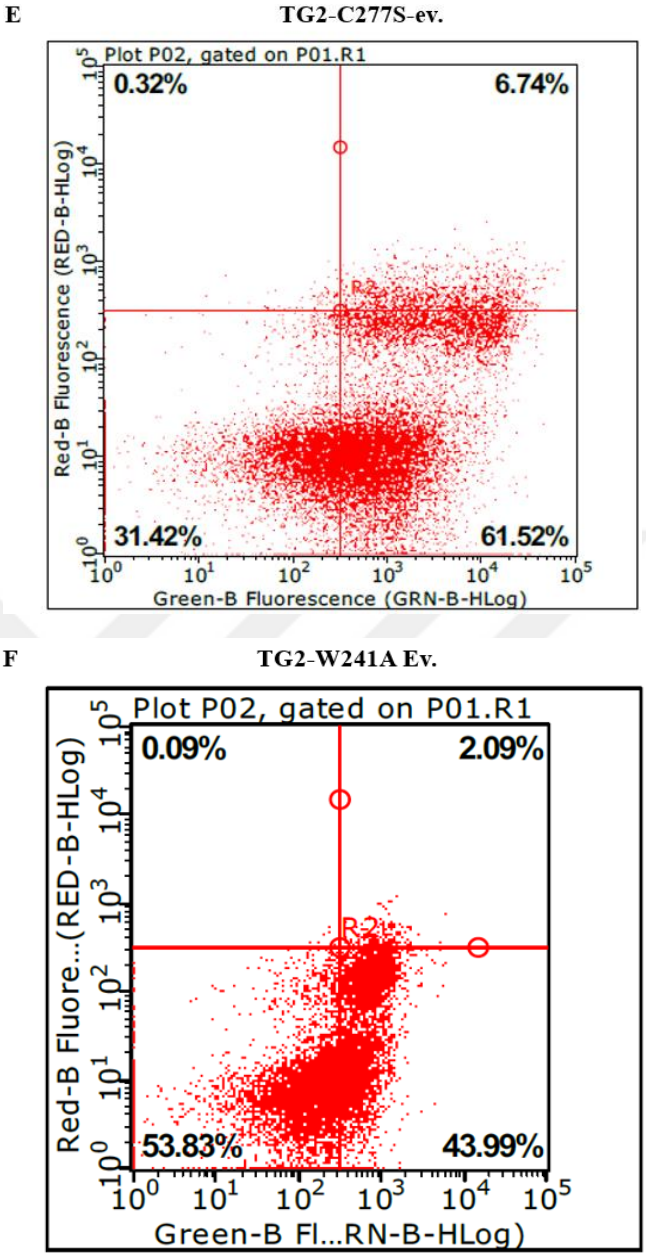

Figure 4.12. Apoptotic cell death of the parental non-transduced, wt-TG2 and mutant TG2 expressing RenCa cells were detected after 1 µM of everolimus treatment for 72h. A-F) The percentages of necrosis (upper left), late apoptosis (upper right), viable cells (lower left), and early apoptosis (lower right) in parental non-transduced, and everolimus treated parental, wt-TG2 and mutant TG2 expressing RenCa cells were represented in respective order. Representative images were selected from three independent Annexin-V experiments.

Table 4.4. Parental, parental-ev., TG2-R580A, TG2-C277S, and TG2-W241A cell populations in necrosis, late and early apoptosis, and viable stages were evaluated after being treated with 1 μM of everolimus for 72h. Standard deviation was calculated according to three independent biological repeats (mean± SD). Statistical significance was determined by comparing each data to control parental cells via two-way ANOVA, p<0.0001(****) were considered significant.

	Viable	**Early Apoptosis**	**Late Apoptosis**	**Necrosis**	**p-value**
Parental	97.58 ± 2.93	0.58 ±0.8	0.043±0.0045	0.13±0.2	-
Parental Ev.	18.1±10.5	77.3±11.8	4.5±2.3	0.04±0.1	**** P<0.0001
wt-TG2	32.9±8.8	74.1±10.7	4.1±2.4	0.12±0.1	**** P<0.0001
TG2-R580A	20.7±6.3	76.0±10.2	3.0±0.3	1.18±1.4	**** P<0.0001
TG2-C277S	32.2±14.5	61.1±12.4	6.6±2.1	0.13±0.2	**** P<0.0001
TG2-W241A	55.6±3.0	40.2±6.5	3.2±2.0	0.06±0.0	**** P<0.0001

As seen in Figure 4.12., after 72h treatment with everolimus, parental, wt-TG2, TG2-R580A, TG2-C277S, and TG2-W241A cells underwent early apoptosis by 72.5, 66.5, 61.6, 61.2, and 44 percent. Necrosis-induced cell population of wt-TG2, TG2-R580A, TG2-C277S, and

TG2-W241A cells were detected to be 0.20, 8, 0.32, and 0.09 percent respectively. Parental RenCa did not go into the necrosis process. Moreover, parental, wt-TG2, TG2-R580A, TG2-C277S, and TG2-W241A cells were detected in the late apoptosis stage with 3.25, 6.47, 8, 6.74, and 2.1 percent in respective order.

Table 4.5. The summary data for cell population of Annexin-V Positive cells were evaluated for the parental non-transduced, wt-TG2 and mutant TG2 expressing RenCa cell lines after being treated with 1 μM of everolimus for 48 and 72h. Standard deviation was calculated according to three independent biological repeats (mean± SD). Statistical significance was determined by comparing each data to control parental cells via one-way ANOVA, $p<0.05$(*), $p<0.005$ (**), and $p<0.001$(***) were considered significant.

	48h		**72h**	
	Annexin-V Assay percent of positive cells	**p-value**	**Annexin-V Assay percent of positive cells**	**p-value**
Parental	0.01±0	-	0.62±0	-
Parental-ev.	62.7±11.8	*** p<0.001	79.7± 12.9	** p<0.005
wt-TG2	52.8±5.6	** p<0.005	67±22.2	* p<0.05
TG2-R580A	58.2±14.9	*** p<0.001	79±15.7	** p<0.005
TG2-C277S	55.6±5.9	** p<0.005	67.7±14.5	* p<0.05
TG2-W241A	32±2.4	* p<0.05	48.8±12.2	ns p>0.05

Overall, Figure 4.11-4.12 and Table 4.5. demonstrate that Annexin-V positive cell population which involves early, and late apoptosis stages were observed to be least in TG2-W241A cells by having 32 and 48 percent of all its population in 48 and 72h of 1 μM of everolimus-administration. On the other hand, Annexin-V positive parental, wt-TG2, TG2-R580A, and TG2-C277S cells were assessed as 62, 53, 58, and 55 percent for 48h of the drug administration while 80, 67, 79, 68, percent of early and late apoptotic cells were present after 72h of everolimus treatment.

5. DISCUSSION

RCC is about to account for 90 percent of all kidney-related malignancies and the most relevant type of renal neoplasms in adults [162]. The most prominent type of RCC is CCRCC which has the lowest prognosis than the other histologic subtypes. Due to the low survival rate and recurrence of RCC, it is one of the top 10 causes of cancer-related deaths [163]. Although early discovery may allow for surgical resection, at the time of diagnosis, 25-30 percent of patients have already established metastasis [164]. Transglutaminase family member, TG2, exhibits crosslinking activity on proteins and calcium-independent GTPase activity. Up-regulation of TG2 has been in several pathological conditions such as tissue fibrosis and cancer. Moreover, in numerous cancer types such as pancreatic, ovarian, melanoma, and lung cancers, over-expression of TG2 was traced and shown to participate in metastasis and cancer progression by mediating tumor survival, alterations in ECM, EMT, and tumor cell growth. In addition to the aforementioned tumor cells, the presence of TG2 overexpression is also detected in RCC by a study published by Hidaki *et al*. [148]. The prognostic significance of TG2 in RCC was also reported by Park *et al.* [165]. Together with all previous findings, as defining new therapeutic approaches in RCC is important to prevent recurrence and invasion of RCC, TG2 may interplay a significant role in RCC metastasis, chemoresistance, and progression due to its different enzymatic functions. In this study, we aimed to that how active site mutants of TG2 can contribute to RCC malignancy by modulating cell cycle and everolimus response regarding GTPase and transamidase functions.

The multifunctional enzyme, TG2, affiliates both tumor cell survival and death based on its functional variants, intracellular localization, cell type, and the received stimuli. Based on these variations, TG2 can demonstrate both pro-apoptotic or anti-apoptotic roles [166]. Moreover, while the GTP-binding active form of TG2 is known to be mostly associated with the promotion of cell survival, catalytically active transamidase forms of TG2 have been demonstrated in both cell survival and apoptosis-inducing mechanisms depending on the cell type and received stimuli [161,166]. In addition, recent evidence suggests that transamidase activity of TG2 is associated with cellular death-inducing mechanisms by increasing apoptosis [87].

In the light of all these previous findings, we firstly focused on how TG2-active site mutant can affect cell proliferation which is an important element for tumor progression. According to our findings, TG2-W241A cells showed a statistically significant and progressive increase in cell viability through the 24-72h of incubations. Moreover, when compared to parental RenCa cells, at the end of 72h of incubation, TG2-W241A cells had the highest increase in cell proliferation among the other cells. On the other hand, wt-TG2, TG2-R580A, and TG2-C277S expressing cells shared an almost similar and more sustained cell proliferation profile. Moreover, to support our cell proliferation data, an analysis of the cell cycle among TG2-active site mutants was done. Our findings suggested that GTP-binding activity enhanced cell cycle progression by the end of 24 h of incubation, as TG2-W241A cells were arrested in G2/M phases by 71 percent suggesting an observed increase in cell proliferation rate was due to induction in cell cycle progression from G1/S to G2/M. From this point of view, it can be said that TG2 may have a notable role in molecular mechanisms regulating the cell cycle. Similar to our finding Nadalutti *et al.*, showed that intracellular TG2 had a central role in living cells and was essential for cell cycle progression from G1 to S phase. Moreover, when they downregulated the endogenous TG2, endothelial cells were observed to be in the G0/G1 stages of the cell cycle and not progress into G2/M [157]. In addition, Mian *et al.* reported that hamster fibrosarcoma cell lines (Met B) were previously transduced with wt-TG2 and transamidase inactive and low-GTP binding affinity TG2-C277S genes demonstrated that increased expression of TG2 clearly attenuates the cell cycle progression from S phases to G2/M phases. To sum up previous and our findings suggest that GTP-binding activity of TG2 alone can provide a noteworthy effect on the regulation of cell cycle and proliferation and consequently result in tumor progression in several tumor cells involving RCC.

Furthermore, tumor cells can evade cell death by circumventing growth suppressors or vice versa. To investigate, how increased cell proliferation and alterations in cell cycle progression can affect the RCC survival, we examined drug response of all cell lines depending on administration times and dose-dependent manner by using an mTOR inhibitor everolimus. Indeed, previous studies reported that the murine CCRCC model, RenCa, is sensitive to applied everolimus treatment [159,167]. In consistence with our results, non-transduced parental RenCa cells were observed to be immensely cytotoxically affected by

0.25-1 μM everolimus treatment by losing 80 percent of cell viability at the end of 72h. However, TG2-W241A cells' viability was not cytotoxically affected by everolimus treatment and although a cytostatic effect was evident. Other cell lines approximately exhibited a similar drug response upon the applied everolimus treatment, and their cell viabilities were significantly reduced in the dose and time-dependent manner. From this point of view, it can be stated that the GTP-binding activity of TG2 may have a role in drug tolerance in RCC. In order to further investigate our results, Annexin-V PI dual staining was employed. Our results demonstrated that GTP-binding active and transamidase-deficient variant TG2-W241A significantly protect RCC from cellular death induced by everolimus. In accordance with our results, Rossin *et.al*. showed that MEF cells transduced with C277S mutant form of TG2, which is transamidation inactive but still processing GTP-binding activity, resulted in protecting cells from cellular death upon induction of apoptosis while wt-TG2 expressing MEF cells more easily respond to death stimuli. Similarly, Kumar *et. al.* reported that GTP-binding-deficient TG2 mutant form, R580A, showed decreased ability to protect healthy mammary epithelial cells MCF10A against doxorubicin treatment and to trigger EMT [168]. Finally, a recent paper from our group demonstrated that EMT was induced in TG2-W241A RenCa cell [156]. These results suggested that the GTP binding activity of TG2 played a crucial role in the induction of EMT which is also associated with increased drug resistance.

In summary of all the data represented GTP-binding activity was proven to have an indispensable role in gained drug tolerance and cell growth in RCC. From this point of view, targeting the GTP-binding domain of TG2 in the RCC can be a potential therapeutic approach for patients with mRCC and may provide better survival and prognosis in RCC patients.

6. CONCLUSION AND FUTURE PERSPECTIVES

Tissue transglutaminase 2 is already known as a protein participating in tumor metastasis, progression, cell proliferation, and drug resistance. However, there is still a contradiction in the identification of two well-known activities of TG2 which is transamidating and GTP-binding in renal cell carcinoma. For the first time, the relative contribution of the enzyme activities of TG2 in cell proliferation, cell cycle regulation, and everolimus response have been demonstrated in RCC. According to previous studies done in our lab showing that GTP-binding active and catalytically transamidase inactive TG2-W241A cells had a role in the induction of NF-$_{K}$B modulated EMT which may result in drug resistance, invasiveness, and cancer stemness. Now, with our recent study, that GTP-binding activity is indispensable for acquired drug resistance, and increased cell proliferation was shown. As a future goal, molecular mechanisms underlying increased G2/M progression could be shown with an analysis of important factors in cell cycle regulation. Changes in protein levels of CDK 4/6, CDK2, Cyclin D1/D3, Cyclin E1, p16, and p27 can be investigated in RenCa cells expressing TG2 variants using Western Blot analysis. In order to dissect the evasion of apoptosis observed in TG2-W241A RenCa cells in response to everolimus, cleavage of Caspase 9, -3 and PARP can also be investigated by a series of experiments.

REFERENCES

1. Hallgrímsson B, Benediktsson H, Vize PD. Anatomy and Histology of the Human Urinary System. *Kidney From Norm Dev to Congenit Dis*. 2003:149–67.
2. Treuting PM, Kowalewska J. Urinary System. In Comparative anatomy and histology: A mouse and human atlas. Second ed. Oxford: *Academic Press*.2012:229-251.
3. Hansel D, Kane C, Paner G, Chang S. The Kidney: A Comprehensive Guide to Pathologic Diagnosis and Management. First ed. New York: *Springer-Verlag*.2015.
4. Yu A. S. L., Chertow G. M., Luyckx V., Marsden P. A., Skorecki K. and Taal M. W. Brenner and Rector's the Kidney. 11th ed.Philadelphia: *Elsevier*.2019.
5. Ferlay J, Steliarova-Foucher E, Lortet-Tieulent J, Rosso S, Coebergh JWW, Comber H, et al. Cancer incidence and mortality patterns in Europe: Estimates for 40 countries in 2012. *Eur J Cancer*. 2013;49(6):1374–403.
6. Divatia MK, Guo CC, Rehman A, Ro JY. Major Subtypes of Renal Cell Carcinoma. Divatia MK et al. (eds), *Kidney Cancer*. First ed. Cham: Springer Nature (Switzerland AG).2020:77-114.
7. Sung H, Ferlay J, Siegel RL, Laversanne M, Soerjomataram I, Jemal A, et al. Global Cancer Statistics 2020: GLOBOCAN Estimates of Incidence and Mortality Worldwide for 36 Cancers in 185 Countries. *CA Cancer J Clin*. 2021;71(3):209-249.
8. Thoenes W, Störkel S, Rumpelt HJ. Histopathology and Classification of Renal Cell Tumors (Adenomas, Oncocytomas and Carcinomas): The Basic Cytological and Histopathological Elements and their Use for Diagnostics. *Pathol Res Pract*. 1986;181(2):125-143
9. Lara PN, Jonasch E. (eds.).Kidney cancer: Principles and practice. 2nd ed. Cham:Springer (Switzerland AG).2012:309.
10. Moch H, Cubilla AL, Humphrey PA, Reuter VE, Ulbright TM. The 2016 WHO Classification of Tumours of the Urinary System and Male Genital Organs—Part A: Renal, Penile, and Testicular Tumours. *Eur Urol*. 2016;70(1):93-105.

11. Divatia MK. Kidney Cancer: Recent Advances in Surgical and Molecular Pathology. First ed.Cham: Springer Nature (Switzerland AG). 2020:445.

12. Ferlay J, Soerjomataram I, Dikshit R, Eser S, Mathers C, Rebelo M, et al. Cancer incidence and mortality worldwide: Sources, methods and major patterns in GLOBOCAN 2012. *Int J Cancer*. 2015;136(5):E359-E386.

13. Muglia VF, Prando A. Renal cell carcinoma: histological classification and correlation with imaging findings. *Radiol Bras*. 2015;48(3):166-174.

14. Hu ZY, Pang LJ, Qi Y, Kang XL, Hu JM, Wang L, et al. Unclassified renal cell carcinoma: A clinicopathological, comparative genomic hybridization, and whole-genome exon sequencing study. *Int J Clin Exp Pathol*. 2014;7(7):3865–75.

15. Ficarra V, Righetti R, Martignoni G, D'amico A, Pilloni S, Rubilotta E, et al. Prognostic value of renal cell carcinoma nuclear grading: Multivariate analysis of 333 cases. *Urol Int*. 2001;67(2):130–4.

16. Lohse CM, Cheville JC. A review of prognostic pathologic features and algorithms for patients treated surgically for renal cell carcinoma. *Clin Lab Med*. 2005;25(2):433-464.

17. Lohse CM, Blute ML, Zincke H, Weaver AL, Cheville JC. Comparison of standardized and nonstandardized nuclear grade of renal cell carcinoma to predict outcome among 2,042 patients. *Am J Clin Pathol*. 2002;118(6):877-886.

18. Veiga MPP da, Arija IN, García LB, Velarde LC, Espinosa JC. Kidney cancer. *Med*. 2021;13(26):1431-1440.

19. Mydlo JH, Bard RH. Analysis of papillary renal adenocarcinoma. *Urology*. 1987;30(6):529-534.

20. Mancilla- Jimenez R, Stanley RJ, Blath RA. Papillary renal cell carcinoma. A clinical, radiologic, and pathologic study of 34 cases. *Cancer*. 1976;38(6):2469-2480.

21. Kovacs G, Fuzesi L, Emanuel A, Kung H - F. Cytogenetics of papillary renal cell tumors. *Genes, Chromosom Cancer*. 1991;3(4):249-255.

22. Thoenes W, Störkel S, Rumpelt HJ. Human chromophobe cell renal carcinoma. *Virchows Arch B Cell Pathol Incl Mol Pathol*. 1985;48(3):207-217.

23. Thoenes W, Störkel S, Rumpelt H - J, Moll R, Baum HP, Werner S. Chromophobe cell renal carcinoma and its variants—a report on 32 cases. *J Pathol*. 1988;155(4):277-287.

24. Shuch B, Ricketts CJ, Vocke CD, Komiya T, Middelton LA, Kauffman EC, et al. Germline PTEN mutation Cowden syndrome: An underappreciated form of hereditary kidney cancer. *J Urol*. 2013;190(6):1990-1998.

25. Zbar B, Alvord WG, Glenn G, Turner M, Pavlovich CP, Schmidt L, et al. Risk of renal and colonic neoplasms and spontaneous pneumothorax pneurnothorax in the Birt-Hogg-Dubé syndrome. *Cancer Epidemiol Biomarkers Prev*. 2002;11(4):393-400.

26. Elliott A, Bruner E. Renal medullary carcinoma. *Arch Pathol Lab Med*. 2019;143(12):1556-1561.

27. Dimashkieh H, Choe J, Mutema G. Renal medullary carcinoma: a report of 2 cases and review of the literature. *Arch Pathol Lab Med*. 2003;127(3):e135-138.

28. Yang XJ, Sugimura J, Tretiakova MS, Furge K, Zagaja G, Sokoloff M, et al. Gene Expression Profiling of Renal Medullary Carcinoma: Potential Clinical Relevance. *Cancer*. 2004;100(5):976-985.

29. Hu Y, Zhou H, Wang G, Song Z, Zhao C, Wang Y. Collecting duct carcinoma of the kidney: A case report. *Oncol Lett*. 2015;9(6):2902-2904.

30. Peyromaure M, Thiounn N, Scotté F, Vieillefond A, Debré B, Oudard S. Collecting duct carcinoma of the kidney: A clinicopathological study of 9 cases. *J Urol*. 2003; 170(4 Pt 1);1138-1140.

31. Srigley JR, Eble JN. Collecting duct carcinoma of kidney. *Semin Diagn Pathol*. 1998;15(1):54-67.

32. Argani P, Ladanyi M. Translocation carcinomas of the kidney. *Clin Lab Med*. 2005;25(2);363-378.

33. Takeuchi H, Tokuyama N, Kuroda I, Aoyagi T. Molecular targeted therapies of renal cell carcinoma considering life stage of the patient: Two case reports. *Exp Ther Med*. 2018;15(4):3976-3980.

34. Peña-Llopis S, Christie A, Xie XJ, Brugarolas J. Cooperation and antagonism among cancer genes: The renal cancer paradigm. *Cancer Res*. 2013;73(14):173-179.

35. Kaelin WG. The von Hippel-Lindau tumour suppressor protein: O2 sensing and cancer. *Nat Rev Cancer*. 2008;8(11):865-873.

36. Zarrabi K, Fang C, Wu S. New treatment options for metastatic renal cell carcinoma with prior anti-angiogenesis therapy. *J Hematol Oncol*. 2017;10(1):38.

37. Niu G, Chen X. Vascular Endothelial Growth Factor as an Anti-Angiogenic Target for Cancer Therapy. *Curr Drug Targets*. 2010;11(8):1000-1017.

38. Motzer RJ, Hutson TE, Tomczak P, Michaelson MD, Bukowski RM, Rixe O, et al. Sunitinib versus Interferon Alfa in Metastatic Renal-Cell Carcinoma. *N Engl J Med*. 2007;356(2):115-124.

39. Motzer RJ, Michaelson MD, Redman BG, Hudes GR, Wilding G, Figlin RA, et al. Activity of SU11248, a multitargeted inhibitor of vascular endothelial growth factor receptor and platelet-derived growth factor receptor, in patients with metastatic renal cell carcinoma. *J Clin Oncol*. 2006;24(1):16-24.

40. Motzer RJ, Rini BI, Bukowski RM, Curti BD, George DJ, Hudes GR, et al. Sunitinib in patients with metastatic renal cell carcinoma. *J Am Med Assoc*. 2006;297(21):2516-2524.

41. Esteban-Villarrubia J, Soto-Castillo JJ, Pozas J, Román-Gil MS, Orejana-Martín I, Torres-Jiménez J, et al. Tyrosine kinase receptors in oncology. *Int J Mol Sci*. 2020;21(22):8529.

42. Motzer RJ, Hutson TE, Tomczak P, Michaelson MD, Bukowski RM, Oudard S, et al. Overall survival and updated results for sunitinib compared with interferon alfa in patients with metastatic renal cell carcinoma. *J Clin Oncol*. 2009;27(22):3584-3590.

43. Kollmannsberger C, Soulieres D, Wong R, Scalera A, Gaspo R, Bjarnason G. Sunitinib therapy for metastatic renal cell carcinoma: Recommendations for management of side effects. *J Can Urol Assoc*. 2007;1(2 Suppl):S41-S54.

44. Santoni M, Conti A, De Giorgi U, Iacovelli R, Pantano F, Burattini L, et al. Risk of gastrointestinal events with sorafenib, sunitinib and pazopanib in patients with solid

tumors: A systematic review and meta-analysis of clinical trials. *Int J Cancer*. 2014;71(2):431-439.

45. Motzer RJ, Hutson TE, Cella D, Reeves J, Hawkins R, Guo J, et al. Pazopanib versus Sunitinib in Renal Cancer. *N Engl J Med*. 2013;329(8):722-731.

46. Carlomagno F, Anaganti S, Guida T, Salvatore G, Troncone G, Wilhelm SM, et al. BAY 43-9006 inhibition of oncogenic RET mutants. *J Natl Cancer Inst*. 2006;98(5):326-334.

47. Wilhelm SM, Carter C, Tang LY, Wilkie D, McNabola A, Rong H, et al. BAY 43-9006 exhibits broad spectrum oral antitumor activity and targets the RAF/MEK/ERK pathway and receptor tyrosine kinases involved in tumor progression and angiogenesis. *Cancer Res*. 2004;64(19):7099-7109.

48. Chang YS, Adnane J, Trail PA, Levy J, Henderson A, Xue D, et al. Sorafenib (BAY 43-9006) inhibits tumor growth and vascularization and induces tumor apoptosis and hypoxia in RCC xenograft models. *Cancer Chemother Pharmacol*. 2007;59(5):561-574.

49. Escudier B, Eisen T, Stadler WM, Szczylik C, Oudard S, Siebels M, et al. Sorafenib in Advanced Clear-Cell Renal-Cell Carcinoma. *N Engl J Med*. 2007;356(2):125-134.

50. Wirth LJ, Tahara M, Robinson B, Francis S, Brose MS, Habra MA, et al. Treatment-emergent hypertension and efficacy in the phase 3 Study of (E7080) lenvatinib in differentiated cancer of the thyroid (SELECT). *Cancer*. 2018;124(11):2356-2372.

51. Whiting D, Sriprasad S. Molecular biology and targeted therapy in metastatic renal cell carcinoma. *J Clin Urol*. 2020;13(1):40-49.

52. Kuznar W. Lenvatinib Extends Survival in Metastatic Renal-Cell Carcinoma. *Am Heal Drug Benefits*. 2015;8(Spec Issue):18.

53. Geel RMJM, Beijnen JH, Schellens JHM. Concise Drug Review: Pazopanib and Axitinib. *Oncologist*. 2012;17(8):1081-1089.

54. Rixe O, Bukowski RM, Michaelson MD, Wilding G, Hudes GR, Bolte O, et al. Axitinib treatment in patients with cytokine-refractory metastatic renal-cell cancer: a phase II study. *Lancet Oncol*. 2007;8(11):975-984.

55. Qi WX, He AN, Shen Z, Yao Y. Incidence and risk of hypertension with a novel multi-targeted kinase inhibitor axitinib in cancer patients: A systematic review and meta-analysis. *Br J Clin Pharmacol*. 2013;76(3):348-357.

56. Posadas EM, Limvorasak S, Figlin RA. Targeted therapies for renal cell carcinoma. *Nat Rev Nephrol*. 2017;13(8):496-511.

57. Motzer RJ, Escudier B, Oudard S, Hutson TE, Porta C, Bracarda S, et al. Efficacy of everolimus in advanced renal cell carcinoma: a double-blind, randomised, placebo-controlled phase III trial. *Lancet*. 2008;372(9637):449-456.

58. Eckert RL, Kaartinen MT, Nurminskaya M, Belkin AM, Colak G, Johnson GVW, et al. Transglutaminase regulation of cell function. *Physiol Rev*. 2014;94(2):383-417.

59. Fesus L, Piacentini M. Transglutaminase 2 : an enigmatic. *TRENDS Biochem Sci*. 2002;27(10):543-549.

60. Onyekachi O. History and Biology of Transglutaminase 2: A Synopsis. *Int J Biochem Res Rev*. 2014;4(1):43-65.

61. Satchwell TJ, Shoemark DK, Sessions RB, Toye AM. Protein 4.2 : A complex linker. *Blood Cells, Mol Dis*. 2009;42(3):201-210.

62. Klöck C, DiRaimondo TR, Khosla C. Role of transglutaminase 2 in celiac disease pathogenesis. *Semin Immunopathol*. 2012;34(4):513-522.

63. Szondy Z, Korponay-Szabó I, Király R, Sarang Z, Tsay GJ. Transglutaminase 2 in human diseases. *Biomed*. 2017;7(3):15.

64. Lorand L, Graham RM. Transglutaminases: Crosslinking enzymes with pleiotropic functions. *Nat Rev Mol Cell Biol*. 2003;4(2):140-156.

65. Nurminskaya M V., Belkin AM. Cellular Functions of Tissue Transglutaminase. *Int. Rev. Cell Mol. Biol.* 2012; 294:1-97

66. Griffin M, Casadio R, Bergamini CM. Transglutaminases: Nature's biological glues. *Biochem J*. 2002;368(Pt 2):377-396.

67. Gundemir S, Colak G, Tucholski J, Johnson GVW. Transglutaminase 2: A molecular Swiss army knife. *Biochim Biophys Acta - Mol Cell Res*. 2012;1823(2):406-419.

68. Lu S, Saydak M, Gentile V, Stein JP, Davies PJA. Isolation and characterization of the human tissue transglutaminase gene promoter. *J Biol Chem*. 1995;270(17):99748-9756.

69. Shimada J, Suzuki Y, Kim SJ, Wang PC, Matsumura M, Kojima S. Transactivation via RAR/RXR-Sp1 interaction: Characterization of binding between Sp1 and GC box motif. *Mol Endocrinol*. 2001;15(10):1677-1692.

70. Nagy L, Saydak M, Shipley N, Lu S, Basilion JP, Yan ZH, et al. Identification and characterization of a versatile retinoid response element (retinoic acid receptor response element-retinoid X receptor response element) in the mouse tissue transglutaminase gene promoter. *J Biol Chem*. 1996;271(8):4355-4365.

71. Mirza A, Liu SL, Frizell E, Zhu J, Maddukuri S, Martinez J, et al. A role for tissue transglutaminase in hepatic injury and fibrogenesis, and its regulation by NF-κB. *Am J Physiol - Gastrointest Liver Physiol*. 1997;72 (2 Pt 1):G281-G288.

72. Jang GY, Jeon JH, Cho SY, Shin DM, Kim CW, Jeong EM, et al. Transglutaminase 2 suppresses apoptosis by modulating caspase 3 and NF-κB activity in hypoxic tumor cells. *Oncogene*. 2010;29(3):356-367.

73. Suto N, Ikura K, Sasaki R. Expression induced by interleukin-6 of tissue-type transglutaminase in human hepatoblastoma HepG2 cells. *J Biol Chem*. 1993;268(10):7469-7473.

74. Johnson K, Hashimoto S, Lotz M, Pritzker K, Terkeltaub R. Interleukin-1 induces pro-mineralizing activity of cartilage tissue transglutaminase and factor XIIIa. *Am J Pathol*. 2001;159(1):149-163.

75. Kuncio GS, Tsyganskaya M, Zhu J, Liu SL, Nagy L, Thomazy V, et al. TNF-α modulates expression of the tissue transglutaminase gene in liver cells. *Am J Physiol - Gastrointest Liver Physiol*. 1998;274(2):G240-245.

76. Chen R, Gao B, Huang C, Olsen B, Rotundo RF, Blumenstock F, et al. Transglutaminase-mediated fibronectin multimerization in lung endothelial matrix in response to TNF-α. *Am J Physiol - Lung Cell Mol Physiol*. 2000;279(1):L161-174.

77. Ai L, Kim WJ, Demircan B, Dyer LM, Bray KJ, Skehan RR, et al. The transglutaminase 2 gene (TGM2), a potential molecular marker for chemotherapeutic

drug sensitivity, is epigenetically silenced in breast cancer. *Carcinogenesis*. 2008;5(9):2756-2776.

78. Park KS, Kim HK, Lee JH, Choi YB, Park SY, Yang SH, et al. Transglutaminase 2 as a cisplatin resistance marker in non-small cell lung cancer. *J Cancer Res Clin Oncol*. 2010;44:63-72.

79. Dyer LM, Schooler KP, Ai L, Klop C, Qiu J, Robertson KD, et al. The transglutaminase 2 gene is aberrantly hypermethylated in glioma. *J Neurooncol*. 2011;101(3):429-440.

80. Zemskov EA, Loukinova E, Mikhailenko I, Coleman RA, Strickland DK, Belkin AM. Regulation of platelet-derived growth factor receptor function by integrin-associated cell surface transglutaminase. *J Biol Chem*. 2009:284(24);16693-16703.

81. Zemskov EA, Mikhailenko I, Smith EP, Belkin AM. Tissue transglutaminase promotes PDGF/PDGFR-mediated signaling and responses in vascular smooth muscle cells. *J Cell Physiol*. 2012;227(5):2089-2096.

82. Zemskov EA, Janiak A, Hang J, Waghray A, Belkin AM. The role of tissue transglutaminase in cell-matrix interactions. *Front Biosci*. 2006;11:1057-1076.

83. Lai TS, Lin CJ, Greenberg CS. Role of tissue transglutaminase-2 (TG2)-mediated aminylation in biological processes. *Amino Acids*. 2017;49(3);501-515.

84. Király R, Demény MÁ, Fésüs L. Protein transamidation by transglutaminase 2 in cells: A disputed Ca 2+-dependent action of a multifunctional protein. *FEBS J*. 2011;579(15):3297-3302.

85. Sarang Z, Molnár P, Németh T, Gomba S, Kardon T, Melino G, et al. Tissue transglutaminase (TG2) acting as G protein protects hepatocytes against Fas-mediated cell death in mice. *Hepatology*. 2005;42(3):578-587.

86. Begg GE, Carrington L, Stokes PH, Matthews JM, Wouters MA, Husain A, et al. Mechanism of allosteric regulation of transglutaminase 2 by GTP. *Proc Natl Acad Sci U S A*. 2006;103(52):19683-19688.

87. Tatsukawa H, Furutani Y, Hitomi K, Kojima S. Transglutaminase 2 has opposing roles in the regulation of cellular functions as well as cell growth and death. *Cell*

Death Dis. 2016;7:e2244.

88. Liu S, Cerione RA, Clardy J. Structural basis for the guanine nucleotide-binding activity of tissue transglutaminase and its regulation of transamidation activity. *Proc Natl Acad Sci U S A*. 2002;99(5):2743-2477.

89. Gundemir S, Johnson GVW. Intracellular localization and conformational state of transglutaminase 2: Implications for cell death. *PLoS One*. 2009;4(7):e6123.

90. Pinkas DM, Strop P, Brunger AT, Khosla C. Transglutaminase 2 undergoes a large conformational change upon activation. *PLoS Biol*. 2007.

91. Prasanna Murthy SN, Iismaa S, Begg G, Freymann DM, Graham RM, Lorand L. Conserved tryptophan in the core domain of transglutaminase is essential for catalytic activity. *Proc Natl Acad Sci U S A*. 2002;5(12):e327.

92. Chen JSK, Mehta K. Tissue transglutaminase: An enzyme with a split personality. *Int J Biochem Cell Biol*. 1999;31(8):817-836.

93. Bergamini CM, Collighan RJ, Wang Z, Griffin M. Structure and regulation of type 2 transglutaminase in relation to its physiological functions and pathological roles. *Adv Enzymol Relat Areas Mol Biol*. 2011;78:1-46.

94. Beninati S, Piacentini M, Bergamini CM. Transglutaminase 2, a double face enzyme. *Amino Acids*. 2017:49(3):415-423.

95. Bianchi N, Beninati S, Bergamini CM. Spotlight on the transglutaminase 2 gene: A focus on genomic and transcriptional aspects. *Biochem J*. 2018;475(9):1643-1667.

96. Fisher ML, Keillor JW, Xu W, Eckert RL, Kerr C. Transglutaminase is required for epidermal squamous cell carcinoma stem cell survival. *Mol Cancer Res*. 2015;13(7):1083-1094.

97. Cellura D, Pickard K, Quaratino S, Parker H, Strefford JC, Thomas GJ, et al. miR-19-mediated inhibition of transglutaminase-2 leads to enhanced invasion and metastasis in colorectal cancer. *Mol Cancer Res*. 2015;13(7):1095-1105.

98. Yakubov B, Chelladurai B, Schmitt J, Emerson R, Turchi JJ, Matei D. Extracellular tissue transglutaminase activates noncanonical NF-κB signaling and promotes metastasis in ovarian cancer. *Neoplasia (United States)*. 2013;15(6):609-619.

99. Agnihotri N, Kumar S, Mehta K. Tissue transglutaminase as a central mediator in inflammation-induced progression of breast cancer. *Breast Cancer Res*. 2012;15(1):202.

100. Kumar A, Xu J, Sung B, Kumar S, Yu D, Aggarwal BB, et al. Evidence that GTP-binding domain but not catalytic domain of transglutaminase 2 is essential for epithelial-to-mesenchymal transition in mammary epithelial cells. *Breast Cancer Res*. 2012;14(1):R4.

101. Eckert RL. Transglutaminase 2 takes center stage as a cancer cell survival factor and therapy target. *Mol Carcinog*. 2019;58(6):837-853.

102. Nezir AE, Ulukan B, Telci D. Transglutaminase 2: The Maestro of the Oncogenic Mediators in Renal Cell Carcinoma. *Med Sci*. 2019;7(2):24.

103. Telci D, Collighan RJ, Basaga H, Griffin M. Increased TG2 expression can result in induction of transforming growth factor β1, causing increased synthesis and deposition of matrix proteins, which can be regulated by nitric oxide. *J Biol Chem*. 2009;284(43):29547-29558.

104. Telci D, Wang Z, Li X, Verderio EAM, Humphries MJ, Baccarini M, et al. Fibronectin-tissue transglutaminase matrix rescues RGD-impaired cell adhesion through syndecan-4 and β1 integrin co-signaling. *J Biol Chem*. 2008;283(30):20937-20947.

105. Wang Z, Griffin M. TG2, a novel extracellular protein with multiple functions. *Amino Acids*. 2012;42(2-3):939-949.

106. Hanahan D, Weinberg RA. Hallmarks of cancer: The next generation. *Cell*. 2011;144(5):646-674.

107. Mehta K, Fok J, Miller FR, Koul D, Sahin AA. Prognostic significance of tissue transglutaminase in drug resistant and metastatic breast cancer. *Clin Cancer Res*. 2004;10(23):8068-8076.

108. Kok JY, Ekmekcioglu S, Mehta K. Implications of tissue transglutaminase expression in malignant melanoma. *Mol Cancer Ther*. 2006;5(6):1493-1450.

109. Jee YH, Mangala LS, Fok JY, Lin YG, Merritt WM, Spannuth WA, et al. Clinical

and biological significance of tissue transglutaminase in ovarian carcinoma. *Cancer Res*. 2008;68(14):5849-5858.

110. Satpathy M, Cao L, Pincheira R, Emerson R, Bigsby R, Nakshatri H, et al. Enhanced peritoneal ovarian tumor dissemination by tissue transglutaminase. *Cancer Res*. 2007;67(15):7194-7202.

111. Verma A, Wang H, Manavathi B, Fok JY, Mann AP, Kumar R, et al. Increased expression of tissue transglutaminase in pancreatic ductal adenocarcinoma and its implications in drug resistance and metastasis. *Cancer Res*. 2006;66(21):10525-10533.

112. Yuan L, Siegel M, Choi K, Khosla C, Miller CR, Jackson EN, et al. Transglutaminase 2 inhibitor, KCC009, disrupts fibronectin assembly in the extracellular matrix and sensitizes orthotopic glioblastomas to chemotherapy. *Oncogene*. 2007;26(18):2563-2573.

113. Mehta K, Kumar A, Kim HI. Transglutaminase 2: A multi-tasking protein in the complex circuitry of inflammation and cancer. *Biochem Pharmacol*. 2010;80(12):1921-1929.

114. Yuan L, Behdad A, Siegel M, Khosla C, Higashikubo R, Rich KM. Tissue transgluaminase 2 expression in meningiomas. *J Neurooncol*. 2008;90(2):125-132.

115. Belkin AM. Extracellular TG2: Emerging functions and regulation. *FEBS J*. 2011;278(24):4074-4716.

116. Apte M V., Wilson JS. Dangerous liaisons: Pancreatic stellate cells and pancreatic cancer cells. *J Gastroenterol Hepatol*. 2012;27(2):69-74.

117. Levental KR, Yu H, Kass L, Lakins JN, Egeblad M, Erler JT, et al. Matrix Crosslinking Forces Tumor Progression by Enhancing Integrin Signaling. *Cell*. 2009;139(5):891-906.

118. Thiery JP, Acloque H, Huang RYJ, Nieto MA. Epithelial-Mesenchymal Transitions in Development and Disease. *Cell*. 2009;139(5):871-890.

119. Kumar A, Xu J, Brady S, Gao H, Yu D, Reuben J, et al. Tissue transglutaminase promotes drug resistance and invasion by inducing mesenchymal transition in

mammary epithelial cells. *PLoS One*. 2010;5(10):e13390.

120. Kumar A, Gao H, Xu J, Reuben J, Yu D, Mehta K. Evidence that aberrant expression of tissue transglutaminase promotes stem cell characteristics in mammary epithelial cells. *PLoS One*. 2011;6(6):e20701.

121. Shao M, Cao L, Shen C, Satpathy M, Chelladurai B, Bigsby RM, et al. Epithelial-to-mesenchymal transition and ovarian tumor progression induced by tissue transglutaminase. *Cancer Res*. 2009;69(24):9192-9201.

122. Herman JF, Mangala LS, Mehta K. Implications of increased tissue transglutaminase (TG2) expression in drug-resistant breast cancer (MCF-7) cells. *Oncogene*. 2006;25(21):3049-3058.

123. Verma A, Guha S, Diagaradjane P, Kunnumakkara AB, Sanguino AM, Lopez-Berestein G, et al. Therapeutic significance of elevated tissue transglutaminase expression in pancreatic cancer. *Clin Cancer Res*. 2008;14(8):2476-2483.

124. Feitelson MA, Arzumanyan A, Kulathinal RJ, Blain SW, Holcombe RF, Mahajna J, et al. Sustained proliferation in cancer: Mechanisms and novel therapeutic targets. *Semin Cancer Biol*. 2015;35 *Suppl*(Suppl):S25-S54.

125. Condello S, Cao L, Matei D. Abstract C49: Tissue tranglutaminase regulates β-catenin signaling in ovarian cancer cells. 2013;27(8):3100-3112.

126. Cao L, Shao M, Schilder J, Guise T, Mohammad KS, Matei D. Tissue transglutaminase links TGF-B, epithelial to mesenchymal transition and a stem cell phenotype in ovarian cancer. *Oncogene*. 2012;31(20):2521-2534.

127. Fu J, Yang QY, Sai K, Chen FR, Pang JCS, Ng HK, et al. TGM2 inhibition attenuates ID1 expression in CD44-high glioma-initiating cells. *Neuro Oncol*. 2013;15(10):1353-1365.

128. Wang X, Yu Z, Zhou Q, Wu X, Chen X, Li J, et al. Tissue transglutaminase-2 promotes gastric cancer progression via the ERK1/2 pathway. *Oncotarget*. 2016;7(6):7066-7079.

129. Mehta K, Kumar A, Kim HI. Transglutaminase 2: A multi-tasking protein in the complex circuitry of inflammation and cancer. *Biochem Pharmacol*.

2010;80(12):1921-1929.

130. Roché H, Vahdat LT. Treatment of metastatic breast cancer: Second line and beyond. *Ann Oncol*. 2011;22(5):1000-1010.

131. Pistritto G, Trisciuoglio D, Ceci C, Alessia Garufi, D'Orazi G. Apoptosis as anticancer mechanism: Function and dysfunction of its modulators and targeted therapeutic strategies. *Aging (Albany NY)*. 2016;8(4):603-619.

132. Mehta K, Fok JY. Targeting transglutaminase-2 to overcome chemoresistance in cancer cells. Siddik Z and Mehta K (ed.), *Drug Resist. Cancer Cells*.Springer (N*ew York NY*). 2009:95-114.

133. Oliverio S, Amendola A, Rodolfo C, Spinedi A, Piacentini M. Inhibition of "tissue" transglutaminase increases cell survival by preventing apoptosis. *J Biol Chem*. 1999;274(4):34123-34128.

- 134. Tatsukawa H, Fukaya Y, Frampton G, Martinez-Fuentes A, Suzuki K, Kuo TF, et al. Role of Transglutaminase 2 in Liver Injury via Cross-linking and Silencing of Transcription Factor Sp1. *Gastroenterology*. 2009;136(5): 1783-95.e10.

135. Yamaguchi H, Wang H-G. Tissue Transglutaminase Serves as an Inhibitor of Apoptosis by Cross-Linking Caspase 3 in Thapsigargin-Treated Cells. *Mol Cell Biol*. 2006;26(2):569-579.

136. Cho SY, Lee JH, Bae HD, Jeong EM, Jang GY, Kim CW, et al. Transglutaminase 2 inhibits apoptosis induced by calciumoverload through down-regulation of Bax. *Exp Mol Med*. 2010;42(9):639-650.

137. Yoo JO, Lim YC, Kim YM, Ha KS. Transglutaminase 2 promotes both caspase-dependent and caspase-independent apoptotic cell death via the calpain/bax protein signaling pathway. *J Biol Chem*. 2012.

138. Eligini S, Fiorelli S, Tremoli E, Colli S. Inhibition of transglutaminase 2 reduces efferocytosis in human macrophages: Role of CD14 and SR-AI receptors. *Nutr Metab Cardiovasc Dis*. 2016;287(18):14377-14388.

139. Yen JH, Yang DJ, Chen MC, Yi-Ying W, Hsieh YF, Cheng YM, et al. Daidzein enhances efferocytosis via transglutaminase 2 and augmentation of Rac1 activity. *Mol*

Immunol. 2014;60(2):135-142.

140. Nicholas B, Smethurst P, Verderio E, Jones R, Griffin M. Cross-linking of cellular proteins by tissue transglutaminase during necrotic cell death: A mechanism for maintaining tissue integrity. *Biochem J*. 2003;371(Pt 2):413-422.

141. Frese-Schaper M, Schardt JA, Sakai T, Carboni GL, Schmid RA, Frese S. Inhibition of tissue transglutaminase sensitizes TRAIL-resistant lung cancer cells through upregulation of death receptor 5. *FEBS Lett*. 2010.

142. Tempest R, Guarnerio S, Maani R, Cooper J, Peake N. The biological and biomechanical role of transglutaminase-2 in the tumour microenvironment. *Cancers (Basel)*. 2021;584(13): 2867-2871.

143. Mehta K. High levels of transglutaminase expression in doxorubicin- resistant human breast carcinoma cells. *Int J Cancer*. 1994;58(3):400-406.

144. Huang L, Xu AM, Liu W. Transglutaminase 2 in cancer. *Am J Cancer Res*. 2015;5(9):2756-2776.

145. Boroughs LK, Antonyak MA, Cerione RA. A novel mechanism by which tissue transglutaminase activates signaling events that promote cell survival. *J Biol Chem*. 2014;289(4):10115–10125.

146. Cao J, Huang W. Compensatory increase of transglutaminase 2 is responsible for resistance to mTOR inhibitor treatment. *PLoS One*. 2016;11(2):e0149388.

147. Carbone C, Di Gennaro E, Piro G, Milone MR, Pucci B, Caraglia M, et al. Tissue transglutaminase (TG2) is involved in the resistance of cancer cells to the histone deacetylase (HDAC) inhibitor vorinostat. *Amino Acids*. 2017;49(3):517-528.

148. Hidaka H, Seki N, Yoshino H, Yamasaki T, Yamada Y, Nohata N, et al. Tumor suppressive microrna-1285 regulates novel molecular targets: Aberrant expression and functional significance in renal cell carcinoma. *Oncotarget*. 2012;3(1):44-57.

149. Ku BM, Kim SJ, Kim N, Hong D, Choi YB, Lee SH, et al. Transglutaminase 2 inhibitor abrogates renal cell carcinoma in xenograft models. *J Cancer Res Clin Oncol*. 2014;140(5):757-767.

150. Kang JH, Lee JS, Hong D, Lee SH, Kim N, Lee WK, et al. Renal cell carcinoma

escapes death by p53 depletion through transglutaminase 2-chaperoned autophagy. *Cell Death Dis*. 2016;7(3):e2163.

151. Ku BM, Kim DS, Kim KH, Yoo BC, Kim SH, Gong YD, et al. Transglutaminase 2 inhibition found to induce p53 mediated apoptosis in renal cell carcinoma. *FASEB J*. 2013;27(9):3487-3495.

152. Ku BM, Lee CH, Lee SH, Kim SY. Increased expression of transglutaminase 2 drives glycolytic metabolism in renal carcinoma cells. *Amino Acids*. 2014;46(6):1527-1536.

153. Min B, Park H, Lee S, Li Y, Choi JM, Lee JY, et al. CHIP-mediated degradation of transglutaminase 2 negatively regulates tumor growth and angiogenesis in renal cancer. *Oncogene*. 2016;35(28):3718-3728.

154. Bagatur Y, Ilter Akulke AZ, Bihorac A, Erdem M, Telci D. Tissue transglutaminase expression is necessary for adhesion, metastatic potential and cancer stemness of renal cell carcinoma. *Cell Adhes Migr*. 2018;12(2):138-151.

155. Song M. Recent developments in small molecule therapies for renal cell carcinoma. *Eur J Med Chem*. 2017;142: 383-392.

156. Ulukan B, Bihorac A, Sipahioglu T, Kiraly R, Fesus L, Telci D. Role of tissue transglutaminase catalytic and guanosine triphosphate-binding domains in renal cell carcinoma progression. *ACS Omega*. 2020:43(5):28273-28284.

157. Nadalutti C, Viiri KM, Kaukinen K, Mäki M, Lindfors K. Extracellular transglutaminase 2 has a role in cell adhesion, whereas intracellular transglutaminase 2 is involved in regulation of endothelial cell proliferation and apoptosis. *Cell Prolif*. 2011;44(1):49-58.

158. Mian S, El Alaoui S, Lawry J, Gentile V, Davies PJA, Griffin M. The importance of the GTP-binding protein tissue transglutaminase in the regulation of cell cycle progression. *FEBS Lett*. 1995:27-31.

159. Nayman AH, Siginc H, Zemheri E, Yencilek F, Yildirim A, Telci D. Dual-inhibition of mTOR and Bcl-2 enhances the anti-tumor effect of everolimus against renal cell carcinoma in vitro and in vivo. *J Cancer*. 2019;10(6):1466-1478.

160. Banumathy G, Cairns P. Signaling pathways in renal cell carcinoma. *Cancer Biol*

Ther. 2010;10(7):658-664.

161. Tatsukawa H, Furutani Y, Hitomi K, Kojima S. Transglutaminase 2 has opposing roles in the regulation of cellular functions as well as cell growth and death. *Cell Death Dis*. 2016;7:e2244.

162. Ljungberg B, Hanbury DC, Kuczyk MA, Merseburger AS, Mulders PFA, Patard JJ, et al. Renal Cell Carcinoma Guideline. *Eur Urol*. 2007;51(6)Ç1502-1510.

163. Kabaria R, Klaassen Z, Terris MK. Renal cell carcinoma: Links and risks. *Int J Nephrol Renovasc Dis*. 2016;9:45-52.

164. Cairns P. Renal cell carcinoma. *Cancer Biomarkers*. 2011;9(1-6):461-473.

165. Jee Park M, Baek HW, Rhee YY, Lee C, Park JW, Kim HW, et al. Transglutaminase 2 expression and its prognostic significance in clear cell renal cell carcinoma. *J Pathol Transl Med*. 2015;49(1):37-43.

166. Fésüs L, Szondy Z. Transglutaminase 2 in the balance of cell death and survival. *FEBS Lett*. 2005;579(15):3297-3302.

167. Larkin J, Esser N, Calvo E, Tsuchihashi Z, Fiedler U, Graeser R, et al. Efficacy of sequential treatment with sunitinib-everolimus in an orthotopic mouse model of renal cell carcinoma. *Anticancer Res*. 2012;32(7):2399-2406.

168. Kumar A, Xu J, Brady S, Gao H, Yu D, Reuben J, et al. Tissue transglutaminase promotes drug resistance and invasion by inducing mesenchymal transition in mammary epithelial cells. *PLoS One*. 2010;5(10):e13390.